


Spring 2017

Groundwater and Tidal Controls on Wetland Hydrology, Julie J. Metz Wetland Mitigation Bank, Woodbridge, Virginia

Benjamin Stuart Hiza
Old Dominion University

Follow this and additional works at: https://digitalcommons.odu.edu/oeas_etds

 Part of the [Fresh Water Studies Commons](#), [Geology Commons](#), [Hydrology Commons](#), and the [Oceanography Commons](#)

Recommended Citation

Hiza, Benjamin S.. "Groundwater and Tidal Controls on Wetland Hydrology, Julie J. Metz Wetland Mitigation Bank, Woodbridge, Virginia" (2017). Master of Science (MS), thesis, Ocean/Earth/Atmos Sciences, Old Dominion University, DOI: 10.25777/7j8s-k388
https://digitalcommons.odu.edu/oeas_etds/6

This Thesis is brought to you for free and open access by the Ocean, Earth & Atmospheric Sciences at ODU Digital Commons. It has been accepted for inclusion in OEAS Theses and Dissertations by an authorized administrator of ODU Digital Commons. For more information, please contact digitalcommons@odu.edu.

**GROUNDWATER AND TIDAL CONTROLS ON WETLAND
HYDROLOGY, JULIE J. METZ WETLAND MITIGATION BANK,
WOODBIDGE, VIRGINIA**

by

Benjamin Stuart Hiza
B.S. May 2000, Virginia Polytechnic Institute and State University
B.S. May 2013, Old Dominion University

A Thesis Submitted to the Faculty of
Old Dominion University in Partial Fulfillment of the
Requirements for the Degree of

MASTER OF SCIENCE

OCEAN AND EARTH SCIENCES

OLD DOMINION UNIVERSITY
May 2017

Approved by:

G. Richard Whittecar (Director)

Jennifer Georgen (Member)

Xixi Wang (Member)

ABSTRACT

GROUNDWATER AND TIDAL CONTROLS ON WETLAND HYDROLOGY, JULIE J. METZ WETLAND MITIGATION BANK, WOODBRIDGE, VIRGINIA

Benjamin Stuart Hiza
Old Dominion University, 2017
Director: Dr. G. Richard Whittecar

Julie J. Metz Wetlands Mitigation Bank, a 92-hectare freshwater wetland located in Woodbridge, Virginia, borders the tidally-influenced Neabsco Creek. Seven pods separated by earthen berms were built by Wetland Studies and Solutions Inc. (WSSI) in 1995 and 1997 by removing the toe of small sandy alluvial fans and covering the underlying coarse gravel bed with a low permeability cap. The basal Quaternary gravels were deposited in a creek valley incised into a thick sand-and-clay Cretaceous delta. The alluvial-fan apron developed at the base of steep slopes along the sides of the valley. Pressure transducer data from five monitoring wells along a transect across Pod 3 were used to generate hydrographs, create groundwater flow maps, calculate hydraulic conductivity (K_{sat}) by performing slug tests, and calibrate wetland water budget models using Wetbud software. Wetbud-generated water budgets using both Basic and Advanced scenarios calculated estimated water levels at Pod 3 for a typical Dry, Normal, and Wet year, and custom periods. Results from the pressure transducer data and the Wetbud Advanced Scenario indicate groundwater is the overall principal water source controlling water variability at Pod 3 in Julie Metz. However, surface water flow and direct precipitation contribute to the variability in Pod 3B. In Pod 3A, closer to Neabsco Creek, the water variability is strongly influenced by tidal forcings and storm surge. The T_TIDE (MATLAB) calculations indicate lunar tides, predominantly semi-diurnal, as

well as wind contribute to fluctuations in Neabsco Creek. Because creek levels control the groundwater gradient they influence how quickly the groundwater leaves Pod 3.

Based upon analyses of storm surge and tidal data, and using the current sea level rise rate (4.14 mm/year), Pod 3A will be consistently inundated in approximately 22 years.

Permanent inundation of Pod 3 is projected in 132 years. The rise in sea level will gradually decrease the gradient and groundwater outflow from the wetland over time and the Julie Metz wetland will transition from a forested shrub-scrub wetland to an emergent wetland.

ACKNOWLEDGMENTS

There are so many people to thank for their support during this journey to obtain a master's degree. I am extremely grateful and thankful to my advisor, Dr. Whittecar, for his support during this process, his ability to push me, provide guidance and encouragement, and his desire for my success.

Together with my advisor, I am indebted to Dr. Jennifer Georgen and Dr. Xixi Wang for being on my committee and guiding me to the completion of my thesis. Thank you for your time and willingness to work with me.

There were several professors that I worked with to improve Wetbud and generate a running model at the Julie Metz wetland. Thank you Dr. Zach Agioutantis, Dr. Lee Daniels, and Dr. Tess Thompson for your recommendations and advice as I worked with the Wetbud software.

Thank you Dr. Ezer for your advice regarding tidal signals and sea level rise. Your input was invaluable.

My wife, son, niece, and daughter endured my working hours, and supported me when I needed them most. They are my pride, joy, and the reason I work so hard. Thank you for your sacrifice and patience.

My parents and grandmother have supported me from the beginning, encouraging me to get an education and later to pursue a master's degree. They have supported my family and me so I could pursue my dreams. Thank you for your support.

Thanks to my friends who have supported and encouraged me during the highs and lows of graduate school. Specifically, I would like to thank Dr. Kurnia Foe, Joe Peterlin, Niall and Dr. Mojic Henshaw, Brad Fitzwater, and Rachel Dunleavy. I would

also like to give a special thanks to Stephen Stone for his steady input and sound advice as we worked together at our respective research sites.

Thank you Nesser and Chamberlain family for your support as I made my final push to finish my thesis. I would not have been able to finish without you.

Finally, I would like to thank the Peterson Family Foundation and Wetland Studies and Solutions, Inc. for giving me this research opportunity through the funding for this project.

TABLE OF CONTENTS

	Page
LIST OF TABLES	viii
LIST OF FIGURES	ix
 Chapter	
I. INTRODUCTION	1
WETLAND IMPORTANCE.....	1
MITIGATION WETLANDS.....	2
SITE DESCRIPTION	4
REGIONAL GEOLOGY AND HYDROGEOLOGY.....	7
SOILS.....	8
IMPORTANCE OF JULIE J. METZ WETLAND.....	10
HYPOTHESIS AND ALTERNATIVE HYPOTHESES	11
RESEARCH OBJECTIVES	11
RESEARCH APPLICATIONS	11
II. METHODS.....	13
SITE SELECTION AND HISTORICAL DATA COLLECTION.....	13
HYDROSTRATIGRAPHIC ANALYSIS	13
HYDRAULIC DATA COLLECTION.....	15
WETLAND WATER BUDGET MODELING - BASIC SCENARIO.....	17
WETLAND WATER BUDGET MODELING - ADVANCED SCENARIO	27
TIDAL ANALYSIS.....	36
SEA LEVEL RISE EFFECTS	39
III. RESULTS.	40
HYDROSTRATIGRAPHIC PROFILE.....	40
HYDROLOGIC DATA	41
WETLAND WATER BUDGET MODELING - BASIC SCENARIO.....	50
WETLAND WATER BUDGET MODELING - ADVANCED SCENARIO	66
TIDAL ANALYSIS.....	79
SEA LEVEL RISE EFFECTS	80
IV. DISCUSSION AND CONCLUSIONS	83
HYDROGEOLOGY.....	83
HYDROLOGIC ANALYSIS	83
TIDAL ANALYSIS.....	85
SEA LEVEL RISE ANALYSIS.....	86
WETLAND WATER BUDGET IMPORTANCE	86

REFERENCES CITED.....	89
-----------------------	----

APPENDICES

A. BOREHOLE LOGS AND WELL COMPLETION REPORTS.....	93
B. COMMON K_{sat} AND S_y VALUES.....	107
C. WETBUD DRAIN CELL ZONE LAYOUT IMAGE.....	109
D. WETBUD GENERAL HEAD CELL ZONE LAYOUT IMAGE.....	111
E. WETBUD MONITORING POINT CELL ZONE LAYOUT IMAGE	113
F. WETBUD NO FLOW CELL ZONE LAYOUT IMAGE.....	115
G. WETBUD RUNOFF WELL IN CELL ZONE LAYOUT IMAGE	117
H. WETBUD HYDRAULIC CONDUCTIVITY GRID ZONE LAYOUT IMAGES.....	119
I. WETBUD SPECIFIC YIELD GRID ZONE LAYOUT IMAGES	122
VITA.....	125

LIST OF TABLES

Table	Page
1. Channel Flow Data	24
2. Inflow Structure (Cipoletti Weir) Data	25
3. Drain Cell Data	29
4. Grid Zone Properties	31
5. Julie Metz Advanced Scenario Layer Attributes	35
6. Pod 3 Hydraulic Conductivity (K_{sat}) Values	41

LIST OF FIGURES

Figure	Page
1. Julie Metz Site Location and Fall Line Map.....	5
2. Julie Metz Pods and Piezometers Location Map	6
3. Julie Metz Geologic Map.....	8
4. Julie Metz Soils Map	9
5. Julie Metz Pod 3 Soil Boring and Monitoring Well Locations Map	14
6. Julie Metz Pod 3 DEM Cell Elevations Map.....	34
7. Northern Potomac Wind Data and Water Elevation Comparison Graph	38
8. Julie Metz Pod 3 Hydrostratigraphic Cross-Sectional Profile	40
9. Julie Metz Hydrograph Pod 3 with Quantico MCAF Station Precipitation	42
10. Julie Metz Hydrograph Pod 3A with Quantico MCAF Station Precipitation	43
11. Julie Metz Hydrograph Pod 3B with Quantico MCAF Station Precipitation.....	44
12. Julie Metz Pod 3 Groundwater Flow Map - Precipitation Event.....	46
13. Julie Metz Pod 3 Groundwater Flow Map - Storm Event	47
14. Julie Metz Pod 3 Groundwater Flow Map - Flood Tide.....	48
15. Julie Metz Pod 3 Groundwater Flow Map - Ebb Tide.....	49
16. Wetbud Basic Scenario Evapotranspiration Graph - Dry Year	51
17. Wetbud Basic Scenario Evapotranspiration Graph - Normal Year	52
18. Wetbud Basic Scenario Evapotranspiration Graph - Wet Year.....	53
19. Wetbud Basic Scenario Evapotranspiration Graph - Custom Period	54
20. Wetbud Basic Scenario Actual Water Level Graph - Dry Year	55
21. Wetbud Basic Scenario Actual Water Level Graph - Normal Year	56

22.	Wetbud Basic Scenario Actual Water Level Graph - Wet Year.....	57
23.	Wetbud Basic Scenario Actual Water Level Graph - Custom Period	58
24.	Wetbud Basic Scenario All Data Graph - Dry Year	59
25.	Wetbud Basic Scenario All Data Graph - Normal Year	60
26.	Wetbud Basic Scenario All Data Graph - Wet Year.....	61
27.	Wetbud Basic Scenario All Data Graph - Custom Period	62
28.	Julie Metz Basic Scenario Calibration with Hydraulic Head Graph	64
29.	Julie Metz Basic Scenario Calibration with Linear Regression Graph.....	65
30.	Wetbud Advanced Scenario MW23 Graph - 1 October 2015	67
31.	Wetbud Advanced Scenario MW23 Graph - 2 October 2015	68
32.	Wetbud Advanced Scenario MW11B Graph - 1 October 2015	69
33.	Wetbud Advanced Scenario MW11B Graph - 2 October 2015	70
34.	Wetbud Advanced Scenario MW7B Graph - 1 October 2015	71
35.	Wetbud Advanced Scenario MW7B Graph - 2 October 2015	72
36.	Julie Metz Advanced Scenario MW23 Calibration - Hydraulic Head Graph	73
37.	Julie Metz Advanced Scenario MW11B Calibration - Hydraulic Head Graph....	74
38.	Julie Metz Advanced Scenario MW7B Calibration - Hydraulic Head Graph.....	74
39.	Julie Metz Advanced Scenario MW23 Calibration - Linear Regression Graph...	76
40.	Julie Metz Advanced Scenario MW11B Calibration - Linear Regression Graph	77
41.	Julie Metz Advanced Scenario MW7B Calibration - Linear Regression Graph..	77
42.	Julie Metz Pod 3 Western Boundary Rack Line Photos	78
43.	Julie Metz Pod 3 Cross-Sectional Profile with Sea Level Rise Effects	81
44.	Julie Metz Pod 3A Hydrograph with Ground Elevations and Precipitation	82

CHAPTER I

INTRODUCTION

Wetland Importance

Wetlands are known to have fertile soils, possess high biodiversity, and perform many environmental functions. They are important nurseries and habitats for many animals and plants such as the more than 5000 plant species, 190 amphibian species, and 270 bird species in United States wetlands. The high animal and plant diversity includes 26% of the wetland plant species and 45% of wetland-reliant animal species that are listed as threatened or endangered by the Endangered Species Act (Hammer, 1989). Wetland areas are excellent buffers of storm surges, tides, and flooding events. The combination of fine grained soils, organic material, and abundant aquatic plants absorbs the erosive power of waves and tides while also reducing the amount of flooding downstream. Floodwater velocities are reduced in wetland areas that allow for temporary floodwater retention. Pollutants such as sediment, nitrate, and phosphate can be filtered from the water because floodwaters and runoff velocities are reduced in wetlands. The excessive amounts of nitrate and phosphate from nonpoint source pollutants are consumed by the aquatic plants as nutrients. Heavy metals found in sediments can be utilized by the aquatic plants, be oxidized, or can settle out, accumulate, and be buried under other sediment layers (Hey and Philippi, 1999).

Even with the abundant benefits from wetlands, more than 50% of U.S. natural wetlands have been destroyed due to human activities since the U.S. was settled (Mitsch and Gosselink, 1993). In 1972, the Clean Water Act began inhibiting the loss of wetlands under Section 404 by assigning the Army Corps of Engineers (USACE) as the regulatory

authority for compensatory mitigation of aquatic waters such as wetlands (National Research Committee, 2001). Following Clean Air Act guidelines, the USACE began protecting wetlands when possible, controlling permit requests related to wetland impairment, and establishing mitigation wetlands to offset natural wetland destruction.

Mitigation Wetlands

Mitigation wetlands are locations where wetlands are created, restored, or enhanced to offset wetland loss due to agriculture or urban development. Prior to the 1980s, mitigation wetland construction efforts were conducted near urban development project locations (Kent, 2001). The success rates for the onsite mitigated wetlands varied from 27% to 50% mainly because 22% to 34% of the mitigation wetlands were never constructed (Redmond, 1991; Gallihugh, 1998; DeWeese, 1994; Brown and Veneman, 1998). Due to the low success rates, the concept of mitigation banking was developed to mitigate wetlands more effectively and efficiently. Mitigation banking is the consolidation of small, mitigated wetland projects into one large mitigated wetland area. Units of the large mitigated wetland, called credits, can be purchased by urban developers to offset wetland destruction incurred at a development site. The benefits of mitigation banking include reduced wetland permit processing, more cost-effective environmental management practices, and the relegation of mitigated wetland construction from the urban developers to wetland professionals (Kent, 2001).

A wetland professional company, Wetland Studies and Solutions, Inc. (WSSI), has been working with wetlands since its inception in 1991, creating and restoring more than 1,300 wetland acres. Most of the projects have been built on shale in the Triassic

basin of northern Virginia and Washington, D.C. area where permeability is low and the groundwater component for wetland construction can be excluded (WSSI, 2011).

Mitigation wetland sites are chosen in low permeability areas to simplify the water budget, calculated using the Pierce method, resulting in higher constructed-wetland success rates. To increase the scope of mitigation wetlands, WSSI saw the need to include the groundwater component in mitigation wetland construction and sponsored the development of a wetland water budget program called Wetbud. The program would be used by wetland construction companies to build wetlands more efficiently and allow regulators to delineate wetlands more accurately. Water budget templates could be generated in Wetbud for various wetland types such as the freshwater tidal wetland.

Efficient mitigation wetland construction may reduce the amount of wetland loss from agricultural and urban development; however, future sea level rise will also impact freshwater tidal wetlands such as Julie J. Metz. Over the next century, a predicted sea level rise of one meter could destroy 26 - 82 % of U.S. coastal wetlands (Mitsch and Gosselink, 1993). Factors influencing coastal wetland loss from sea level rise include wetland accretion rates relative to sea level rise rates and local rates of subsidence. In the Mid-Atlantic region of the U.S., average coastal wetland accretion rates currently exceed the rates of sea level rise and changes in elevation (Titus and Anderson, 2009). Thus, in places where coastal wetlands can migrate landward and accrete sufficiently quickly, tidal wetlands may persist as sea levels rise. Unfortunately, many coastal areas consist of terrace flats that rise abruptly at steep escarpments formed by ancient shorelines. At those scarps, both saline and freshwater tidal wetlands may be "pinched-out" in the future due to both the direction of urban development from land and sea level rise from the

coast. The impact of shoreline-stabilizing barriers such as sea walls might also prevent the migration of coastal wetlands inland as sea level rises and ultimately drowns out tidal wetlands. Calculations using current sea level rise rates and wetland elevations can be used to determine the time period for inundation and wetland loss.

Site Description

Julie J. Metz was the first wetlands mitigation bank in Northern Virginia approved by the USACE. The freshwater tidal wetland is located at the street address 15875 Neabsco Road, Woodbridge, Virginia in Prince William County (Figure 1) and was WSSI's first wetland mitigation project. It is approximately 227 acres with seven pods bordering the tidally-influenced Neabsco Creek (Figure 2). The pods are constructed low-lying areas with raised earthen berms as boundaries. They were constructed in two phases during 1995 and 1997, respectively. The pods generated 19.1 mitigation credits and increased the wetland size from 208 acres to 227 acres (National Mitigation Bank Association, 2011). WSSI constructed Julie Metz by modifying the toe of alluvial fans located along the southern section of the wetland and capping the flattened area with a semi-impermeable clay layer. The alluvial fans were modified to increase the groundwater input to the wetland area.

WSSI monitored the water table fluctuations in the wetland over time by installing 22 piezometer well nests. Depth-to-water data collected from the piezometers were used to confirm the USACE regulations for the hydrogeologic component of the wetland had been met. Under the HGM wetland classification system (Brinson, 1993), Julie Metz is considered a slope and estuarine fringe wetland.

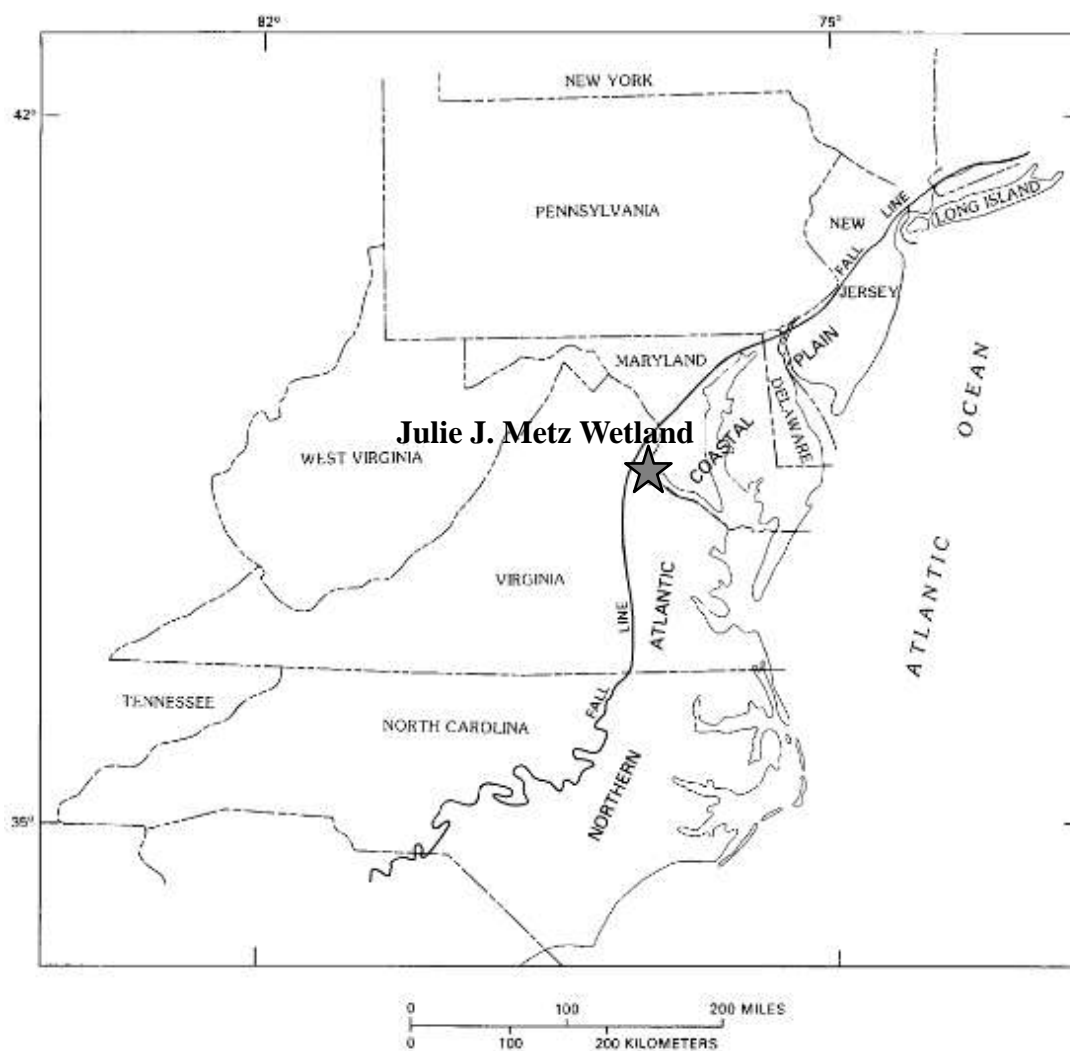


Figure 1. Map displaying the location of the Fall line and the Julie J. Metz wetland location (modified from Meng and Harsh, 1988).

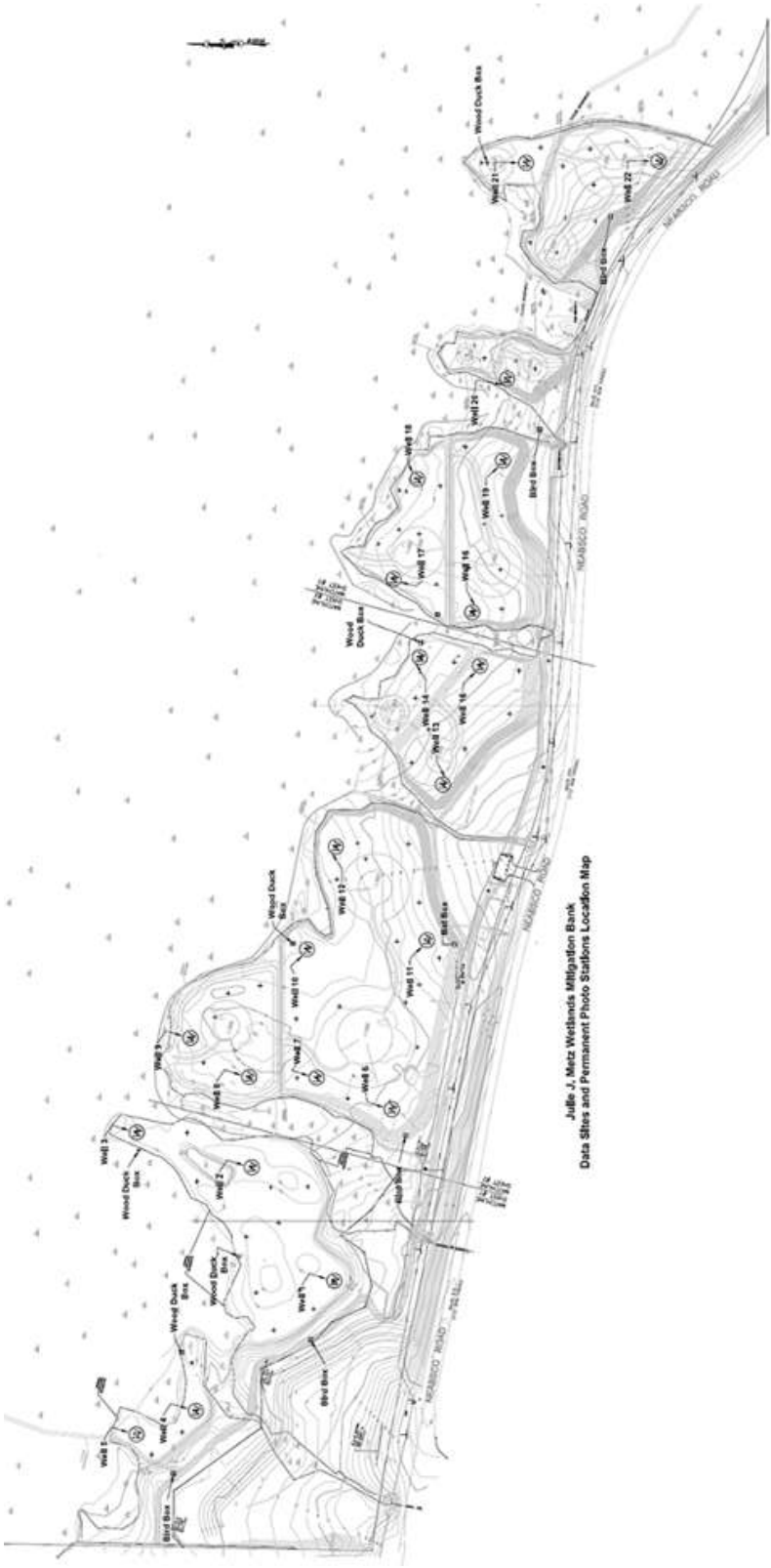


Figure 2. Wetland Studies and Solutions, Inc. (WSSI) well location map displaying the name and location of the piezometer clusters within the Julie J. Metz wetland.

Regional Geology and Hydrogeology

The Julie Metz wetland area is located along the northern fringe of the Virginia Coastal Plain near the Fall Zone separating the Piedmont and Coastal Plain regions (Figure 1). The geology of the Virginia Coastal Plain is mainly thick, unconsolidated sediments originating from several transgressions and regressions of the ocean and weathered material from the nearby Piedmont region (Whittecar et. al., 2016).

At Julie Metz, Neabsco Creek has deeply incised the Potomac Group (K_p), a thick package of medium to coarse Cretaceous sands. Quaternary-aged terraces (Q_{t4}) consisting of pebble and cobble-sized gravels with a sand matrix have filled in the incised creek valley. The terrace material also contains fragments of the Ordovician-aged, Quantico slate from the upstream areas of Neabsco Creek. The flood plains of Neabsco Creek are Quaternary-aged alluvium deposits (Q_{al}) (Figure 3) (Mixon et al., 1972).

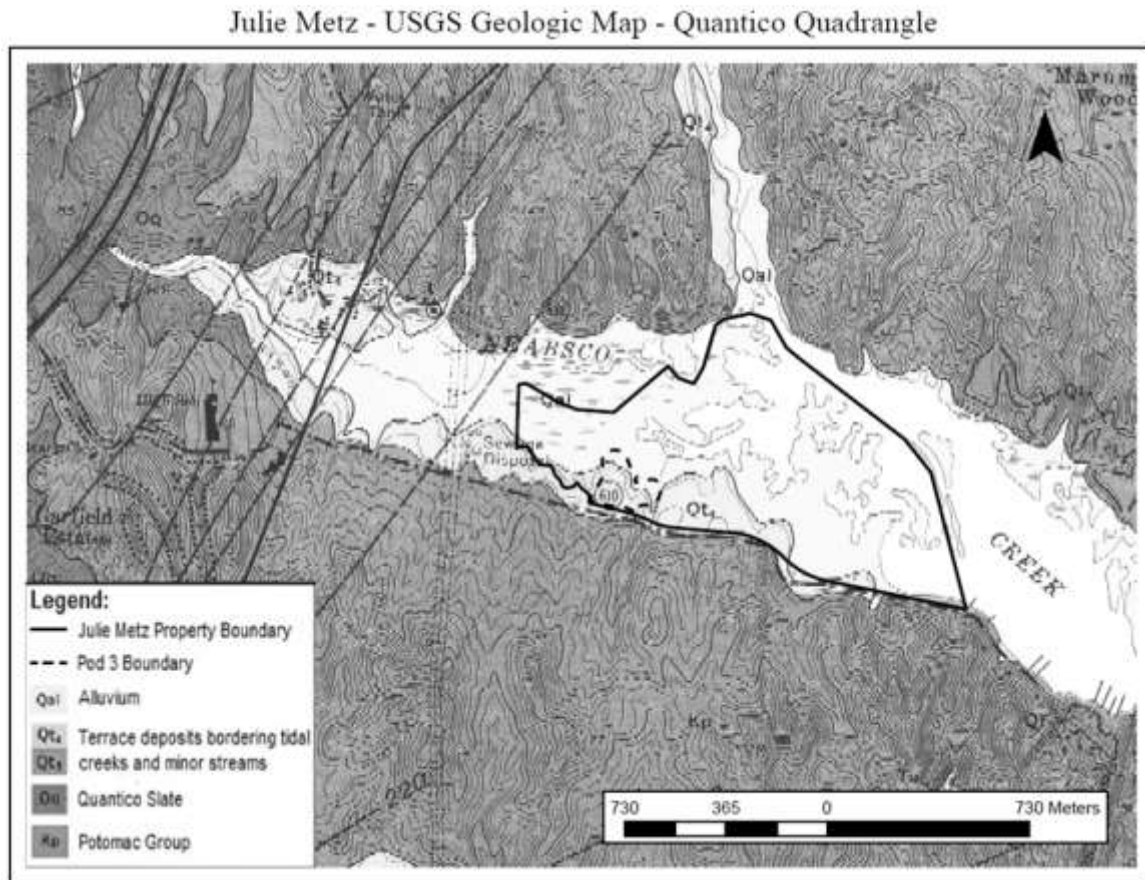


Figure 3. Modified USGS geologic map of the Quantico quadrangle display in the geologic formations, the Julie J. Metz property boundary, and the Pod 3 boundary (modified after Mixon et al., 1972).

Soils

There are three primary soil types at the Julie Metz wetland that are identified and described using the Soil Web (Web Soil Survey, 2016) in combination with Google Earth Pro (Figure 4). The upland areas are classified as Lunt loam soils (34B) with 2-7% slopes and comprise 9.6 acres (4.5%) of the wetland.

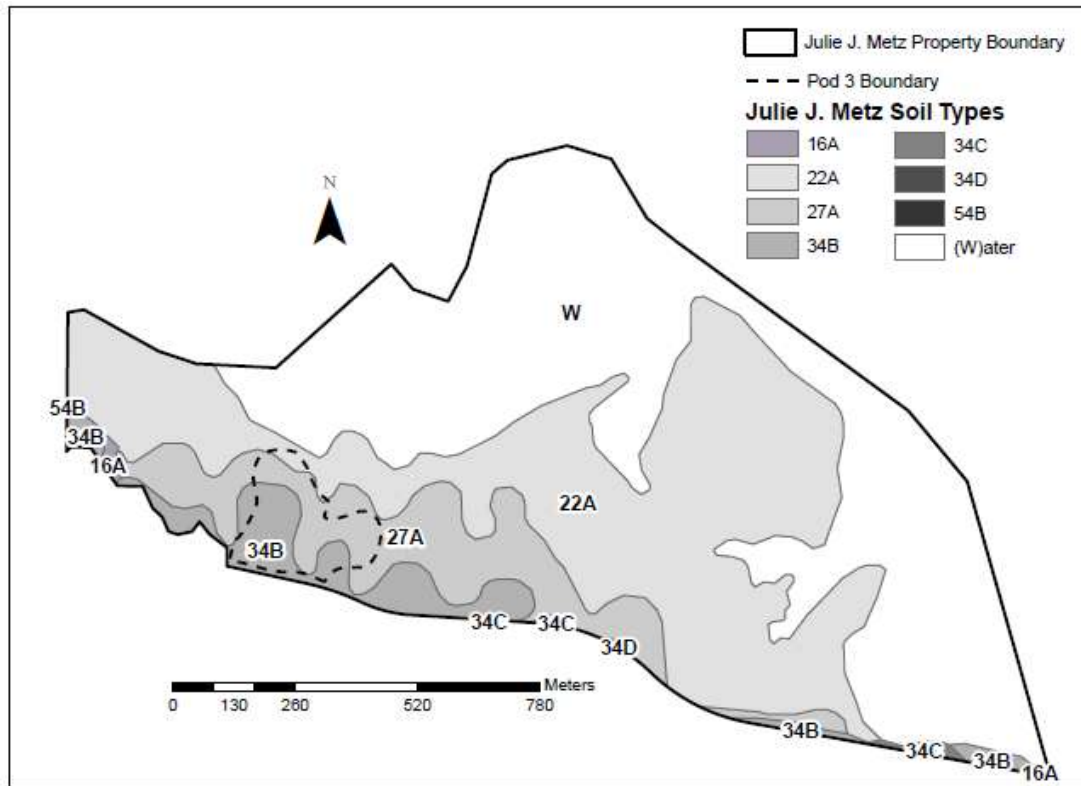


Figure 4. Arcmap image displaying the soil types within the Julie J Metz wetland.

Soil series boundaries obtained via Web Soil Survey (2016).

Old marine terrace deposits are the parent material for the Lunt loam soil. Lunt loam soils are described as Typic Hapludalfs with medium runoff and well drained soil characteristics. This soil is non-hydric and its hydrologic soil group is B. Hydric soils form in wet conditions where there is sufficient ponding to creating anaerobic soil conditions (NRCS, 2016).

Downgradient of the Lunt loam soil group are two hydric soil types located in flood plain settings: the Hatboro-Cordorus Complex (27A) and the Featherstone mucky silty loam (22A). The Hatboro-Cordorus Complex is 45% Hatboro and 35% Cordorus soils with 0-2% slopes that covers 22.5 acres (10.5%) of the Julie Metz wetland. The silty loam soil is classified as

Fluvaquentic Endoaquepts (Hatboro) and Fluvaquentic Dystrudepts (Cordorus). The Hatboro and Cordorus soils are derived from alluvium material with a B/D hydrologic soil group classification. The Hatboro soils are identified as poorly drained while Cordorus soils are labeled as moderately well drained. Both soils have low runoff characteristics.

The Featherstone mucky silty loam is located downgradient of the Hatboro-Cordorus Complex and is the main soil type at the Julie Metz, covering 79.1 acres (36.9%) of the wetland. This soil originates from marine deposits with 0-2% slopes, low runoff, and very poorly drained soil features. The Featherstone soil has a B/D hydrologic soil group classification.

Importance of Julie J. Metz Wetland

Julie Metz is a unique freshwater mitigated wetland with seven constructed pods. The earthen berm pod boundaries provide an ideal setting for generating a water budget in Wetbud to understand the wetland hydrology. For this study, Pod 3A and 3B will be analyzed (Figure 2). A water budget using Wetbud will be generated for the upper pod, 3B. Water input to Pod 3B comes as surface runoff from the upland alluvial fan, precipitation, and groundwater at the toe of the modified alluvial fan. The lower pod, 3A, is tidally influenced by the nearby Neabsco Creek. It is anticipated that the dominant hydraulic controls in Pod 3B will be groundwater while the dominant controls will be tidal forcings in the lower pod, 3A. Precipitation will also be a factor in affecting wetland hydrology throughout the wetland.

In addition to tidal forcings, Pod 3A will be affected by sea level rise. The rise in sea level at the tidal creek will change the hydrologic dynamics in the lower pod and eventually also affect the upper pod. Governing equation calculations and tidal component analysis will be used to evaluate the tidal influence on the wetland.

Hypothesis and Alternative Hypotheses

The hypothesis for this study is that groundwater will be the principal water source that controls water table variations across the highly permeable freshwater tidal wetland named Julie Metz. Alternative hypotheses are that precipitation or tidal forcings will be the principal water source that controls water table variations across the Julie Metz wetland.

Research Objectives

The following research objectives drove the collection of data needed to test the project hypotheses:

1. Generate a water budget analysis for a highly permeable freshwater tidal wetland using Wetbud. The beta-testing and development of both Basic and Advanced models in Wetbud to characterize the hydrogeology of the Julie Metz wetland will also provide a valuable test of the use, ability, and limits of this new software package.
2. Investigate potential future changes in the Julie Metz water budget caused by tidal variations, storm surges, and sea level rise. The Wetbud inputs and outputs will be manipulated to model the effects of tidal variations, storm surges, and sea level rise on the freshwater tidal wetland. GIS maps will be created to display various flooding scenarios caused by tidal variations, storm surges, and sea level rise.

Research Applications

Regulators can use the Wetbud freshwater tidal wetland template to delineate wetlands with similar characteristics, and mitigation wetland companies can use the template to build

freshwater tidal wetlands more efficiently. Additionally, the impact of varying sea level rise and flooding scenarios on coastal environments such as freshwater tidal wetlands can be shown.

CHAPTER II

METHODS

The Julie Metz site is unique because it is a sloping wetland located in a freshwater tidal setting. Several procedures were conducted to characterize the hydrostratigraphy and hydrology in one pod of the tidally-influenced, Julie Metz wetland and to develop a water budget using modeling software.

Site Selection and Historical Data Collection

Pod 3 was chosen for this research project because of its close proximity to the freshwater tidal creek and an earthen weir located at the northern edge of Pod 3. Following the Pod 3 selection, historical data were requested from the company that constructed the Julie Metz wetland, Wetland Studies and Solutions, Inc. (WSSI). These data included contour maps with the piezometer well cluster locations and elevations as well as historical depth-to-water readings at the piezometer locations within the wetland.

Hydrostratigraphic Analysis

Absent from the historical data was the site stratigraphy. At Julie Metz, the stratigraphy was determined by placing soil borings at selected locations using hand augers with three-inch diameter auger heads (Figure 5).

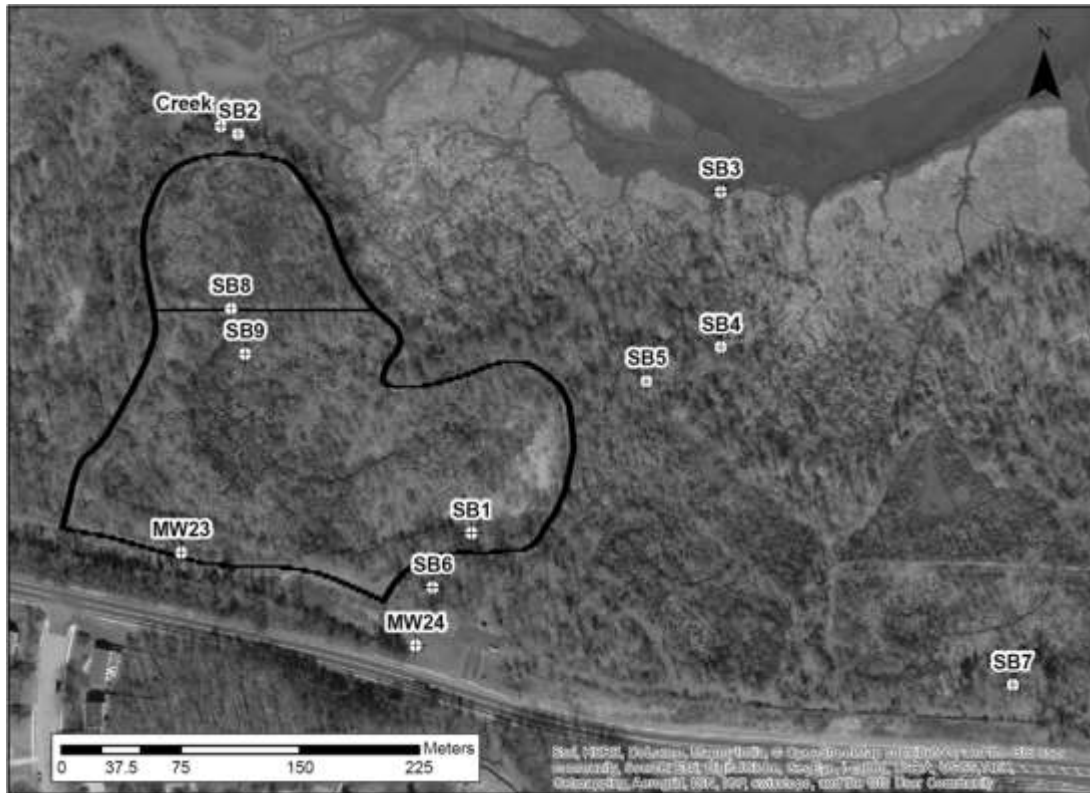


Figure 5. ArcGIS map showing the Julie Metz Pod 3 boundary with soil boring and monitoring well locations.

The soil boring locations were determined by analyzing soil maps, geologic maps, and topographic maps. Soil cuttings collected from soil borings SB1, SB2, and SB6 were placed in an open three-inch PVC pipe and described. A soil sample was collected between each of the determined soil profile breaks (Appendix A). The soil samples and profile descriptions were used to create soil boring logs and a geologic cross-section displaying the hydrostratigraphy and anticipated groundwater movement within Pod 3. The stratigraphic data obtained from the soil borings were explained in a geologic context by analyzing the USGS geologic map of the Quantico, Virginia quadrangle (1:24000) (Mixon et al., 1972).

Hydrologic Data Collection

Groundwater movement within Pod 3 of the Julie Metz wetland was determined with depth-to-water measurements obtained at monitoring wells and piezometer well clusters. Beginning in May 2014, depth-to-water measurements were collected from the existing, surveyed piezometer nests located in Pod 3. In August 2014, a Solinst Levellogger Edge M5/F15 was placed in piezometer MW9B to provide water level measurements from pressure and temperature data that were collected on an hourly interval. During the month of August, a monitoring well was installed in the nearby tidal Neabsco Creek with two of the six feet of well screen below the surface in Featherstone silt loam (22A). Refusal occurred during well installation at the depth of two feet, due to large cobbles and gravels. The Neabsco Creek monitoring well was surveyed using laser level equipment and the nearby MW9B as a known elevation point. A Solinst Levellogger Edge M5/F15 was placed in the monitoring well to provide water level measurements. The levelloggers, spaced 25 meters apart in MW9B and the Neabsco Creek well, provided information related to tidal forcings and storm events.

Groundwater and surface water input to Pod 3 of the Julie Metz wetland were evaluated by installing two upslope monitoring wells labeled MW23 and MW24 (Figure 5). Solinst levelloggers were installed at MW23 and MW24, in addition to placing levelloggers in piezometers located within Pod 3. In November 2014, colleagues at Virginia Tech mobilized a drill rig trailer to the Julie Metz wetland. The drill rig uses 6.25-inch ID and 8-inch OD hollow stem augers. Two upslope locations were selected based on drill rig access, and spatial distribution for groundwater data collection.

Hydraulic head values were calculated from well elevation points and the water level data collected from transducers located at MW9B, Neabsco Creek, MW23, and MW24. Solinst

leveloggers were placed in MW11B and MW7B to gather a better distribution of groundwater data and determine the amount of influence precipitation has on the wetland hydrology and water budget in Pod 3. Precipitation data were obtained from the nearest NOAA weather station to Julie Metz, located 7.5 miles southeast at the Quantico Marine Base (Quantico MCAF 724035). The hydrograph data were used to generate groundwater flow maps during several episodic events such as flood tides, ebb tides, storm events, and large precipitation events.

Within Pod 3, slug tests were used to calculate hydraulic conductivity. Three trials of falling slug tests were performed at the following piezometers in Pod 3: MW6B, MW7B, MW8B, MW9B, MW10B, MW11B, and MW12B. For each falling head slug test, a Solinst levelogger was placed in the piezometer approximately 2 - 3 inches above the bottom. The levelogger was set to one-second data collection intervals and allowed to stabilize in the piezometer well water for a minimum of two minutes. Next, approximately two gallons of Neabsco Creek water was added to the well and the levelogger recorded how quickly the water in the piezometer dropped. Depth-to-water measurements were periodically collected from the piezometers during each trial to estimate the rate of return to the initial water level. The slug test ended when 90% of the added water had dropped and the water level was within 10% of the initial depth-to-water measurement prior to the slug test. Slug tests at MW10B and MW11B were ended prior to the 10% recovery because of the slow recovery rates. After ending the slug tests, the levelogger data were analyzed using the Bouwer-Rice method to calculate the hydraulic conductivity. The Hvorslev method was not used because the piezometer well screens were not submerged below the water table (Fetter, 2001). The three trials at each piezometer were averaged to give the average hydraulic conductivity value (m/sec).

Three trials of falling head slug tests were also conducted at the upslope wells, MW23 and MW24. A Solinst levellogger was placed in the screened interval for the upslope wells and was set to one-second data collection intervals. Once in the well, the levellogger was given a minimum of two minutes to stabilize to the groundwater temperature and water level. Then, a one-inch diameter SCH 40 PVC pipe slug was lowered into the well to displace the water. The concrete-filled, PVC slug was 4.1 feet (1.25 meters) long and capped on both ends with a looped cable running through the slug to attach the rope. The levellogger recorded how quickly the displaced water in the upslope well dropped. The slug test ended when 90% of the added water had dropped and the water level was within 10% of the initial depth-to-water measurement prior to the slug test. When the slug was pulled from the upslope well, a rising head slug test was performed. The levellogger already in the upslope well for the falling head slug test was used to record the water level recovery rate when the slug was pulled from the upslope monitoring well. Three falling head and three rising head slug tests were performed at each upslope well. The Bouwer-Rice method as well as the Hvorslev method were used to calculate the hydraulic conductivity (m/sec) (Fetter, 2001). The well screens for the upslope wells were submerged below the water table, making the Hvorslev method applicable for hydraulic conductivity calculations. The calculated hydraulic conductivity values were used as a starting point for calibrating wetland water budget models.

Wetland Water Budget Modeling - Basic Scenario

A water budget is the net gain or loss of water from a natural system, such as a wetland, based on its water inputs (gains) and water outputs (losses). Wetland water budgets are important because they help to predict the hydrology of a wetland throughout a given year. A

wetland water budget can be broken into several components as illustrated by the following equation 1 from Pierce (1993):

$$P + SWI + GWI = ET + SWO + GWO + \Delta S \quad (1)$$

where the variables are precipitation (P), surface water inflow (SWI), groundwater inflow (GWI), evapotranspiration (ET), surface water outflow (SWO), groundwater outflow (GWO), and change in water storage (ΔS).

Wetland water budget software named Wetbud has been developed to generate water budgets in various wetland settings. The purpose of Wetbud is to generate a site-specific wetland water budget for a selected time period and typical Dry, Normal, and Wet years using WETs tables and the terms in the Pierce water budget equation (Pierce, 1993). WETs tables are a statistical summary of long-term precipitation data from National Weather Service (NWS) stations. The precipitation data is divided into values less than the 30%, values greater than 70%, and values greater than 30% and less than 70%. Using the WETs table for a specific location, the precipitation values less than 30% for a given year are considered a Dry year. Values greater than 70% are considered a Wet Year, and precipitation values falling between 30% and 70% for a given year are labeled a Normal year (Sprecher and Warne, 2000).

Wetbud has two versions, the Basic and Advanced Scenarios. The Basic Scenario generates modeled groundwater hydrographs on a monthly scale from weather station data, groundwater data, WETs tables, and site-specific characteristics such as a National Resources Conservation Service (NRCS) curve number and hydraulic conductivity. Basic Scenario data uses the United States imperial unit of measure while the Advanced Scenario uses the metric

system. The Advanced Scenario models groundwater hydrographs on a daily scale, has a time solver component, and uses cells to provide more realistic hydrologic site conditions, topography, and site dimensions. The methods described below are outlined in a manner that allows a Basic and Advanced Scenario to be constructed using Wetbud.

Basic Scenario Projects

A Julie Metz project was created in Wetbud (Dobbs et al., 2016) by entering the name of the project, the latitude (38.605601 decimal degrees), the longitude (-77.277559 decimal degrees), and the wetland bottom elevation (2.64 feet). The bottom wetland elevation was calculated by averaging the ground elevations at the piezometers within Pod 3 of the wetland.

NOAA Stations

Wetbud uses National Oceanic and Atmospheric Administration (NOAA) Global Summary of the Day (GSOD) stations in conjunction with NOAA Global Historical Climatology Network (GHCN) stations to generate solar, weather, and precipitation data for an area. The nearest NOAA GSOD station (Quantico MCAF 724035), approximately 7.5 miles southwest of the wetland, provided most of the data used in Wetbud to model the Julie Metz wetland. Dates with missing data for the Quantico station were patched using nearby GSOD stations. Values from Davison AAF (724037) and Washington Dulles (724030) were used to fill in missing weather and precipitation data. Solar data not directly imported using the Wetbud software were downloaded and imported from the National Solar Radiation Database (NSRB) 1991 - 2010 Update (http://rredc.nrel.gov/solar/old_data/nsrdb/1991-2010/hourly/list_by_state.html) or the Remote Automated Weather Stations (RAWS) USA Climate Archive (<http://www.raws.dri.edu/index.html>). Solar data are divided into two components in Wetbud: meteorological statistical global (METSTAT GLO) (Watt-hr/m^2) and extraterrestrial solar

radiation (ETR) (Watt-hr/m²). METSTAT GLO is a statistical global model that incorporates several parameters such as ozone, water vapor, cloud cover, and aerosols in calculating the solar data (Myers, 2002). RAWS stations record METSTAT GLO solar data. The RAWS data were downloaded and imported from the Cedarville, Maryland station (2010-2012) or from the Prince William, Virginia station (2013-2015) to patch the missing METSTAT GLO solar data at the Quantico MCAF station. Then, the METSTAT GLO solar data were converted from langley (ly) to Watt-hr/m² prior to the data import (1 ly = 11.63 Watt-hr/m²). ETR solar data were calculated using equations 2-5 from Maidment (1993):

$$d_r = 1 + 0.033 \cos\left(\frac{2\pi}{365} J\right) \quad (2)$$

where d_r is the relative distance between the Earth and Sun, and J is the Julian day number;

$$\delta = 0.4093 \sin\left(\frac{2\pi}{365} J - 1.405\right) \quad (3)$$

where δ is the solar inclination in radians;

$$\omega_s = \arccos(-\tan \phi \tan \delta) \quad (4)$$

where ω_s is the sunset hour angle in radians, and ϕ is the latitude of the site (positive for Northern Hemisphere, negative for Southern Hemisphere); and

$$S_o = 15.392 d_r (\omega_s \sin \phi \sin \delta + \cos \phi \cos \delta \sin \omega_s) \quad (5)$$

where S_0 is the ETR in mm/day. Calculated ETR solar data for Julie Metz were verified using an online ETR calculator (http://www.engr.scu.edu/~emaurer/tools/calc_solar.cgi.pl). Once verified, the ETR data were converted from mm/day to Watt-hr/m² (1 mm/day = 680.5555556 Watt-hr/m²). ETR and METSTAT GLO solar data for missing dates were combined in an Excel spreadsheet and imported to the Quantico station in Wetbud.

Parameters for ET

The Penman method was chosen to calculate evapotranspiration (ET) for the Julie Metz wetland. Latitude and longitude information for Julie Metz were input into the calculation of clear sky insolation index data from the NASA Surface meteorology and Solar Energy - Location website (<https://eosweb.larc.nasa.gov/cgi-bin/sse/grid.cgi?email=wctauber@aol.com>).

Insolation data were entered in Wetbud for the months where yearly solar data were available for the Quantico station, 1991-2015.

WND Years

Wet (W), Normal (N), and Dry (D) years are used in water budget modeling software, such as Wetbud, to evaluate the effects of precipitation, surface water, and groundwater at a site location for three years selected to represent a range of common climatic conditions. WND years for Julie Metz were calculated using the Wetbud software based on a procedure described in McLeod (2013). Here the calculations used the available precipitation data from Quantico (1991 - 2015) and the NRCS WETS station data from Caroline County, VA (VA2009).

Wetland Watershed Parameters

Several Julie Metz wetland and watershed parameters, such as the constructed wetland area, the watershed area contributing to surface runoff, and a Curve Number are needed to calculate surface water flows derived from adjacent slopes. For the Julie Metz Wetbud project,

the constructed wetland area refers to the Pod 3B area. The acreage for Pod 3B was calculated using the Add polygon tool in Google Earth Pro (7.57 acres). Google Earth Pro was also used to calculate the total area of watershed that influences direct surface runoff to Pod 3B at Julie Metz (60.00 acres). The drainage basin or watershed area influencing Pod 3B was delineated using GIS Arcmap, and was verified using topographic maps. The watershed area was measured using Google Earth Pro tools.

The NRCS developed a runoff Curve Number system with values ranging from 30 to 100. The Curve Number quantifies the amount of runoff potential of a watershed area based on the land cover type, the land treatment and hydrologic conditions, and the hydrologic soil group (Lim et al., 2006). As the Curve Number increases, the runoff potential increases. The NRCS method to calculate the Curve Number for the Julie Metz watershed area was performed using Google Earth Pro and the Web Soil Survey. The Web Soil Survey information, derived from NRCS soil maps and published on the Google Earth Pro platform, was used to determine the hydrologic soil groups. Aerial photography from Google Earth Pro was used to establish the land cover type and the hydrologic condition of the land within the watershed area. Using the watershed boundary, a grid was generated to calculate the area-weighted NRCS Curve Number. The NRCS Curve Number result was 70. A second method, using GIS Arcmap, was also used to calculate the NRCS Curve Number. A toolbox called HEC-GeoHMS was used by Arcmap. The toolbox was developed by the USGS, and informative instructions were generated by Venkatesh Merwade from the School of Civil Engineering at Purdue University (Merwade, 2012). Input layers needed to calculate the NRCS Curve Number from the HEC-GeoHMS toolbox included the digital elevation model (DEM), the soils type, and the USGS land cover grid. Following the

detailed instructions, a curve number similar to the NRCS curve number was obtained. The curve number result using Arcmap was 65.

Wetland Water Inputs

A wetland water budget model for Julie Metz has several inputs to the wetland that include the initial fill, precipitation, groundwater, surface runoff, and stream overbank flow. The initial fill depth, the level of water in the wetland when the model simulation begins, was set to zero inches for the Dry, Normal and Wet years. The precipitation data were obtained from the Quantico MCAF (724035) weather station. Groundwater input to the Julie Metz wetland was calculated by the Wetbud software.

The Wetbud software calculates effective monthly recharge (W_{em}) using a method that was developed by Whittecar and Lawrence in 1999 and later improved (Whittecar et al., 2017). Effective monthly recharge generates artificial antecedent groundwater hydrographs using known water levels in monitoring wells. The W_{em} requires at least six months of water level data from hillslope monitoring wells, the distance between the hillslope and toeslope, the ground surface elevation or the water elevation at the toeslope, and data from the nearest weather station. At Julie Metz, MW23 was used for the hillslope well; the horizontal distance between MW23 and the toeslope was calculated to be 100 ft using Google Earth Pro, and the ground elevation at the toeslope was also calculated from Google Earth Pro (0.69 meters). Additional wetland hillslope properties at Julie Metz Pod 3B were needed to use effective monthly recharge (W_{em}) to calculate the groundwater input to Pod 3B using Darcy's Law. Google Earth Pro was used to determine the width of the constructed wetland, Pod 3B, at the toeslope (700 feet), and the thickness of the constructed wetland from the hillslope to the toeslope (6.75 feet). The results from the slug tests at MW23 were used to determine the hydraulic conductivity of the hillslope

(8.06 inches/day). These wetland dimensions and the hydraulic conductivity were used in conjunction with MW23 water level data, toeslope ground elevations, the distance between MW23 and the toeslope, and the precipitation data to calculate the groundwater input to the Julie Metz wetland using Darcy's Law (Fetter, 2001) and the effective monthly recharge method.

Direct surface runoff for Julie Metz was calculated from the Wetbud software, using the watershed area and the calculated, average NRCS curve number (average CN = 68.5). The stream over bank flow for Julie Metz was determined by using the Wetbud software and Google Earth Pro via the TR-55 Method (USDA, 1986 & Pitt, 2005). Google Earth Pro was used in conjunction with topographic maps to determine sheet flow length (A to B) and slope, shallow concentrated flow (B to C) and slope, and open channel flow (C to D) and slope (Table 1). Sheet flow (A to B) is the shallow flow depth (<0.1ft) within the first 100ft of a stream in a watershed area. The shallow concentrated flow (B to C) starts after the sheet flow and can extend up to 1,400ft. The shallow concentrated flow (B to C) uses paved versus unpaved conditions, flow length, and slope to calculate the flow velocity. The shallow concentrated flow (B to C) transitions to open channel flow (C to D) after 1,400ft stream length. The open channel flow (C to D) extends up to 7,300ft and is distinguished by a clear, visible channel (USDA, 1986).

TABLE 1. CHANNEL FLOW DATA

Variable ID	Sheet Flow (A to B)	Shallow Concentrated Flow (B to C)	Open Channel Flow (C to D)
Manning's N	0.011	N/A	0.020
Flow Length (ft)	100	965	1436
Slope (ft/ft)	0.01	0.06	0.03
Channel Bottom Width (ft)	N/A	N/A	4
Channel Side Slope (z:1)	N/A	N/A	1
Channel Depth (ft)	N/A	N/A	2

Other open channel flow dimensions such as channel bottom width, channel side slope ratio, channel depth, the weir type (Cipoletti), and the various inflow structure elevations (Table 2) were determined from measurements and estimations made during site visits to Julie Metz.

TABLE 2. INFLOW STRUCTURE (CIPOLETTI WEIR) DATA

Description	Value (ft)
Weir Length	2.50
Elevation of Streambed at Inflow Structure	6.93
Elevation of Inflow Invert	7.18
Elevation (Top) of Wetland Berm	7.18
Wetland Bottom Elevation	2.64

Wetland Water Outputs

There are two contributors to water exiting the Julie Metz wetland, potential evapotranspiration (PET) and groundwater. PET, the major source of water loss, is defined as how much water is removed from an area via evaporation and plant transpiration if there is a sufficient amount of water (Dingman, 2015). Wetbud uses two methods used to measure PET—the Penman-Monteith and Thornthwaite methods (Allen, 2005 & Fetter, 2001). The Penman-Monteith inputs are solar radiation, air temperature, vapor content, and wind speed (Allen, 2005). The Thornthwaite method relies on weather data such as the daylight length and temperature (Lu et al., 2005). The Penman-Monteith method was chosen for calculating evapotranspiration for the Julie Metz wetland because the Penman-Monteith method calculates daily PET values while the Thornthwaite method calculates PET on a monthly scale (Allen, 2005). The PET was calculated using Penman-Monteith from the Wetbud software. The inputs needed to calculate

PET in Wetbud were the clear sky insolation index data for the Quantico MCAF station (724035) and the albedo (0.23).

The groundwater-out component for the Julie Metz water budget was calculated using Darcy's Law. The dimensions of Pod 3B, the hydraulic conductivity derived from slug tests, and the hydraulic gradient between MW11B and MW7B were used as inputs for Darcy's Law to produce a groundwater flow rate.

Other Site Parameters

There are three other site parameter values that are needed to execute the Julie Metz Basic Scenario in Wetbud: the soil storage factor, the surface storage factor, and the outlet weir depth. The soil storage factor relates to the specific yield for the uppermost soil zone that affects evapotranspiration. Soil storage factors range from zero to one, where low values equate to lower specific yields and higher values result in higher specific yields. Soils with high specific yields, such as the cobbles and gravels with a loamy soil matrix at Julie Metz, have values near 0.50 (Appendix B). As described in the Wetbud user manual (Dobbs et al., 2016), the surface storage factor is a percentage ranging from zero to five that quantifies the actual amount of ponded water not displaced by vegetation. The surface zone at Pod 3B in the Julie Metz wetland was estimated to have 2% of vegetation so a surface storage factor of 0.98 was used for the Basic Scenario model.

Model Calibration

Once the inputs were entered and the Julie Metz Basic model was run, the model results were compared with the groundwater hydrographs at monitoring wells MW11B and MW7B from 1 August 2015 to 27 January 2016. A sensitivity analysis was performed using Matlab to

calculate the Nash-Sutcliffe Efficiency (NSE) (Nash and Sutcliffe, 1970), the Root Mean Squared Error (RMSE), the R^2 value, the p-value, and the linear regression equation. A linear regression graph and an actual versus simulated hydrograph were also generated from the Matlab software. Adjustments were made to the NRCS Curve Number, the soil storage factor, and the surface storage factor in Wetbud until the NSE and R^2 values were closest to one, the RMSE value was at its minimal value during the sensitivity analysis, and the p-value was less than 0.05. Achieving these numerical conditions indicated the model results were representative of the actual water levels collected at MW11B and MW7B in the Julie Metz wetland.

Wetland Water Budget Modeling - Advanced Scenario

The wetland water budget model for the Wetbud Basic Scenario uses the Pierce model where there are various inputs and outputs in a depressional, bathtub-like setting (Pierce, 1993). Wetbud modifies the Pierce method by including groundwater as both an input and an output component to the water budget model. The Wetbud Advanced Scenario builds on the Basic Scenario by including several more parameters in the Wetbud model: time steps and solvers, model dimensions, cell zones, and grid zones.

Time Steps and Solvers

The Wetbud Advanced Scenario is a graphical user interface (Dobbs et al., 2016) for MODFLOW, a United States Geological Survey (USGS) finite difference groundwater model (Barlow and Harbaugh, 2006). The Advanced Scenario incorporates the precipitation rate, the evapotranspiration rate, and the runoff rate for a number of time steps selected by the user. For the Julie Metz water budget model, 181 time steps were used. The precipitation, evapotranspiration, and runoff data were imported for the time period from 1 August 2015 to 27

January 2016. For each time step, the hydraulic head values were converted to meters and the rates were displayed as seconds. Hydraulic head values were acquired from the levellogger data at MW23. The head values collected at the 2300 hour of each day were placed in the Head In column corresponding to that day. Surface runoff values were calculated using the NRCS Curve Number (69) derived from the Wetbud Basic Scenario model runs and the runoff area (60 acres). The first time step was meant to approximate steady-state conditions, and was used as a calibration period with a time step length of 31,540,000 seconds (one year). The Head In value for the first time step was calculated by averaging the head values at the 2300 hour from 1 August 2015 to 27 January 2016. Initially, the precipitation and evapotranspiration rates from 1 August 2015 to 27 January 2016 were averaged and placed in the first time step for the calibration period. However, the results showed evapotranspiration rates were greater than the precipitation rates. The precipitation and evapotranspiration rates were calculated and updated using the estimated annual precipitation and evapotranspiration 1971-2000 data from U.S. maps shown in Figure 2 and Figure 14 of Sanford and Selnick (2013). Afterwards, the precipitation rates were appropriately greater than the evapotranspiration rates. Average runoff rates were used from 1 August 2015 to 27 January 2016 for the first time step. Default values were used for the number of sub-steps (3) and the time step multiplier (1.2). The remaining 180 time steps were transient with a time length of 86,400 seconds (one day). Once the time steps were generated for Julie Metz, the solver was created. The default settings in Wetbud were used to create the Newton (NWT) Solver for the Julie Metz model. A site-specific name was the only entry needed to generate the NWT solver.

Cell Zones

There are several parameters within the Advanced Scenario that are used to establish cell water flow properties. In the Julie Metz Advanced Scenario, cell types called drains, general heads, monitoring points, no-flow areas, and wells were used.

Drain cell properties were created by entering the elevation head and the hydraulic conductance. Three drains were created for layers 1, 2, and 3 where groundwater is leaving Pod 3B. An image showing the drain location for layer 1 is shown in Appendix C. The drain location is the same for layers 2 and 3. The elevation head for each of the drains was determined from the imported bottom elevations of each layer. The hydraulic conductivity for each drain was estimated from multiple model run results (Table 3).

TABLE 3. DRAIN CELL DATA

Drain ID	Layer Bottom Elevation (m)	Drain Elevation Head (m)	Drain Hydraulic Conductivity (m/s)
Pod 3B Outlet1	2.86	2.87	0.01
Pod 3B Outlet2	2.70	2.71	0.01
Pod 3B Outlet3	2.09	2.10	0.005

Hydraulic conductance is expressed as m^2/s and its estimation is derived from width, length, hydraulic conductivity, and thickness. The width, length, and thickness were set to five meters, the cell dimensions used for the Julie Metz wetland. The drain cell for each layer was placed on the bermed path separating Pod 3B from Pod 3A, where the earthen weir is located.

General head cell properties were used to establish a head boundary at the upslope area near MW23 for the Julie Metz model. A Wetbud cell zone layout image with the general head

locations and conductance value is shown in Appendix D. The general head cells required conductance values and general head values. General head conductance values for Julie Metz were calculated in the same way as the drain cell properties. The width, length, and thickness were set to five meters, the cell dimensions used for the Julie Metz wetland. The hydraulic conductivity (K_{sat}) value for the upslope general head ($4.00E-5 \text{ m}^2/\text{s}$) was calculated from the slug tests conducted at nearby MW23. The MW23 slug test results from each trial, using the Hvorslev and Bower-Rice methods, were averaged. General head values were pulled from the Head In column of the time step array to generate daily, variable head values from 1 August 2015 to 27 January 2016 for the general head cells.

Once the drain and general head cell properties were established, monitoring points were created to show groundwater movement through Pod 3B. Monitoring point cells were designated for each of the piezometer nests located within Pod 3B: MW6B, MW7B, MW10B, MW11B, MW12B, and MW23 (Appendix E). The monitoring point cells provided necessary groundwater hydrographs of water level fluctuations at the piezometer locations. Values from MW23, MW11B, and MW7B were needed for model calibration.

No-flow cell properties are needed to create the shape of the site to be modeled. The inactive cell property (no-flow cell, $IBOUND = 0$) was selected for the no-flow cells in the Julie Metz model (Appendix F). The no-flow cells were placed on the grid setup of the Julie Metz model to create a boundary that represents the raised berm and boundary of Pod 3B at the Julie Metz wetland.

A runoff well was created in Wetbud to represent the surface runoff entering Pod 3B near MW11B. The well used the runoff rate values located in the runoff rate column of the time step array to generate surface runoff values from 1 August 2015 to 27 January 2016. In the Advanced

Grid Setup, the runoff well was placed in the vegetation layer (layer 1), 10 meters southwest of MW11B (Appendix G).

Grid Zones

Grid zones are created in Wetbud to designate cells with specific parameters related to hydraulic conductivity (Ksat), specific yield, the precipitation rate, and the evapotranspiration rate. The hydraulic conductivity and specific yield values are associated with the various soil types. For the Julie Metz model, the hydraulic conductivity values were generated from the slug test results or from estimated values for common types of sediments (Appendix B).

Eight grid zone properties were generated for hydraulic conductivity using the sediment or material type as the description (Table 4).

TABLE 4. GRID ZONE PROPERTIES

Grid Zone ID	Hydraulic Conductivity (m/s)	Specific Yield / Storage
Forested Vegetation	4E-04	1
Shrub Vegetation	2.3E-03	1
Lunt Loam	2.55E-05	0.1
Clay	6E-06	5E-04
Clay Loam	1E-06	0.025
Gravel-Cobble-1	5E-04	0.08
Gravel-Cobble-2	5.7E-05	0.08
Gravel-Cobble-3	1E-03	0.08

The vegetation Ksat values were obtained from Dr. Tess Thompson at Virginia Tech (T. Thompson, personal communication, October 15, 2015). Lunt Loam and gravels-cobbles Ksat values were acquired from slug tests at MW23 and MW7B, respectively. The hydraulic

conductivity values for the remaining soil types were estimated from the table in Appendix B. The Wetbud hydraulic conductivity grid zone layout for each layer is shown in Appendix H.

Eight grid zone properties were also generated for specific yield, using the sediment or material type as the description (Table 4). The same values were entered for specific yield and storage in the Julie Metz model. The specific storage values were estimated from the table in Appendix B. The specific yield grid zone layout in Wetbud for each layer is shown in Appendix I. Specific yield and hydraulic conductivity values were adjusted after each iteration until model calibration was achieved. Wetbud does not allow empty grid cells. Therefore, a no-flow grid zone property was generated with arbitrary hydraulic conductivity and specific yield values (Table 4).

Precipitation and evapotranspiration rates for the cell properties in the first layer of the Julie Metz model were called from the precipitation and evapotranspiration rates in the time step array from 1 August 2015 - 27 January 2016. The evapotranspiration zone for the cells in the Julie Metz model used a constant evapotranspiration surface for all time steps. Additionally, the ET extinction depth was held constant for all time steps.

Advanced Grid Setup

The grid setup in the Advanced Scenario allows the user to accurately place cell and grid zones in locations that depict the site location. Appendices C - I display the cell and grid zones for each layer in the Julie Metz model.

Advanced Scenario Setup

In the Advanced Scenario project setup, there are several inputs needed to construct the model grid. The setup needs the number of layers, the layer parameters, the number of columns and rows, and the dimensions of each cell. For the Julie Metz model, four layers were generated

with 58 rows and 54 columns to represent Pod 3B. The dimension of each cell was determined by the column width (5 m) and the row width (15 m). Meters was selected as the length units and seconds was selected for the time units in the Advanced Scenario project setup.

The Grid Setup Wizard and GIS Arcmap were used to generate an accurate, topographic grid setup for the Julie Metz Advanced Scenario model. In Wetbud, the box indicating flat layers was unchecked. A USGS digital elevation model (DEM) file was downloaded from GeoCommunity (www.geocomm.com) and added to Arcmap. The DEM map extent was set to meters with the following boundary values: (Top) 2105180, (Bottom) 2104910, (Left) 3606264, and (Right) 3606554. The DEM file was adjusted to a five meter pixel grid size. Afterwards, the raster file was modified using the Fishnet, Raster to Vector, Vector to Raster, Raster to Points, Merge, Rotate, Shift, and Raster to Ascii tools. After merging the fishnet and elevation points, there were several outlier cells with abnormal elevations. The outlier cells were corrected by taking the average of the surrounding cells and using the value as the updated cell elevation (Figure 6).

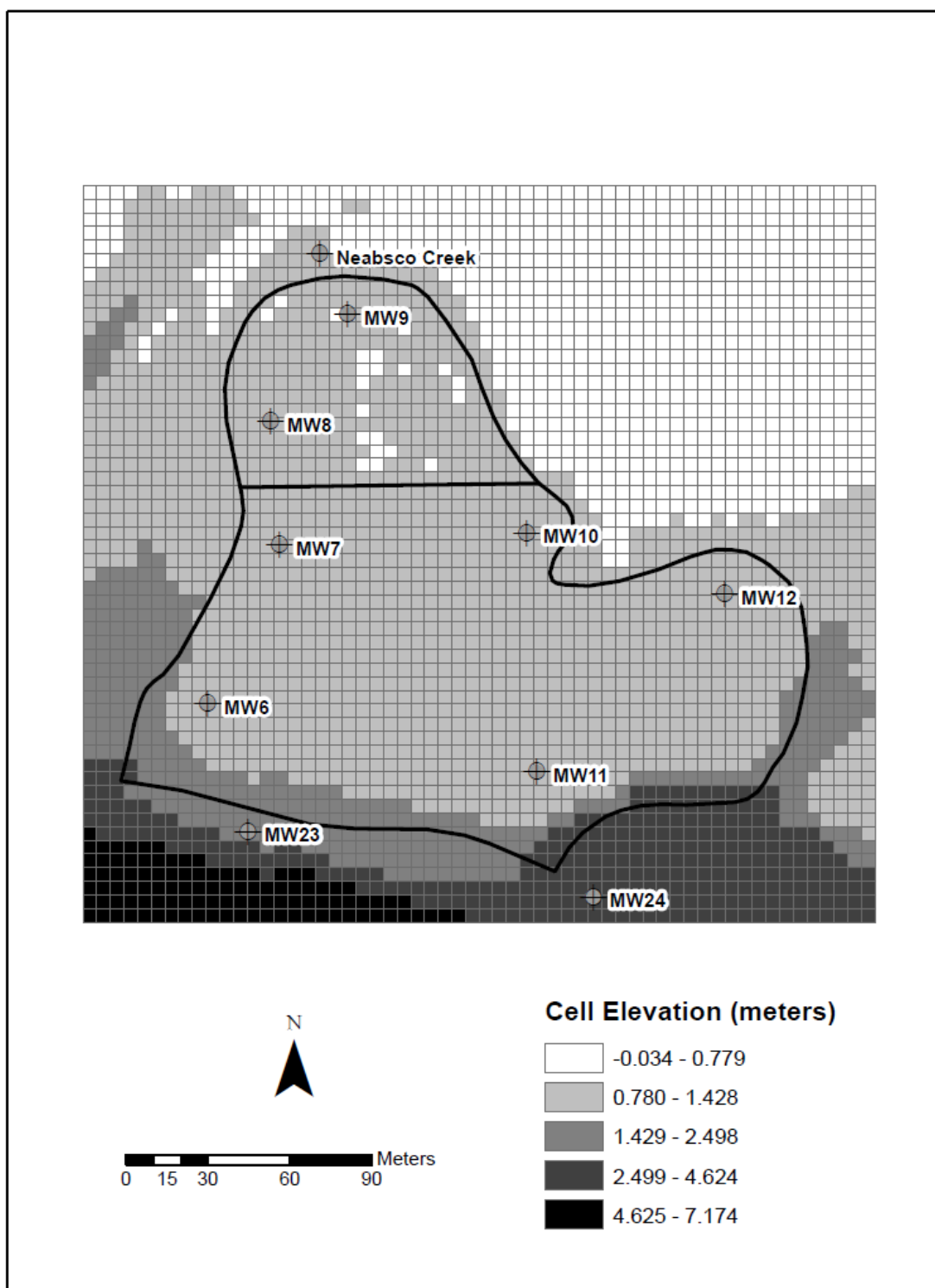


Figure 6. Julie Metz Pod 3 Arcmap DEM cell elevations used to create the topography in the Wetbud Advanced Scenario.

Once the elevation file in Arcmap was saved as an Ascii file, the Ascii file was imported in the Julie Metz Advanced Scenario. Then, the elevation file in Wetbud was exported as an Excel file and two meters were added to all elevation values. The two meters were added to ensure all elevation values would remain positive for each layer in the Julie Metz Advanced Scenario. With the elevations adjusted, the values were re-imported into Wetbud.

There were several layer attributes that were required for the Julie Metz model. The layer description, the top and bottom elevations for each layer, the initial head, the layer type, the layer condition, the vertical conductivity, and the horizontal anisotropy were entered. The initial head was set at 3.10 m and the ET extinction depth at 3.00 m. The layer condition was variable for all layers. Additionally, the vertical conductivity was set to Value and the horizontal anisotropy was set to an isotropic condition for all layers. The ground surface was set to the bottom elevation values from layer 1. The remaining layer attributes are shown in Table 5.

TABLE 5. JULIE METZ ADVANCED SCENARIO LAYER ATTRIBUTES

Layer ID	Layer Description	Top Elevation (m)	Bottom Elevation (m)	Layer Type
Layer 1	Surface Vegetation	10.174	1.966	Unconfined (Lyr 1)
Layer 2	Soil	9.174	1.814	Unconfined (Lyr 1)
Layer 3	Clay	9.022	1.204	Unconfined (T varies)
Layer 4	Gravel	8.412	0.290	Unconfined (T varies)

Model Calibration

Similar to the Basic Scenario calibration, the Advanced model results were compared with the groundwater hydrographs at monitoring wells MW23, MW11B, and MW7B from 1

August 2015 to 27 January 2016. Again, a sensitivity analysis was performed using Matlab to calculate the Nash-Sutcliffe Efficiency (NSE) (Nash and Sutcliffe, 1970), the Root Mean Squared Error (RMSE), the R^2 value, the p-value, and the linear regression equation. A linear regression graph and an actual versus simulated hydrograph were also generated from the Matlab software. Hydraulic conductivity (Ksat) and specific yield values were adjusted in Wetbud until the NSE and R^2 values were closest to one, the RMSE value was at its minimal value during the sensitivity analysis, and the p-value was less than 0.05. Achieving these numerical conditions indicated the model results were representative of the actual water levels collected at MW23, MW11B, MW7B in the Julie Metz wetland.

Tidal Analysis

The tidal influence on Pod 3 at the Julie Metz wetland was assessed in several ways. First, the distance of measurable tidal influence inland from the tidal creek was calculated. Then, the T_Tide Matlab function was used to quantify the primary contributors to the tidal forcings at Neabsco Creek. Finally, Neabsco Creek and regional hydrograph data were compared to wind speed and direction during the same time period.

A one-dimensional equation (Jacob, 1950 & Fetter, 2001), shown below as equation 6, was used to quantify the distance inland from Neabsco Creek to a negligible tidal influence within Pod 3A of the Julie Metz wetland:

$$H_x = H_o e^{\left(-x \sqrt{\frac{\pi S}{t_o T}}\right)} \quad (6)$$

where H_x is the amplitude of the tidal fluctuation (0.02 m), H_o is the amplitude of the tidal change (0.3048 m), x is the distance inland from the coast, S is the aquifer storativity (0.02), t_o is

the tidal period (21600 s), and T is the aquifer transmissivity (6E-3 m/s). For unconfined aquifers, such as the aquifer at Julie Metz, the storativity equals the specific yield (S_y). The aquifer transmissivity is solved using the equation 7 (Fetter, 2001):

$$T = b \cdot K \quad (7)$$

where b (6 m) is the thickness and K is the hydraulic conductivity (1E-3 m/s). The site-specific values for Julie Metz parameters are provided in parenthesis.

The tidal forcing in Neabsco Creek can be influenced by the gravitational effects from the Sun and Moon, as well as the wind and regional watershed flow to the creek. The `T_Tide` Matlab function was used to separate the tidal signal into its various components (Pawlowicz et al., 2002). Then, the Matlab function separated the lunar and solar components from the remaining components that are influenced by wind and regional watershed flow. The results from the separation were quantified as percentages. Additionally, the solar and lunar components were used to determine the tidal signal type at Neabsco Creek (diurnal, semidiurnal, or mixed) using the Form Factor shown as equation 8 (Xiong & Berger, 2010):

$$F = \frac{(K_1 + O_1)}{(M_2 + S_2)} \quad (8)$$

where F is the Form Factor, K_1 is lunisolar diurnal component, O_1 is the principal lunar diurnal component, M_2 is the principal lunar semidiurnal component, and S_2 is the principal solar semidiurnal component. Form factor values less than 0.25 are considered semidiurnal while values greater than 3.0 are considered diurnal. Form factor values between 0.25 and 1.5 are

called mixed tides, mostly semidiurnal while values between 1.5 and 3.0 are called mixed tides, mostly diurnal (Aungsakul et al., 2011). The Form Factor value at Neabsco Creek was used to verify the tidal signal type shown in the Neabsco well hydrograph.

Wind speed and direction data from the Washington, D.C. station were compared to several hydrographs to support the percentage results from the T_Tide Matlab function. A combined hydrograph displayed the Neabsco Creek tidal signal, the MW9B groundwater hydrograph, and the Washington, D.C. tidal signal from 1 October 2014 to 8 October 2014 (Figure 7). A graph displayed the wind data during the same time period.

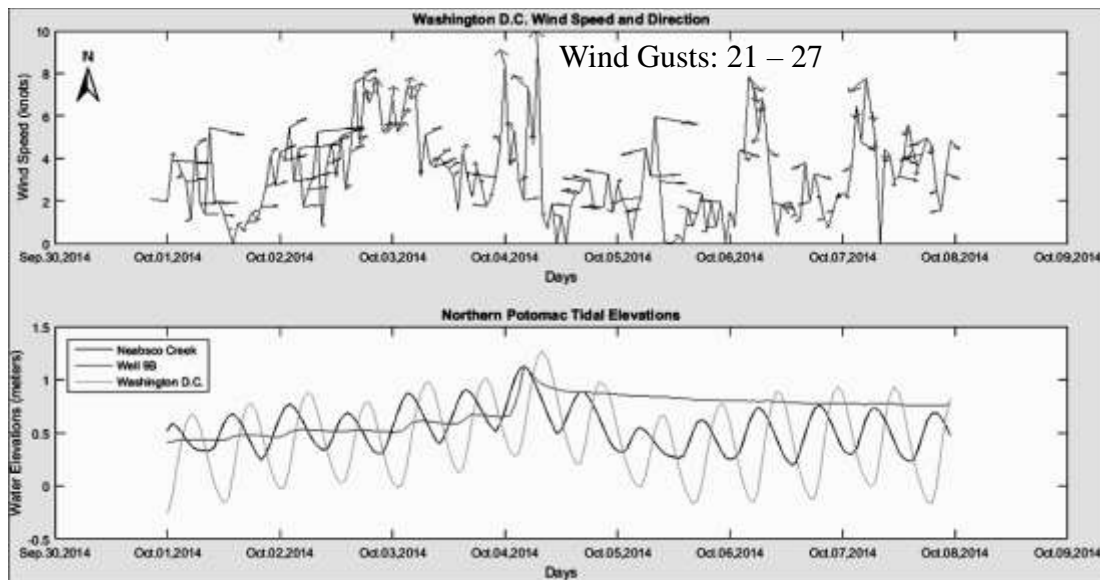


Figure 7. Matlab graphs showing northern Potomac wind speed and direction, tidal elevations, and groundwater elevations from 1 - 8 October 2014.

Sea Level Rise Effects

The effects of sea level rise on Pod 3 within the Julie Metz wetland were investigated by constructing a cross-sectional profile of the pod with various water elevations. The cross-sectional profile of Pod 3A and 3B, with a vertical exaggeration of 24, was generated using ground elevations from the monitoring wells and piezometer nests as well as Google Earth Pro to determine the distances between the ground elevation points. Then, the mean low water level (MLW), the mean high water level (MHW), the local mean sea level, and the peak storm surge level were determined from the hydrograph at the Neabsco Creek well for year 2014 - 2015. These levels were added to the cross-sectional profile to display the current tidal trends at Neabsco Creek for 2014 - 2015. Anticipated water level changes for Pod 3 were added to the cross-sectional profile where the local mean sea level was at the highest elevation point in Pod 3B, causing inundation and wetland loss. The time period for this occurrence at Pod 3B was calculated using the current sea level rise rate at the Washington, D.C. station, 4.14 mm/yr (Ezer and Atkinson, 2015).

CHAPTER III

RESULTS

Hydrostratigraphic Profile

The hydrostratigraphy of an area controls the rate and direction of groundwater flow. At the Julie Metz wetland, eleven boreholes were completed in and around Pod 3 (Figure 6) to generate the hydrostratigraphy of the area. Three of the boreholes were used to install upland monitoring wells MW23 and MW24 and a monitoring well in the tidal creek (Appendix A). The twelve boreholes had a silty or sandy clay unit overlying quartz cobbles and gravels with slate fragments (Appendix A). The depths of the boreholes varied from one foot (SB6) to 23 feet (MW24). A cross-sectional profile displaying the hydrostratigraphy of Pod 3 was constructed using MW24, SB1, SB2, and SB6 (Figure 8).

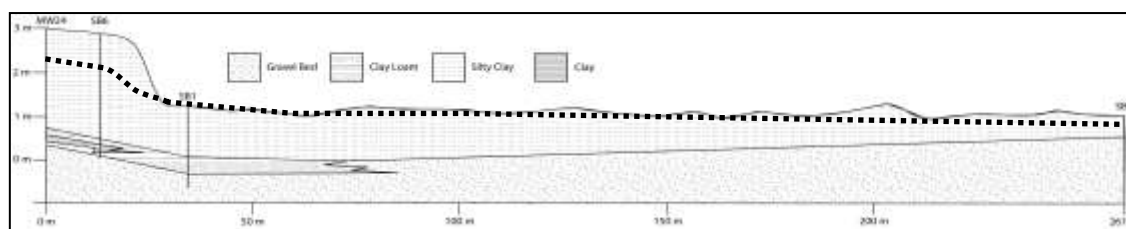


Figure 8. Hydrostratigraphic cross-sectional profile of Pod 3 at Julie Metz.

The hydrostratigraphic cross-sectional profile displays a massive poorly-sorted cobble and gravel unit with slate fragments that is underlying a silty and sandy clay unit. The cobble and gravel unit with the overlying silty and sandy clay unit is the common stratigraphic profile found throughout Pod 3. A thin clay layer located in the upland area pinches down-gradient towards

the creek. The dotted black line on the cross-sectional profile shows the average water table based on topography and depth-to-water measurements from monitoring wells and piezometers.

Hydrologic Data

Hydrologic data were gathered to generate groundwater hydrographs, groundwater flow maps, and determine the hydraulic conductivity. The hydraulic conductivity results are shown in Table 6.

TABLE 6. POD 3 HYDRAULIC CONDUCTIVITY (K_{sat}) VALUES

Well ID	Avg. K_{sat} after 3 trials (ft/s)	Avg. K_{sat} after 3 trials (m/s)
MW6B	8.7E-05	2.7E-05
MW7B	3.5E-04	1.1E-04
MW8B	5.2E-05	4.3E-05
MW9B	1.0E-04	3.1E-05
MW10B	1.7E-05	5.2E-06
MW11B	8.2E-06	2.5E-06
MW12B	1.0E-03	3.1E-04
MW23	2.9E-04	6.4E-05
MW24	5.8E-05	1.8E-05
Cumulative Average	2.2E-04	6.7E-05
Standard Deviation	3.2E-04	9.6E-05

Hydraulic conductivity values range from 3.1E-04 m/s at MW12B to 2.5E-06 m/s at MW11B with a cumulative average of 6.7E-05 m/s and a standard deviation of 9.6E-05 m/s. The hydraulic conductivity values are lower than expected from the cobble and gravel unit because the layer is poorly-sorted, indicating that the void space in the cobble and gravel layer is filled with a loamy soil matrix, thus lowering the hydraulic conductivity.

Pressure transducer data were collected from MW23, MW11B, MW7B, MW9B, and the Neabsco Creek monitoring well. The data are presented as groundwater hydrographs adjoined with the Quantico MCAF (724035) daily precipitation data (Figures 9 - 11).

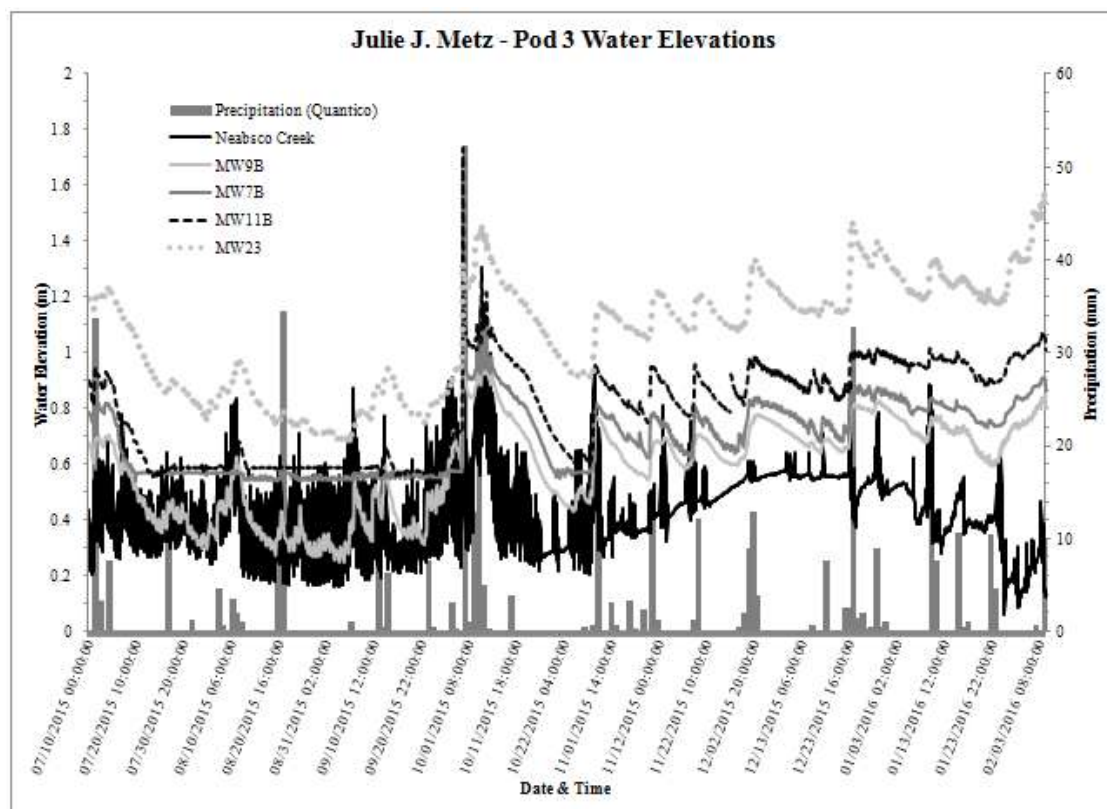


Figure 9. Julie J. Metz Pod 3 Hydrograph with Quantico MCAF Station Precipitation from 10 July 2015 to 4 February 2016.

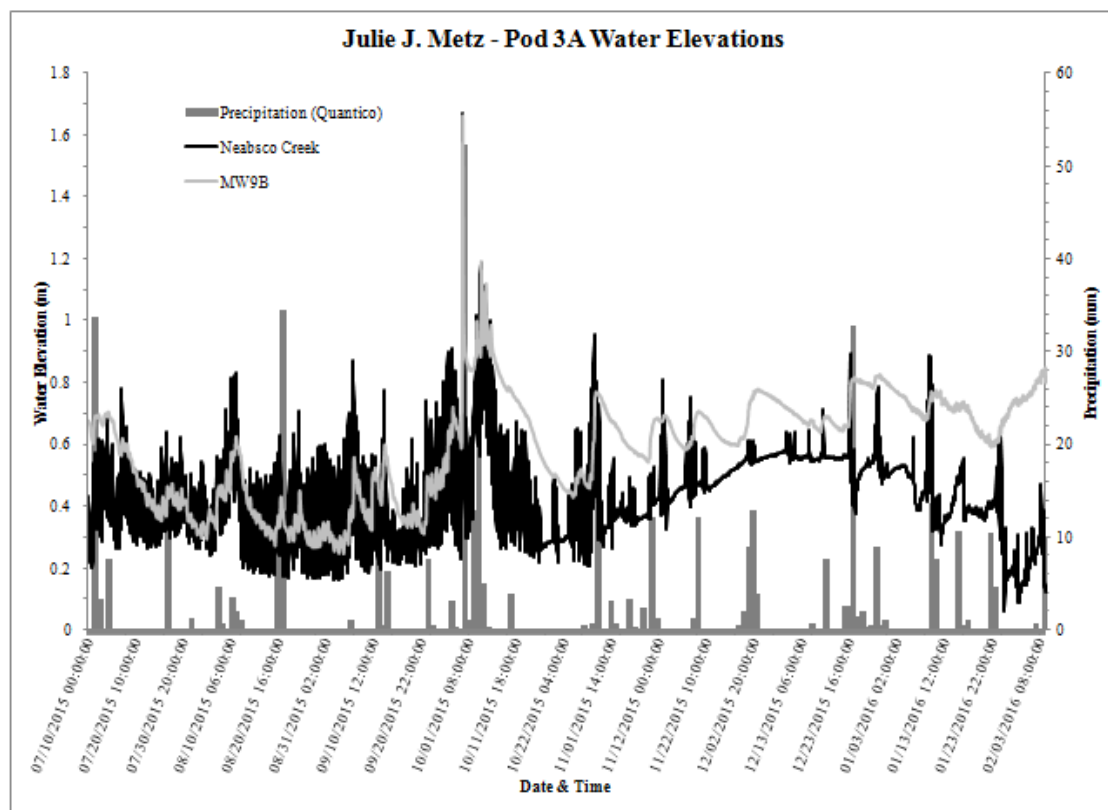


Figure 10. Julie J. Metz Pod 3A Hydrograph with Quantico MCAF Station Precipitation from 10 July 2015 to 4 February 2016.

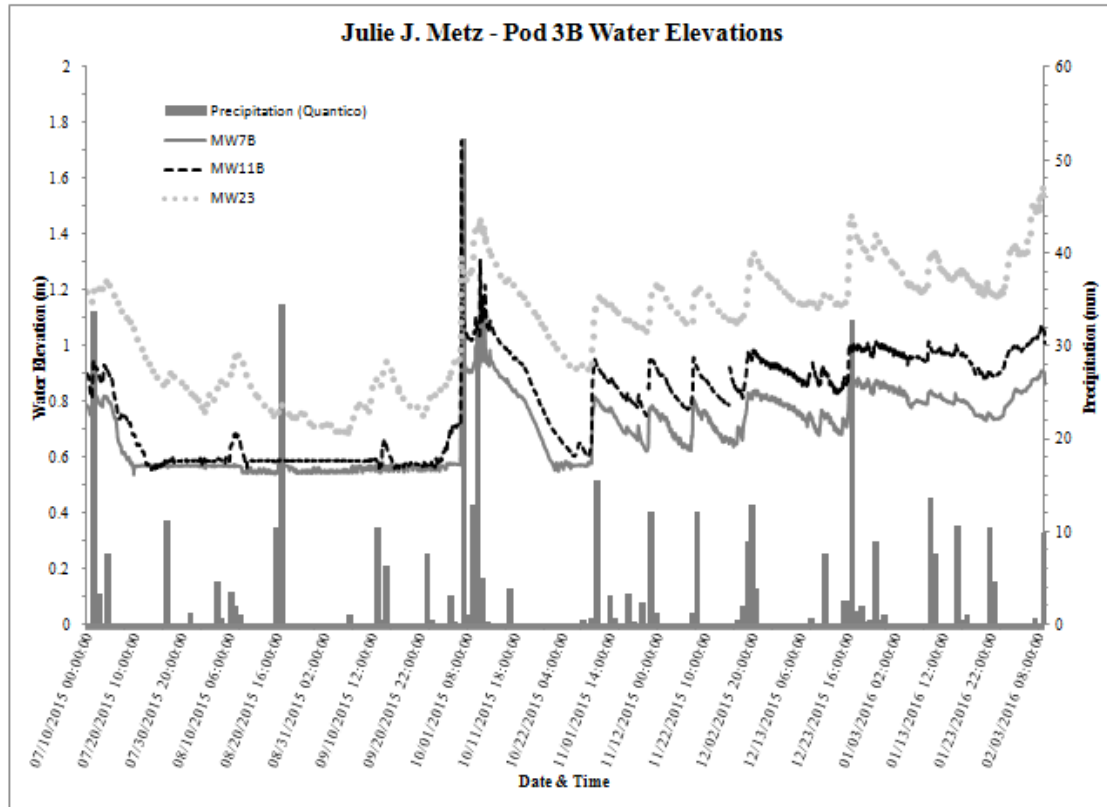


Figure 11. Julie J. Metz Pod 3B Hydrograph with Quantico MCAF Station Precipitation from 10 July 2015 to 4 February 2016.

The Pod 3B hydrograph shows groundwater base flow with flashiness episodes during precipitation events and regional watershed surface runoff to Pod 3B. Surface water influence to Pod 3B is shown in Figure 11 during the 1 October 2015 precipitation event where the hydraulic head at the toeslope well (MW11B) had a higher elevation than the hillslope well (MW23). The toeslope well is located approximately 15 m from a corrugated drainage pipe used to direct surface runoff from the residential upland area south of Neabsco Road to Pod 3B. Surface runoff entered Pod 3B from the corrugated pipe near MW11B and raised the water table at a greater rate than the surface runoff that infiltrated the hillslope area and raised the water table at MW23.

Precipitation events and groundwater input also influenced the groundwater hydrographs at MW7B located near the boundary of Pod 3A and 3B (Figure 11). The base flow of the hydrograph indicates continual groundwater input and the flashiness during precipitation events demonstrates the influence of rainfall on the hydrology at the central area of Pod 3.

At the Neabsco Creek well and MW9B located 25 m inland, the groundwater hydrographs display influence from precipitation events, tidal forcings, and continual groundwater output (Figures 9 and 10). There is flashiness in the hydrograph during precipitation events, but the overwhelming attribute influencing the hydrographs is the tidal forcing. The tidal forcing displays a semidiurnal signal that is shown in hydraulic head data from MW9B as well as the Neabsco Creek well. The semidiurnal signal has a tidal range of approximately 1.5 ft in Neabsco Creek and 1 ft at MW9B with a one hour lag in the tidal signal at MW9B. The Pod 3A hydrograph base flow indicates continual groundwater flow output.

Hydraulic heads measurements that were used to generate groundwater hydrographs were also integrated with the remaining wells and piezometers to generate groundwater flow maps. Hydraulic heads values were taken from MW6B, MW7B, MW8B, MW9B, MW10B, MW11B, MW12B, MW23, MW24, and the Neabsco Creek well. The values were used to generate groundwater flow maps for Pod 3 during an ebb tide, flood tide, following a precipitation event, and after a storm event (Figures 12 - 15).

Julie J. Metz Pod 3 Groundwater Flow Map during
Precipitation Event at Mid Tide – 9 November 2015

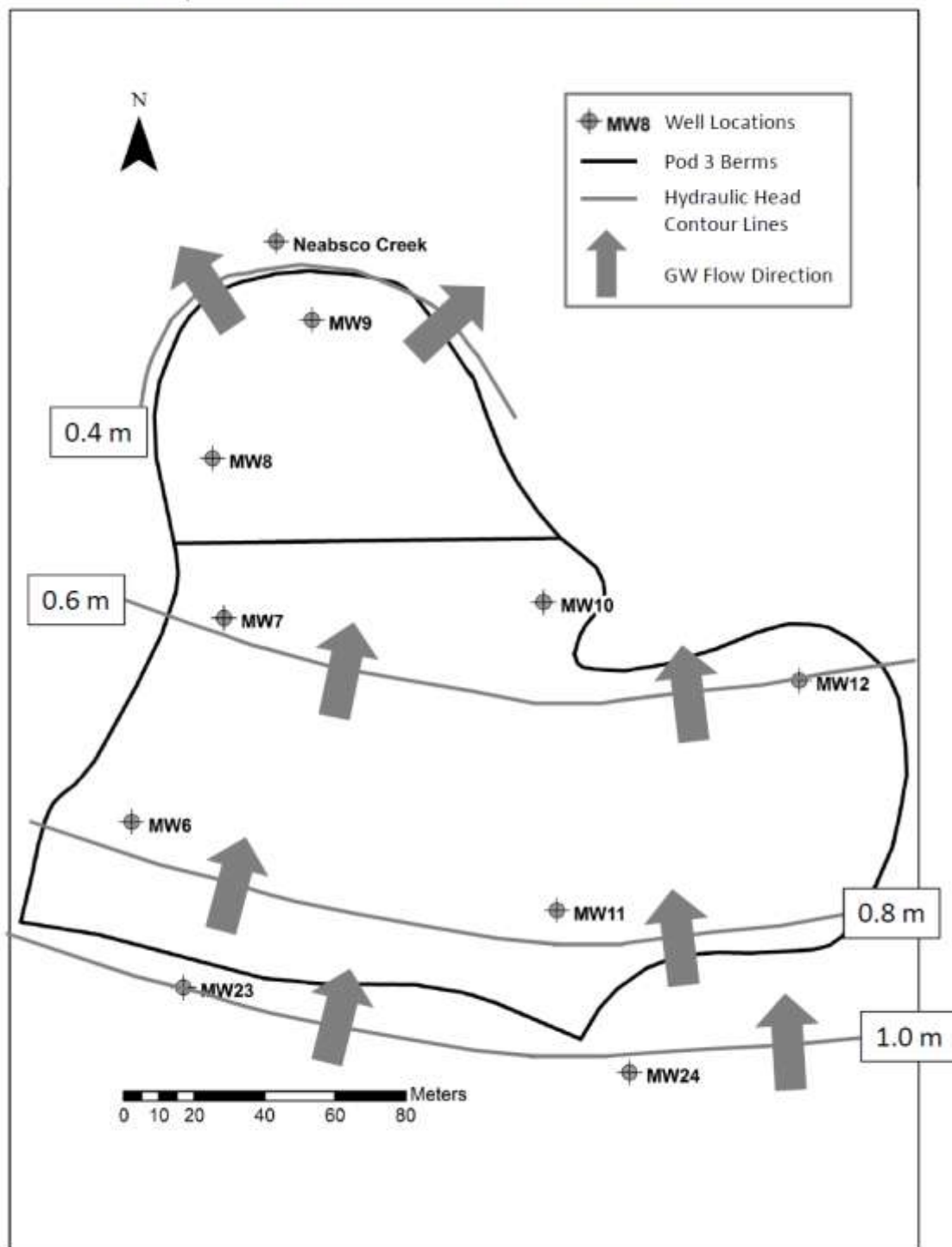


Figure 12. Pod 3 groundwater flow map showing hydraulic head contour lines and flow direction during a precipitation event on 9 November 2015.

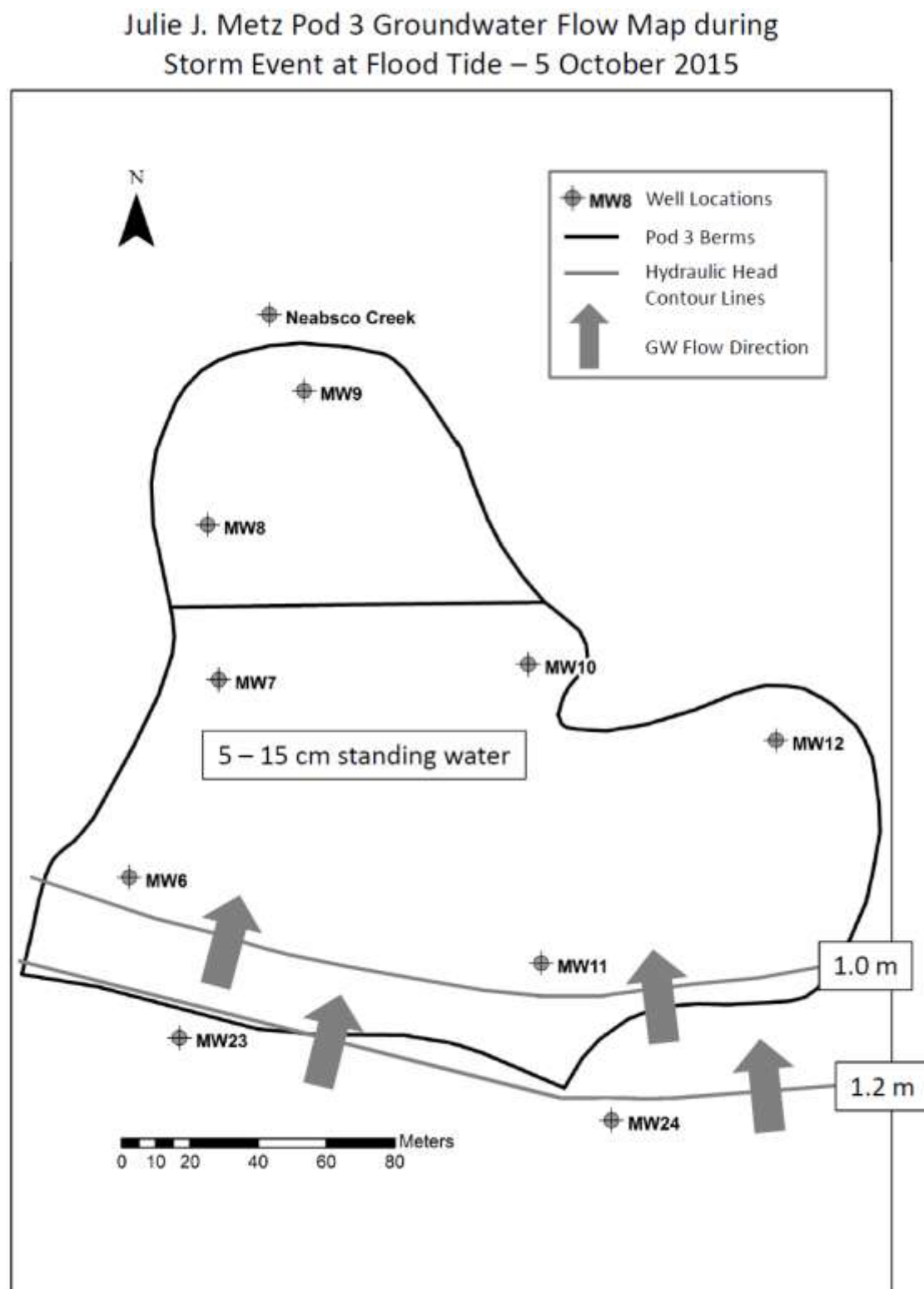


Figure 13. Pod 3 groundwater flow map showing hydraulic head contour lines and flow direction during a storm event on 5 October 2015.

Julie J. Metz Pod 3 Groundwater Flow Map during Flood Tide – 1 July 2015

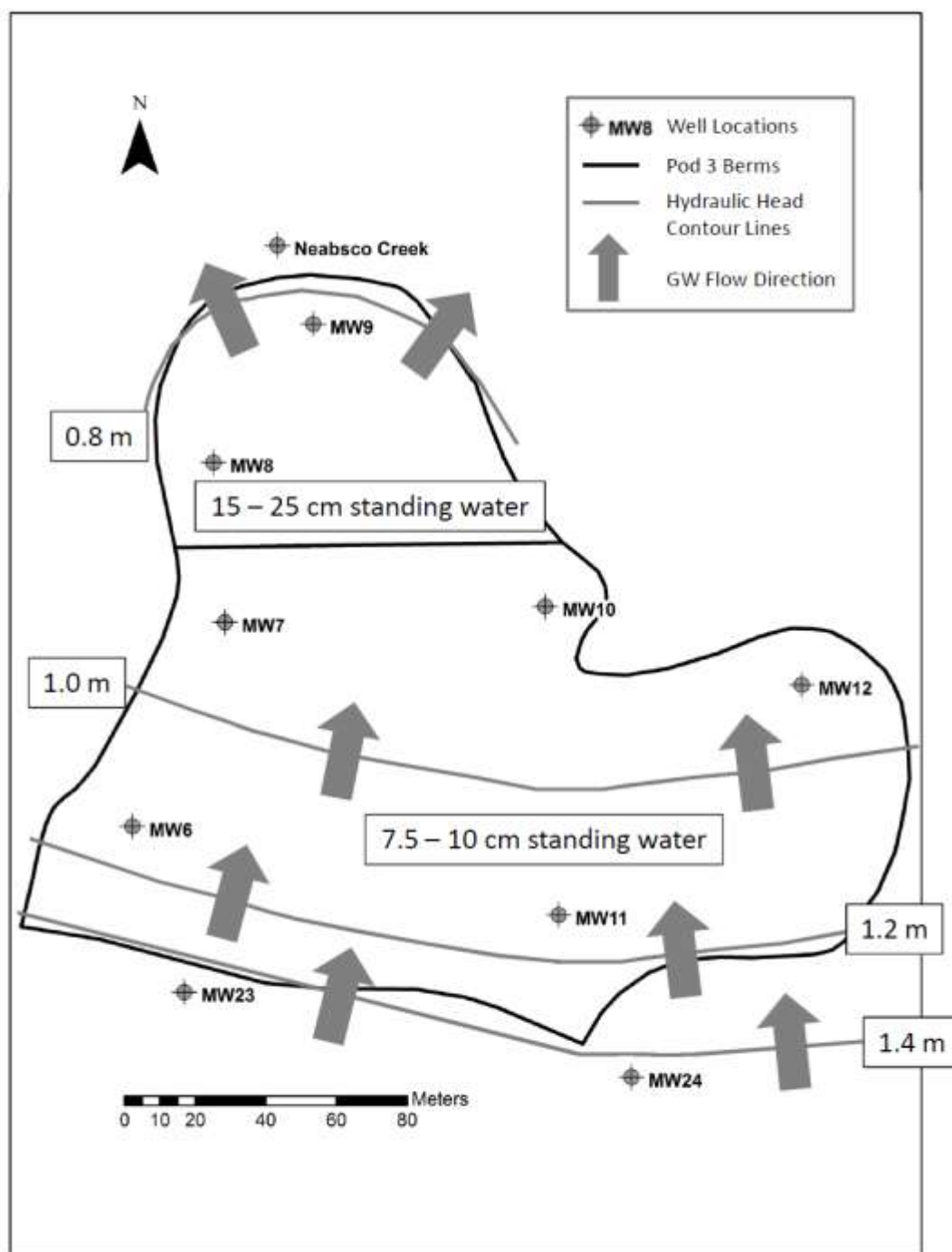


Figure 14. Pod 3 groundwater flow map showing hydraulic head contour lines and flow direction during a flood tide on 1 July 2015.

Julie J. Metz Pod 3 Groundwater Flow Map during Ebb Tide – 1 July 2015

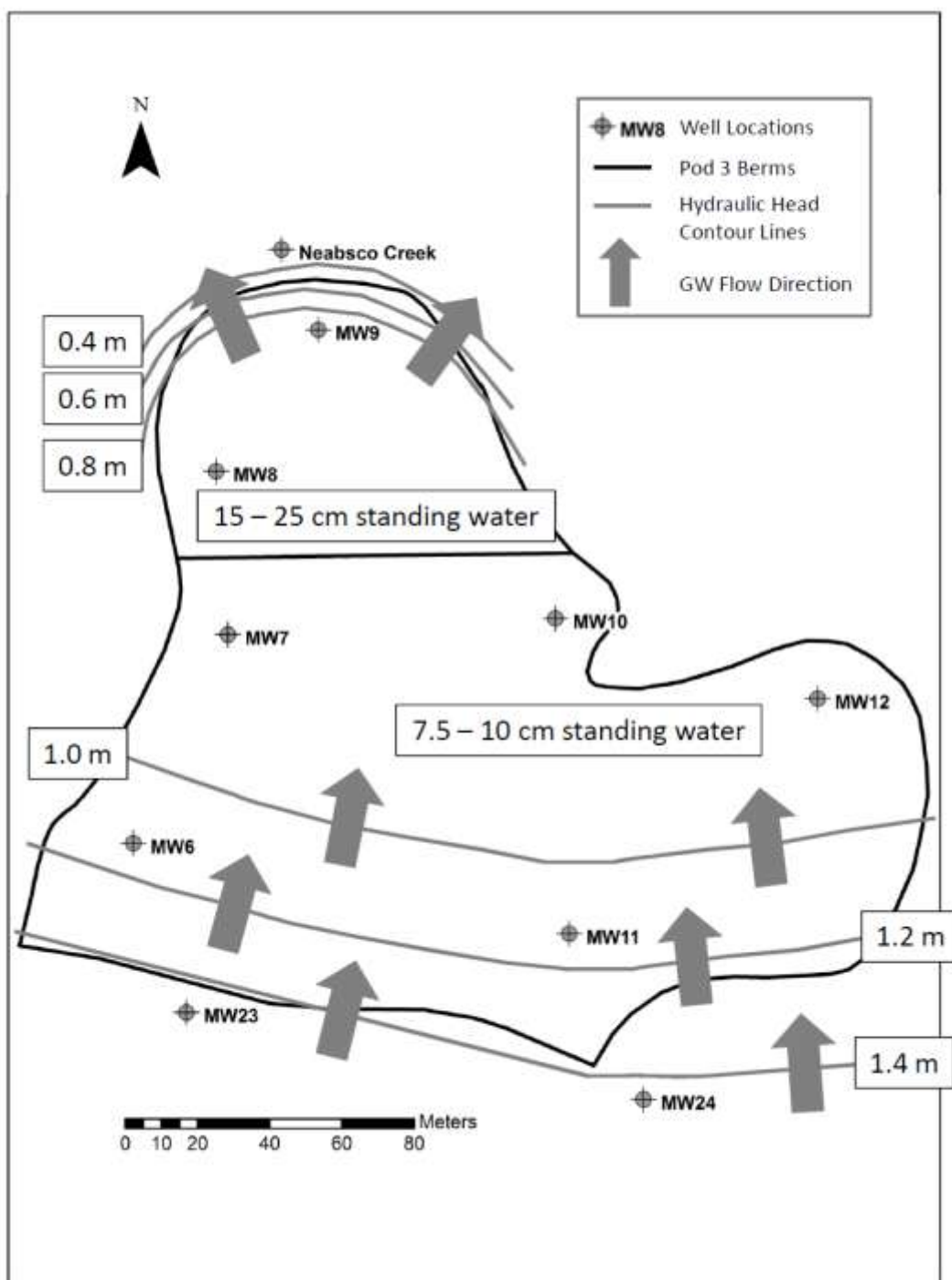


Figure 15. Pod 3 groundwater flow map showing hydraulic head contour lines and flow direction during an ebb tide on 1 July 2015.

All flow maps display a northern flow pattern from the hillslope region to the creek. After the precipitation event and storm surge occurrence, the groundwater flow pattern maintains a northerly direction towards the creek. However, in Pod 3A, the flow is greatly reduced because the gradient has decreased with significant inundation in Pods 3A and 3B.

The groundwater gradient is also controlled by the tidal forcing. During the flood tide, the water table in the creek is higher and close to the water table in Pod 3A. Therefore, the groundwater gradient is minimal and the groundwater flow exiting the pod is reduced. The groundwater flow increases as the creek approaches peak ebb tide because the groundwater gradient is much greater between the creek and Pod 3A. The gradient and groundwater flow exiting Pod 3A oscillates as the semidiurnal tide rises and falls. The groundwater flow maps and the Pod 3A hydrograph illustrate the strong tidal forcing influence on Pod 3A and the lack of influence on Pod 3B. The Pod 3B groundwater hydrograph shows groundwater and surface water influence at Pod 3B due to the sloping landscape position and precipitation.

Wetland Water Budget Modeling - Basic Scenario

The Wetbud Basic Scenario analysis used weather data from the Quantico MCAF (724035) station to calculate evapotranspiration (ET) rates for a typical Dry (2002), Normal (1994), and Wet (1993) years at the Julie Metz wetland. ET rates were also produced for the user-defined custom period from August 2015 to January 2016 (Figures 16 - 19).

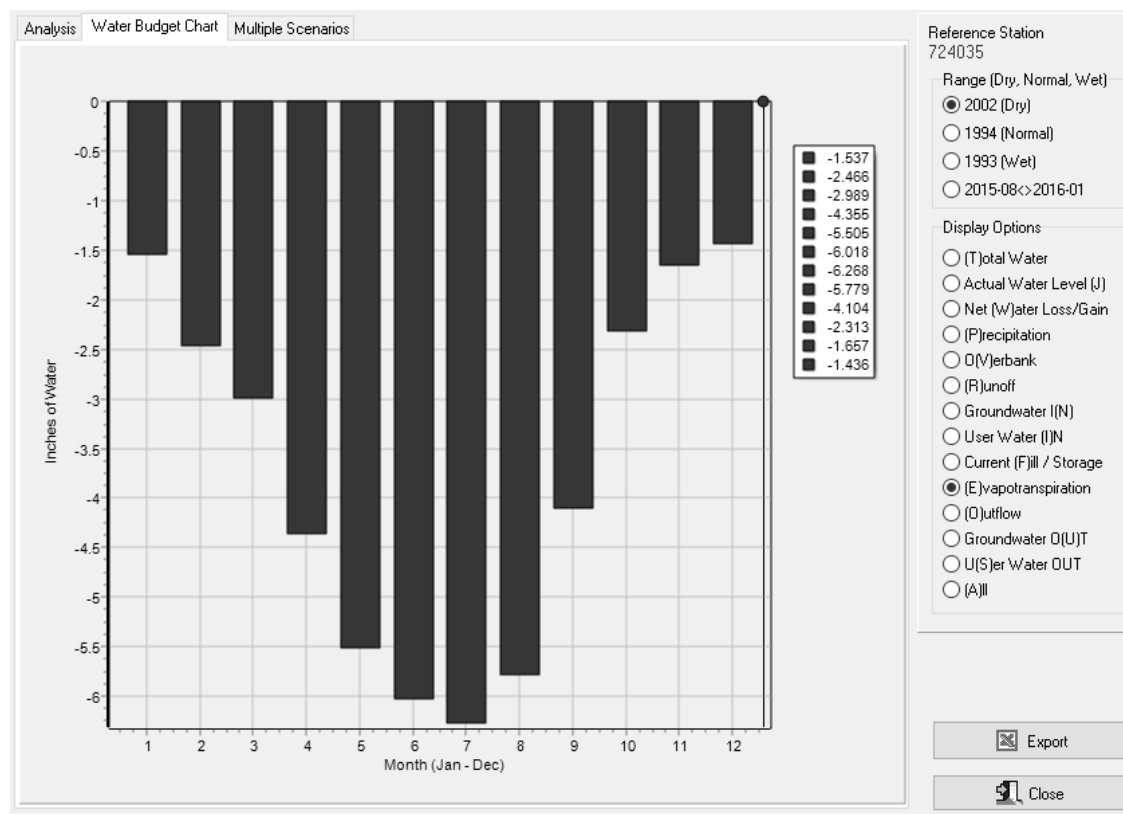


Figure 16. Wetbud evapotranspiration results for the typical Dry year (2002) at Julie Metz.

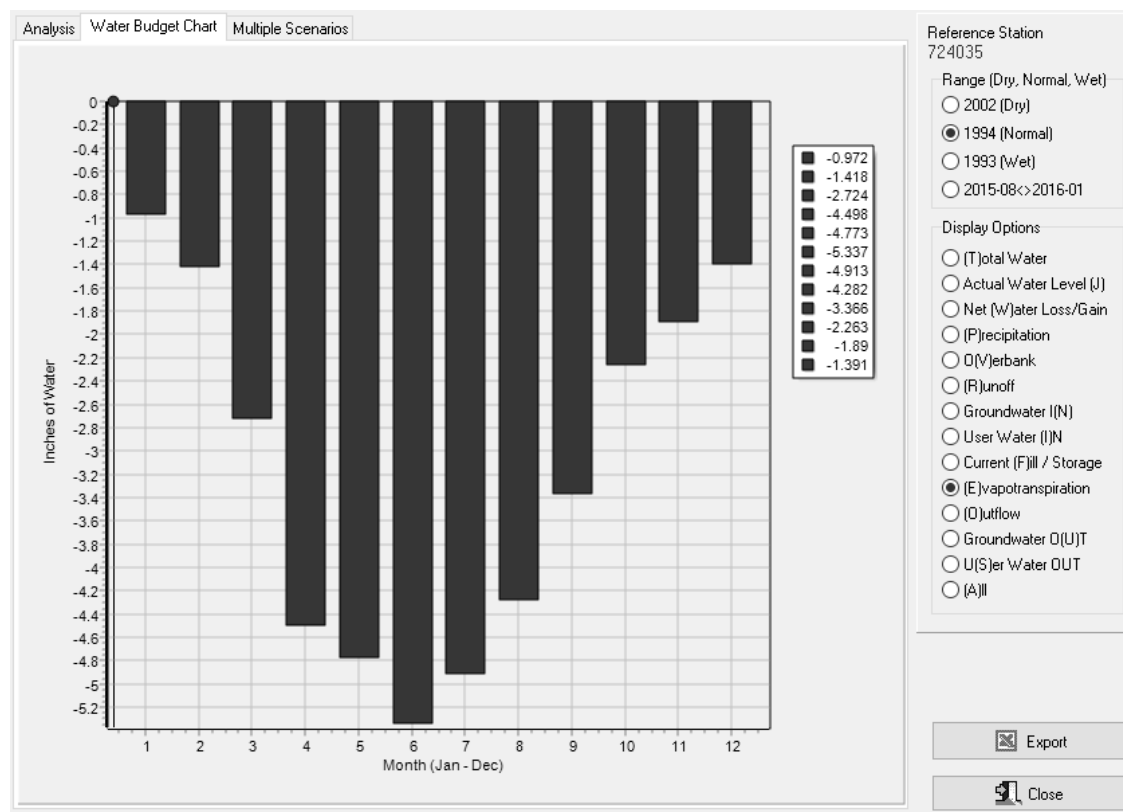


Figure 17. Wetbud evapotranspiration results for the typical Normal year (1994) at Julie Metz.

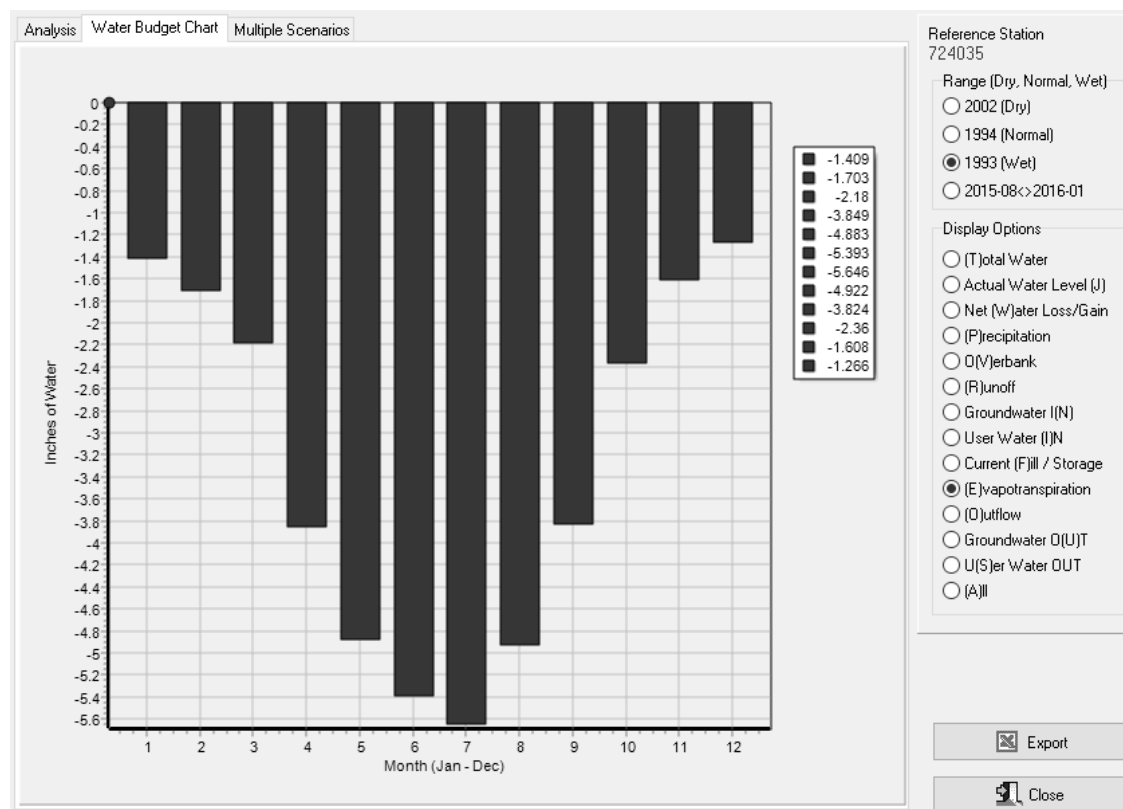


Figure 18. Wetbud evapotranspiration results for the typical Wet year (1993) at Julie Metz.

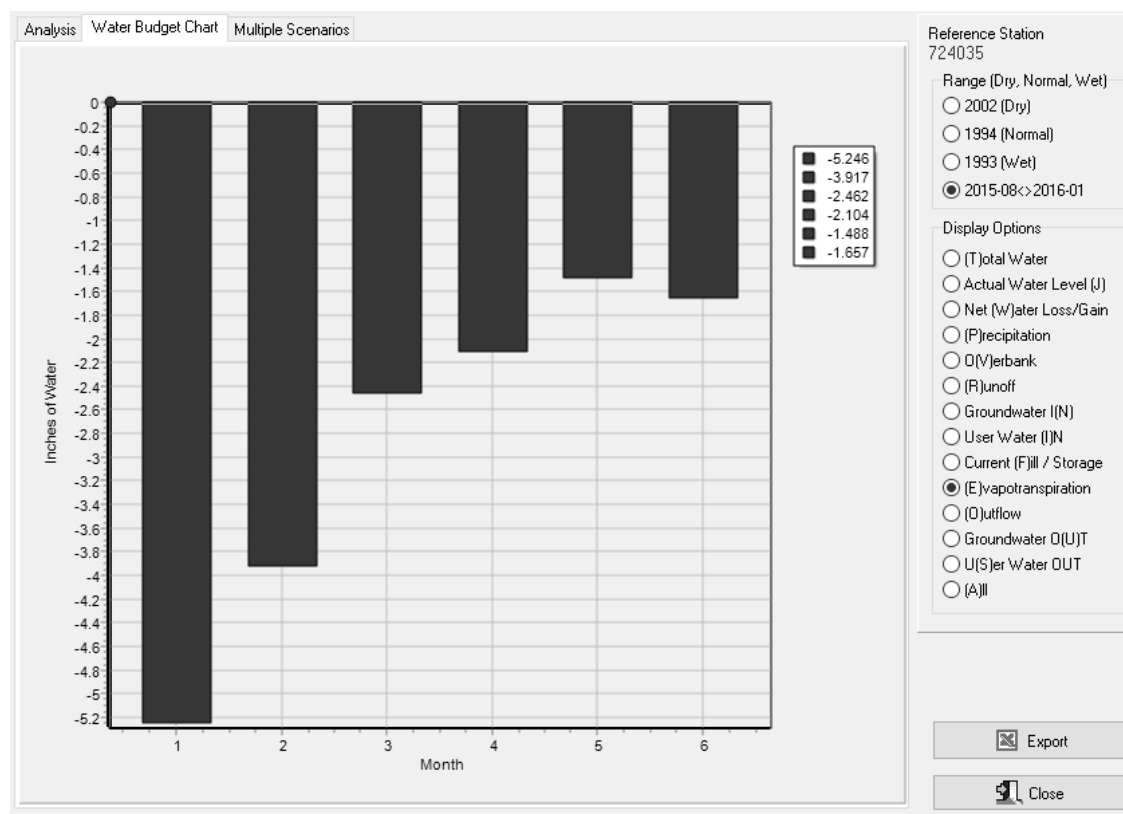


Figure 19. Wetbud evapotranspiration results for the custom period (Aug 2015 - Jan 2016) at Julie Metz.

Evapotranspiration is the principal net loss constituent for the Julie Metz water budget, but groundwater output is also an important component. The net gains for the Julie Metz wetland water budget are precipitation, groundwater input, runoff, and overbank flow. The Wetbud Basic Scenario generated actual water levels for the typical Dry year (2002), Normal year (1994), Wet year (1993), and the custom period from August 2015 to January 2016 based on the monthly net gain and loss values (Figures 20 - 23).

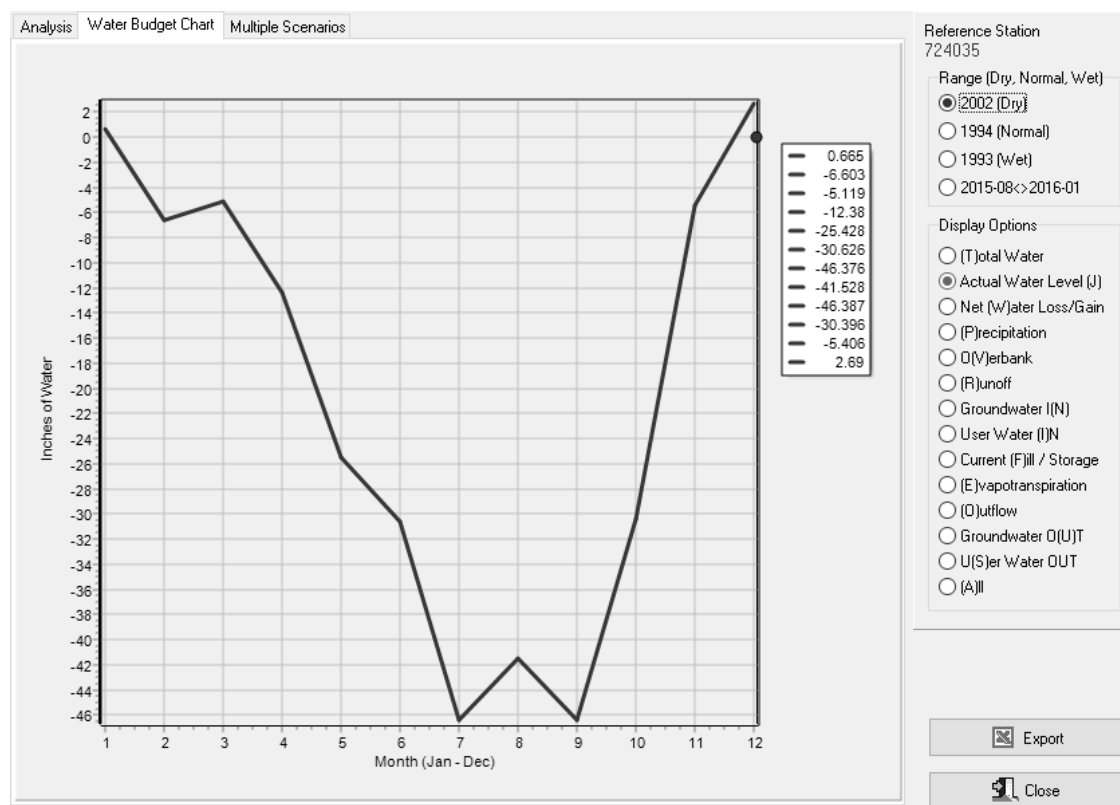


Figure 20. Wetbud actual water level results for the typical Dry year (2002) at Julie Metz.

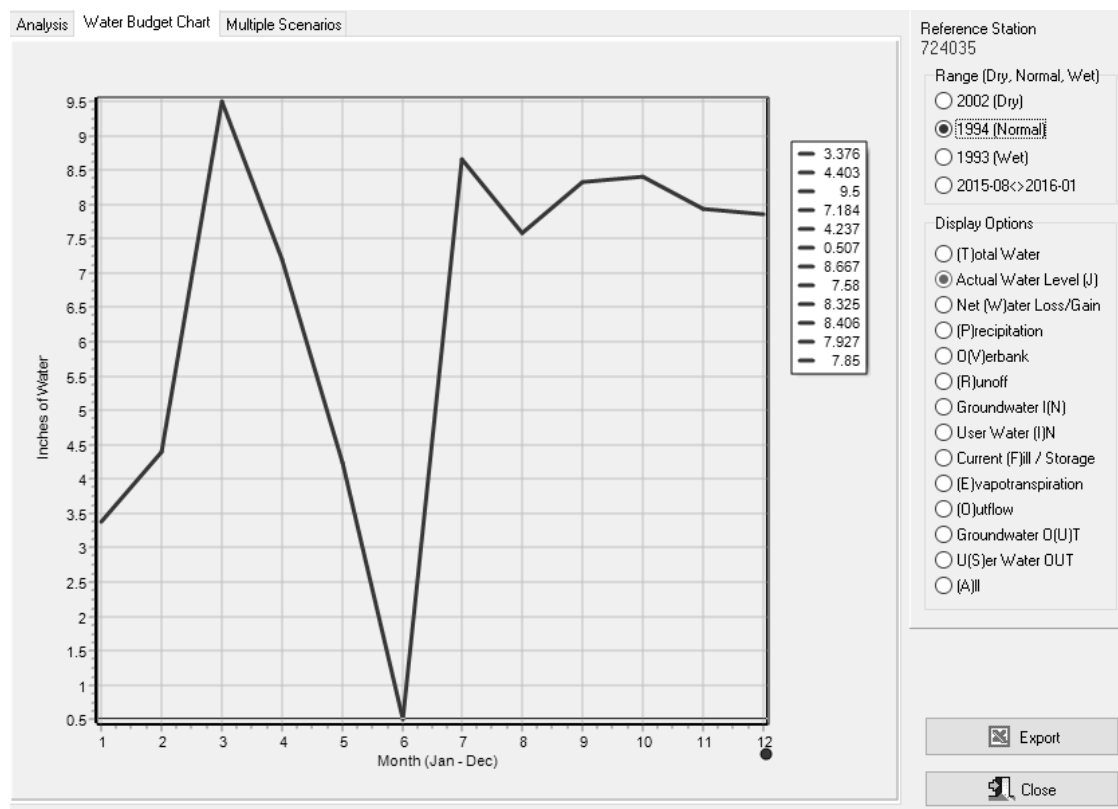


Figure 21. Wetbud actual water level results for the typical Normal year (1994) at Julie Metz.

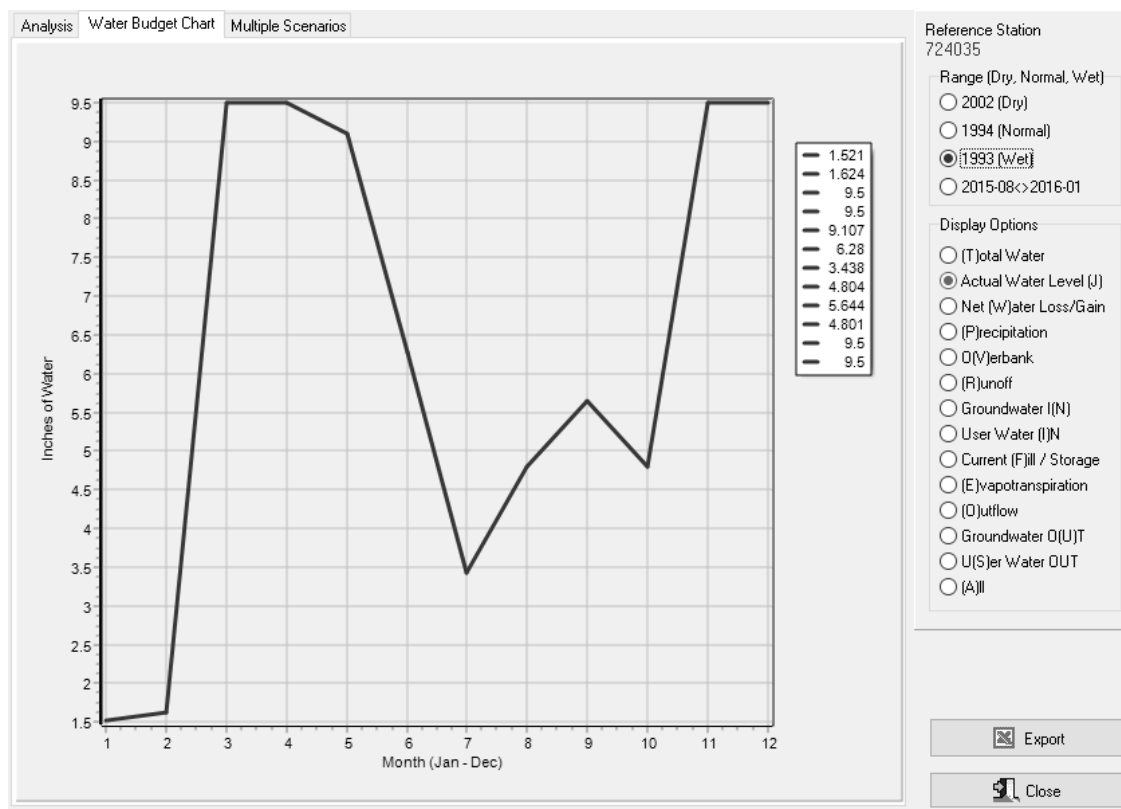


Figure 22. Wetbud actual water level results for the typical Wet year (1993) at Julie Metz.

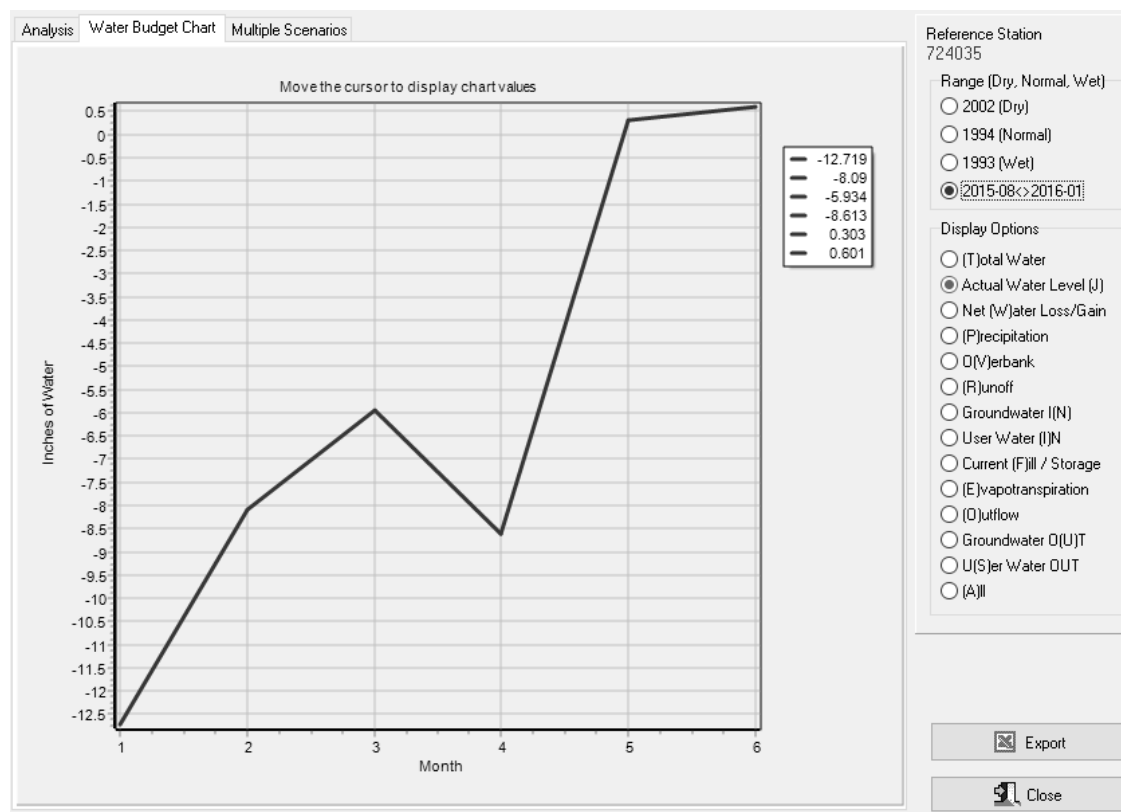


Figure 23. Wetbud actual water level results for the custom period (Aug 2015 - Jan 2016) at Julie Metz.

The Dry year (2002) water budget chart shows actual water levels that decrease from January to July, fluctuate slightly from July to September, and steadily rise from September to December. Actual water levels for the typical Normal year (1994) rise from January to March, decrease from March to June, increase for one month, and fluctuate approximately one inch from July to December. The typical Wet year (1993) water levels increase from January to March, maintain approximately nine inches of ponded water until May, decrease from May to July, increase slightly with small water level fluctuations from July to October, and finally increase from October to December. The custom period from August 2015 to January 2016 displays actual

water levels that increase approximately six inches from August to October, decrease 2.5 inches for one month, and increase nine inches from November to January. The primary water budget components controlling the actual water levels for the Dry, Normal, Wet, and custom periods are precipitation and evapotranspiration.

Basic Scenario Precipitation and Evapotranspiration Values

The Wetbud charts for the calculated Dry (2002), Normal (1994), Wet (1993) years, and the custom six month period from August 2015 to January 2016 show how precipitation and ET influence actual water levels (Figures 24 - 27).

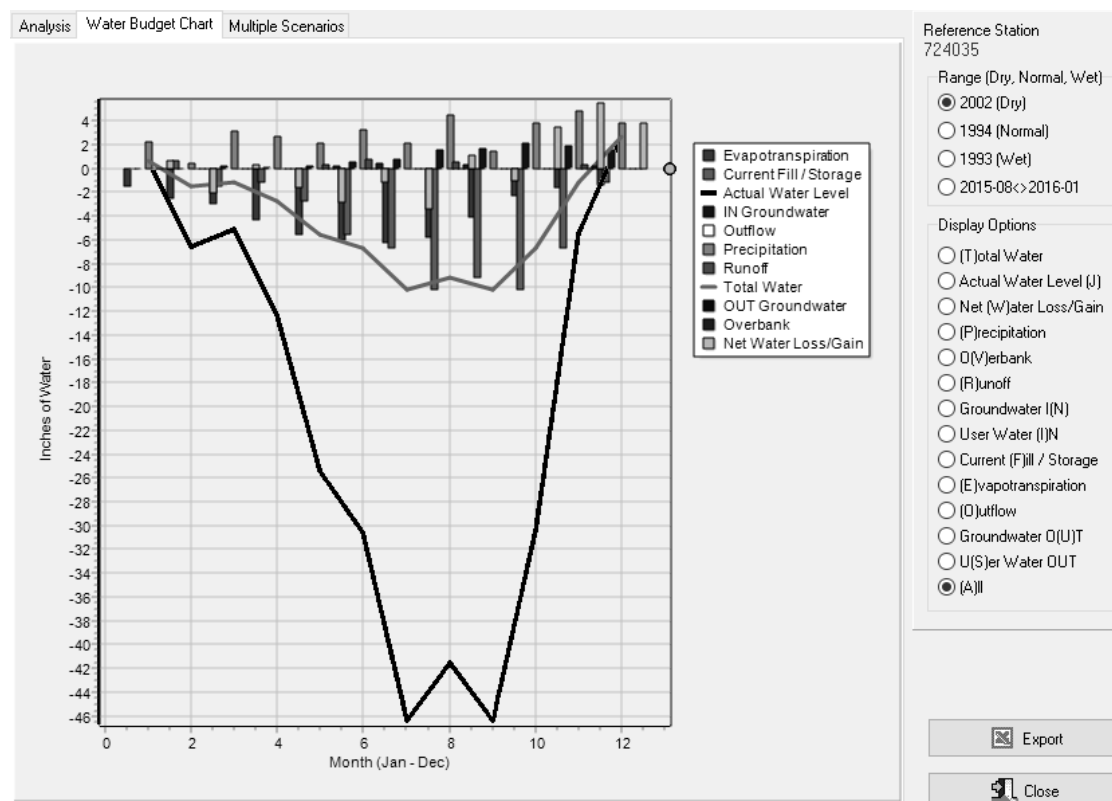


Figure 24. Wetbud all data results for the typical Dry year (2002) at Julie Metz.

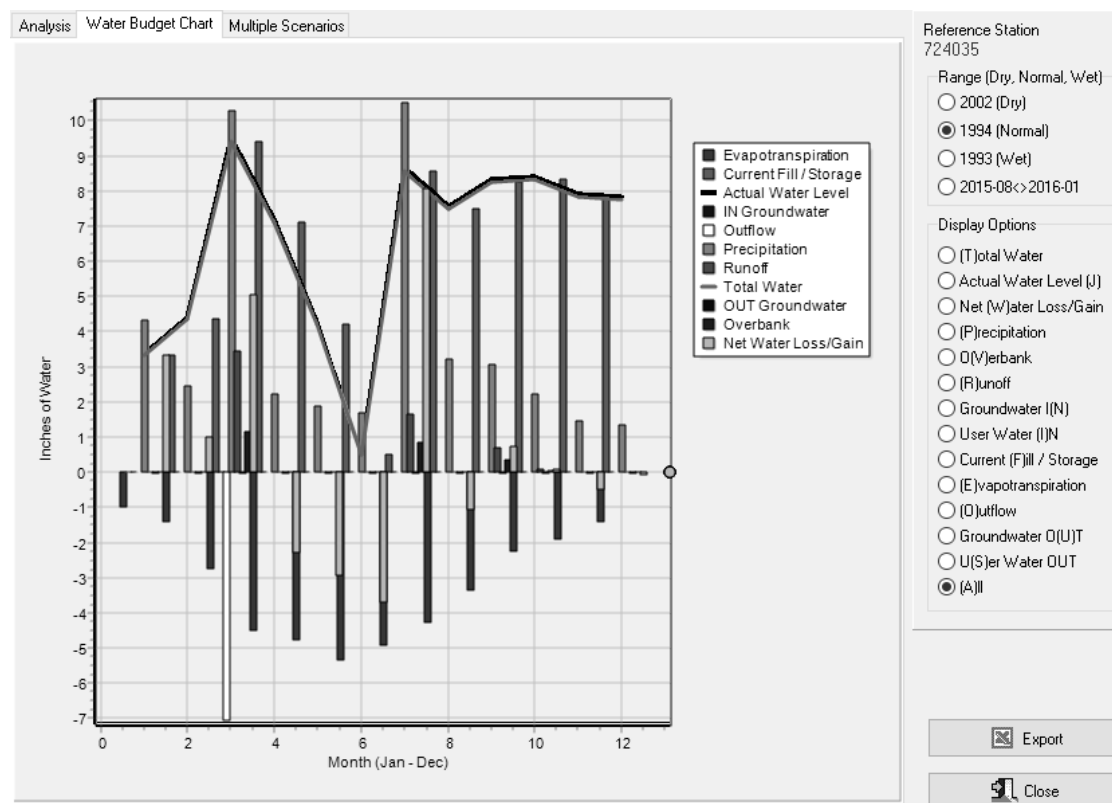


Figure 25. Wetbud all data results for the typical Normal year (1994) at Julie Metz.

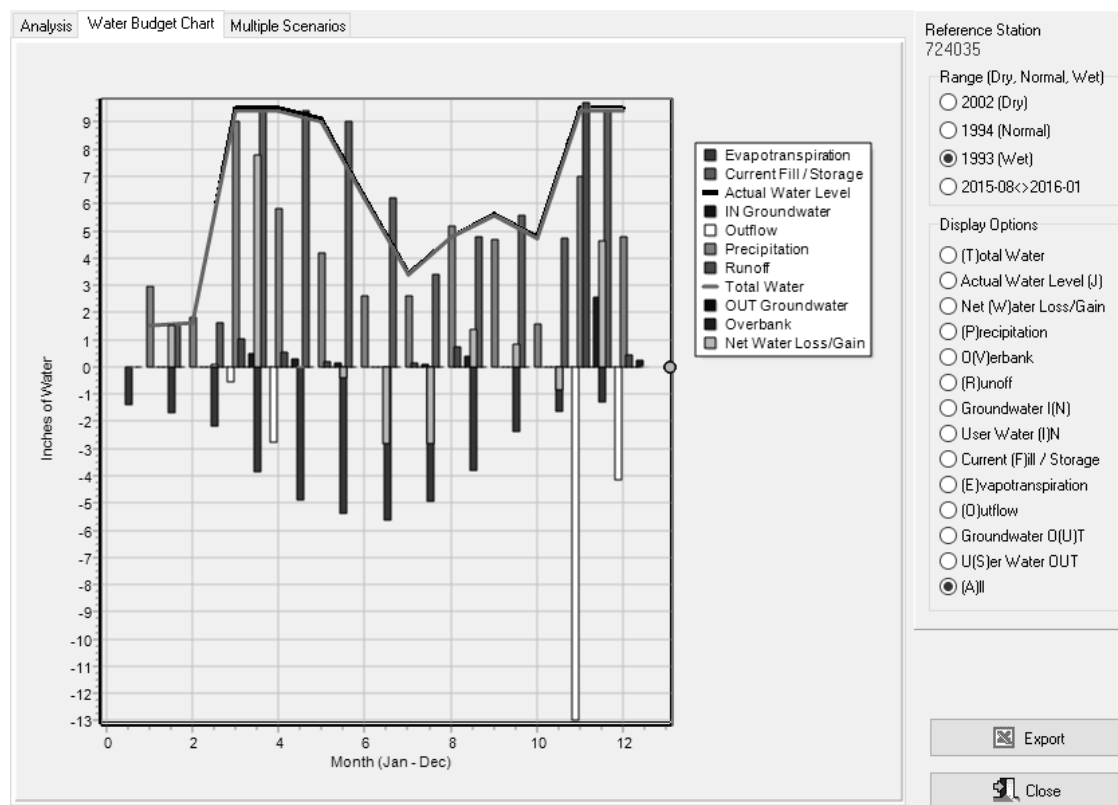


Figure 26. Wetbud all data results for the typical Wet year (1993) at Julie Metz.

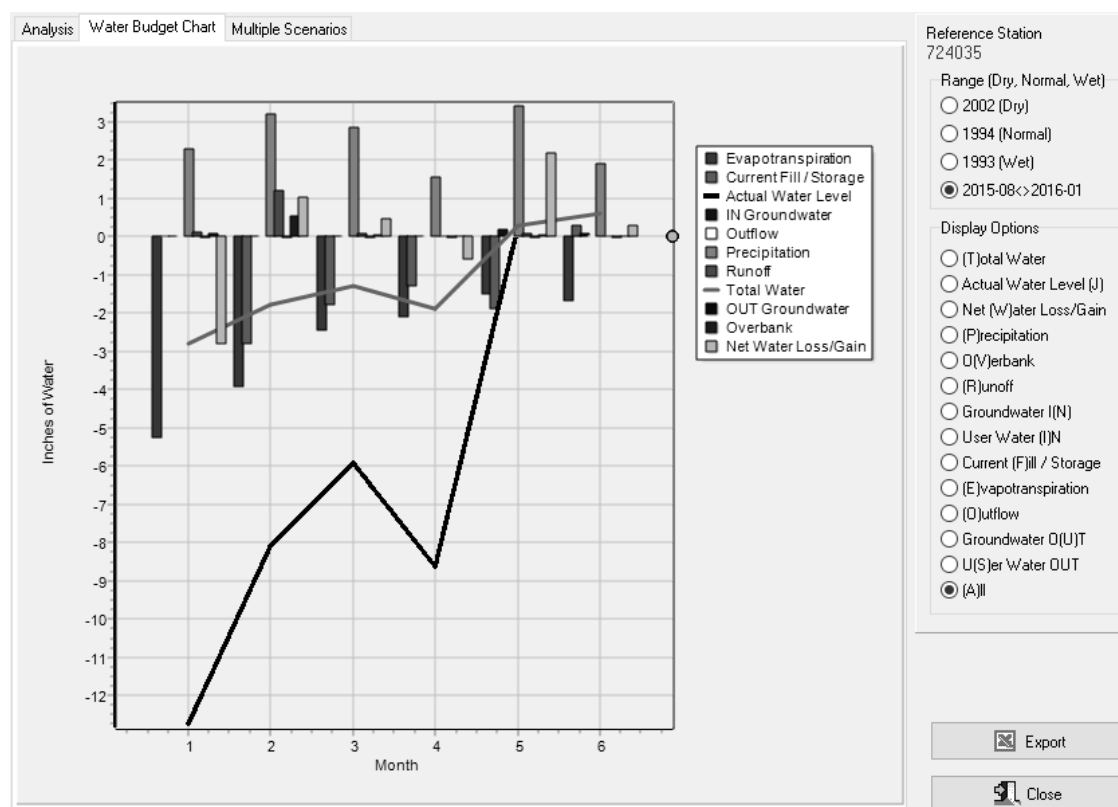


Figure 27. Wetbud all data results for the custom period (Aug 2015 - Jan 2016) at Julie Metz.

Actual water levels decrease from Winter to Spring and into the Summer for a typical Dry year (2002) at Julie Metz. As Fall begins and continues into the Winter, the actual water levels increase dramatically. Following the actual water level trend for year 2002, precipitation values were variable throughout the year. Evapotranspiration (ET) values were lower during the Fall and Winter months, and significantly higher during the Spring and Summer months. The precipitation values were dwarfed by the ET values, indicative of a typical Dry year.

Wetbud calculated year 1994 as a typical Normal year shown in Figure 25. The Normal year illustrates the response of the actual water level to precipitation and ET values. During the year 1994, precipitation values were much greater than the ET values. In March and July, there

was significant precipitation, causing flashiness in the actual water levels. Between March and July, the precipitation was considerably lower while ET values were at their peak during the Summer months. The change in precipitation and the steady increase in ET caused a sharp decline in the actual water levels from March until July.

The year 1993 was calculated as a typical Wet year for Julie Metz using Quantico weather station data (Figure 26). During the year, actual water levels were above the ground surface causing inundation throughout the year. Again, precipitation and ET were the primary constituents controlling the water levels. Actual water levels show inundation because precipitation values were greater than the ET values for most of the year. Water levels decreased from May to June as precipitation decreased and ET increased, but the aquifer storage remained positive indicating the soils were saturated.

The custom period from August 2015 to January 2016 was selected in Wetbud to compare with data collected at the Julie Metz wetland during the same time period and calibrate the model. The Julie Metz Wetbud water budget chart for the custom period displays all water budget data (Figure 27). Month 1 corresponds with August and the subsequent numbers align with the months following August, ending with January 2016 as Month 6. During the six month period, ET values decline and precipitation values range from approximately 1.5 inches in November (Month 4) to approximately 3.5 inches in December (Month 5). There is a sharp increase in the actual water levels from August until January which correlates with the decline in ET during the same six month period.

Basic Scenario Model Calibration

The Wetbud Basic Scenario was calibrated by comparing the monthly water level values to the actual monthly water levels collected at the Julie Metz wetland from August 2015 to January 2016 (Figure 28).

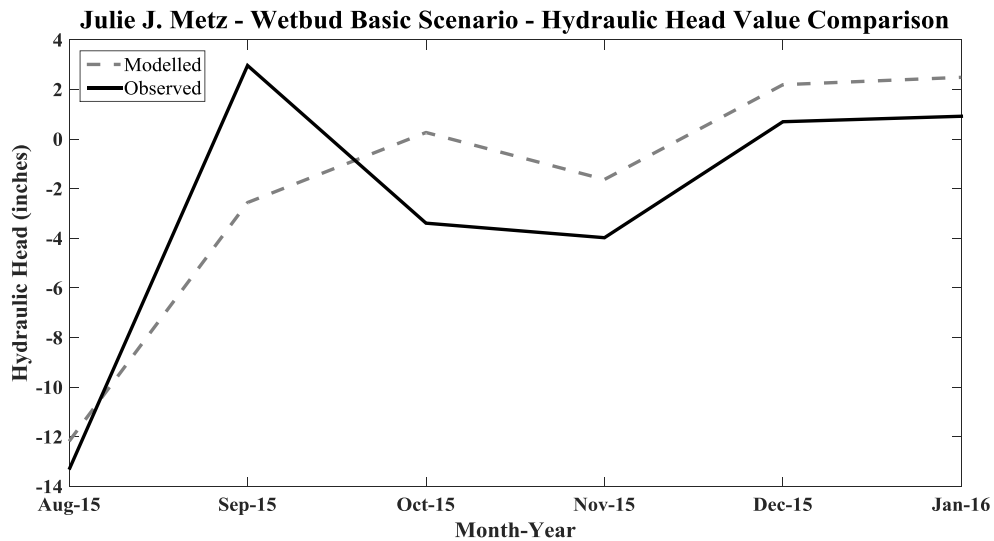


Figure 28. Julie Metz Basic Scenario hydraulic head comparison graph for the custom period with NSE (0.67748) and RMSE (3.0379) results.

Matlab was used to calculate the Nash-Sutcliffe Efficiency (NSE) (1970) and the Root Mean Squared Error (RMSE). It was also used to generate a graphical display comparing the modeled and observed hydraulic head values at Julie Metz. A sensitivity analysis was performed by individually adjusting the NRCS Curve Number, the soil storage factor, and the surface storage factor. Once the highest NSE value was attained by adjusting the NRCS Curve Number, the soil storage factor was adjusted, followed by the surface storage factor. The highest NSE value of

0.67488 was obtained after completing the sensitivity analysis. The highest NSE value corroborated with the lowest RMSE value during the calibration process. NSE values can range from $-\infty$ to 1. Values less than 0.5 are classified as unacceptable, values greater than 0.5 and less than 0.65 are satisfactory, and values greater than 0.65 are labeled as good to very good (Moriassi et al., 2007). Thus, the Wetbud Basic Scenario calibration is considered good to very good based on the NSE value of 0.67488.

A linear regression was performed in Matlab using the modeled and observed hydraulic head values to further establish an acceptable calibration for the Wetbud Basic Scenario at Julie Metz (Figure 29).

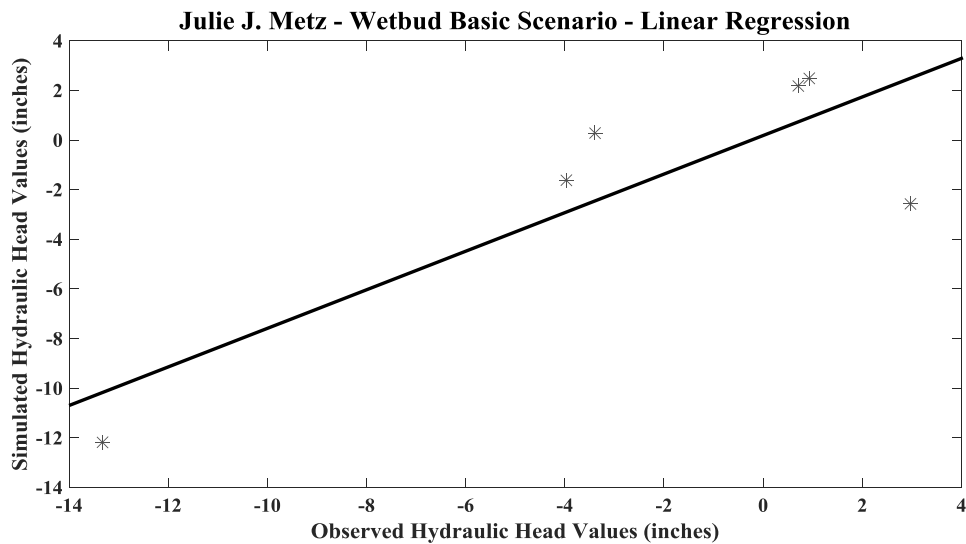


Figure 29. Julie Metz Basic Scenario linear regression graph for the custom period with regression values ($y = 0.77716x + 0.19274$, $R^2 = 0.70596$, $p\text{-value} = 0.036258$).

Best fit linear regressions have R^2 values at or near 1. The R^2 value for the Wetbud Basic Scenario was 0.70596 and the p-value was 0.036258. Acceptable p-values are less than 0.05 and the R^2 value of 0.70596 is sufficiently close to 1. The Wetbud Basic Scenario for the Julie Metz wetland is considered calibrated based on the NSE, RMSE, R^2 , and p-value data.

Wetland Water Budget Modeling - Advanced Scenario

The Wetbud Advanced Scenario calculates water budgets but it also incorporates daily time steps, cell zone and grid zone properties, and a topographic grid to generate hydraulic head values. The hydraulic head values were generated for the time period 1 August 2015 to 27 January 2016. Advanced Scenario outputs were created for each cell, displaying the water and surface elevations for each of the four layers. The hydraulic head output values for layer 2 were chosen because layer 1 is a vegetation layer. The layer 2 hydraulic head values at monitoring points MW23, MW11B, and MW7B were selected to analyze the hydrology of Pod 3B. The monitoring point locations are given a row and column coordinate for reference. The Head Along Row option was selected in the Advanced scenario to show the hydraulic head values for the row containing monitoring points MW23, MW11B, and MW7B at a given time step. After reviewing Figures 9 and 11, time steps 61-62 (1-2 October 2015) were chosen because of the sharp increase in hydraulic head during a storm event.

The layer 2 hydraulic head values for the row containing MW23 are shown in Figures 30 and 31 for time steps 61 and 62 respectively. MW23 is located at column 7, row 13 with a surface elevation of 4.21 meters. On 1 October 2015, the water elevation was 2.99 m prior to a storm event. The water elevation steadily decreased across the row from left to right, displaying a downward water flow gradient across Pod 3B from the upland area to the lowland area. During a

storm event on 2 October 2015, the water elevation at MW23 increased to 3.20 m and the water flow gradient decreased significantly with the water table at or near the surface (Figures 30 and 31).

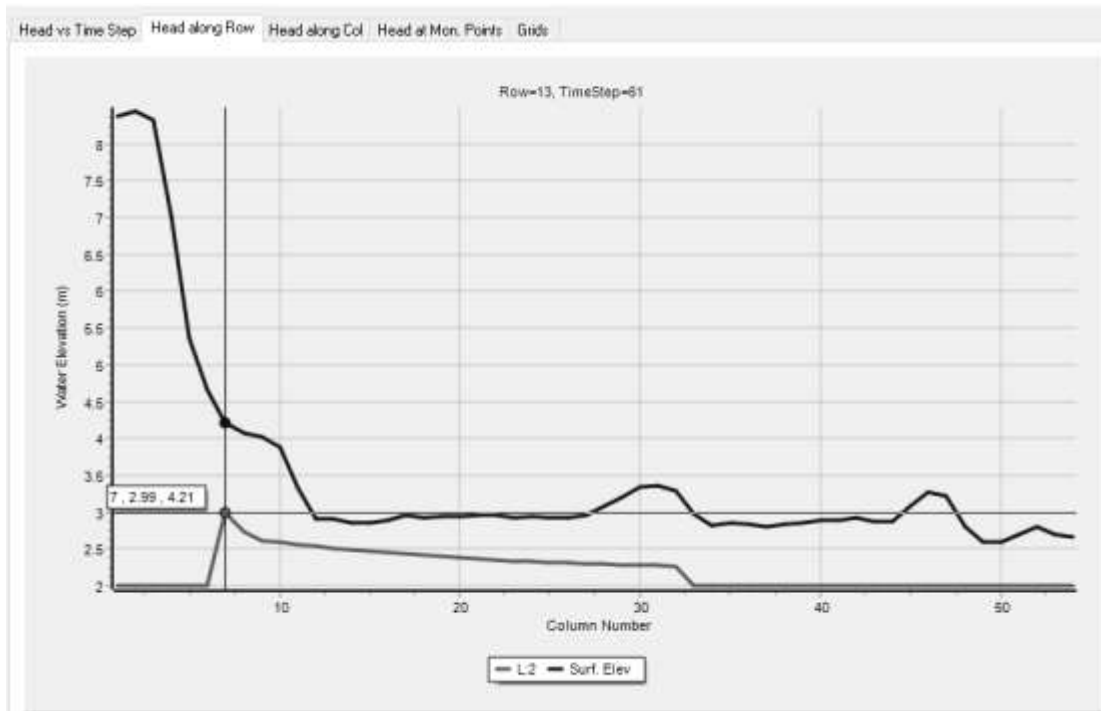


Figure 30. Wetbud Advanced Scenario Output at MW23 (C7, R13) at time step 61 (1 October 2015) prior to a storm event.

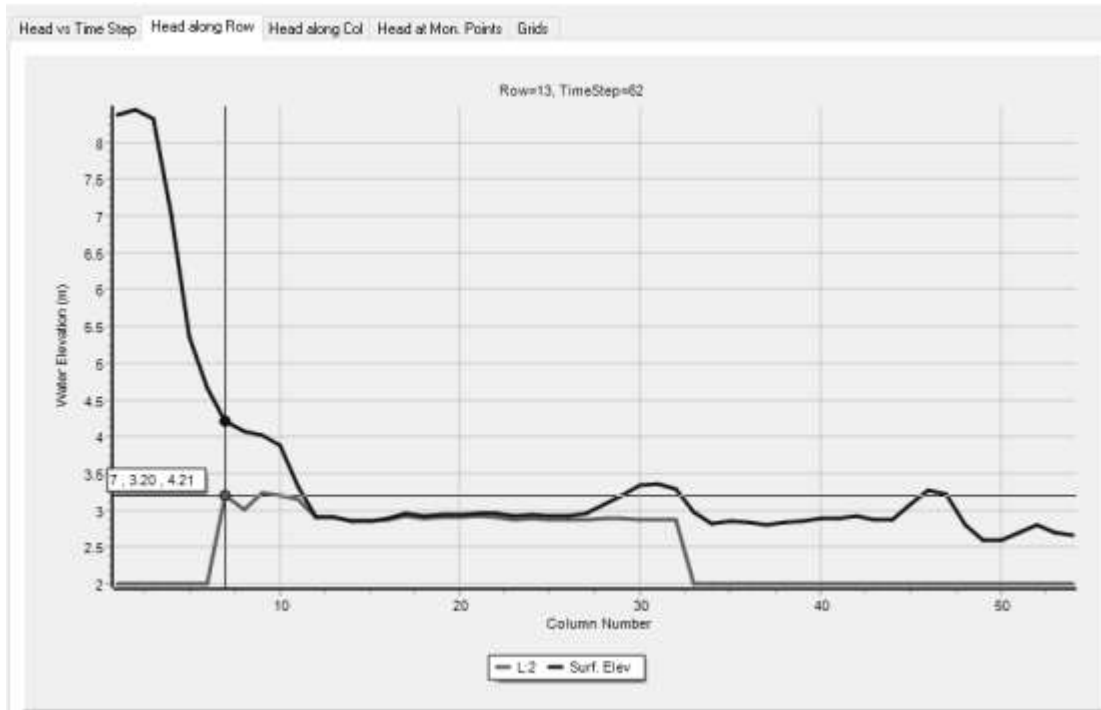


Figure 31. Wetbud Advanced Scenario Output at MW23 (C7, R13) at time step 62

(2 October 2015) during a storm event.

The same groundwater flow pattern occurred for the rows containing monitoring points MW11B and MW7B (Figures 32 - 35). MW11B is located at the toeslope within Pod 3B with a surface elevation of 3.00 m and a water elevation at 2.51 m on 1 October 2015. The following day, the water elevation increased to 3.44 m, 0.44 m above the ground surface as a result of the storm. A corrugated drain pipe located approximately 14 m northwest of MW11B contributed to the inundation by funneling surface runoff from the upland area to the toeslope near MW11B.

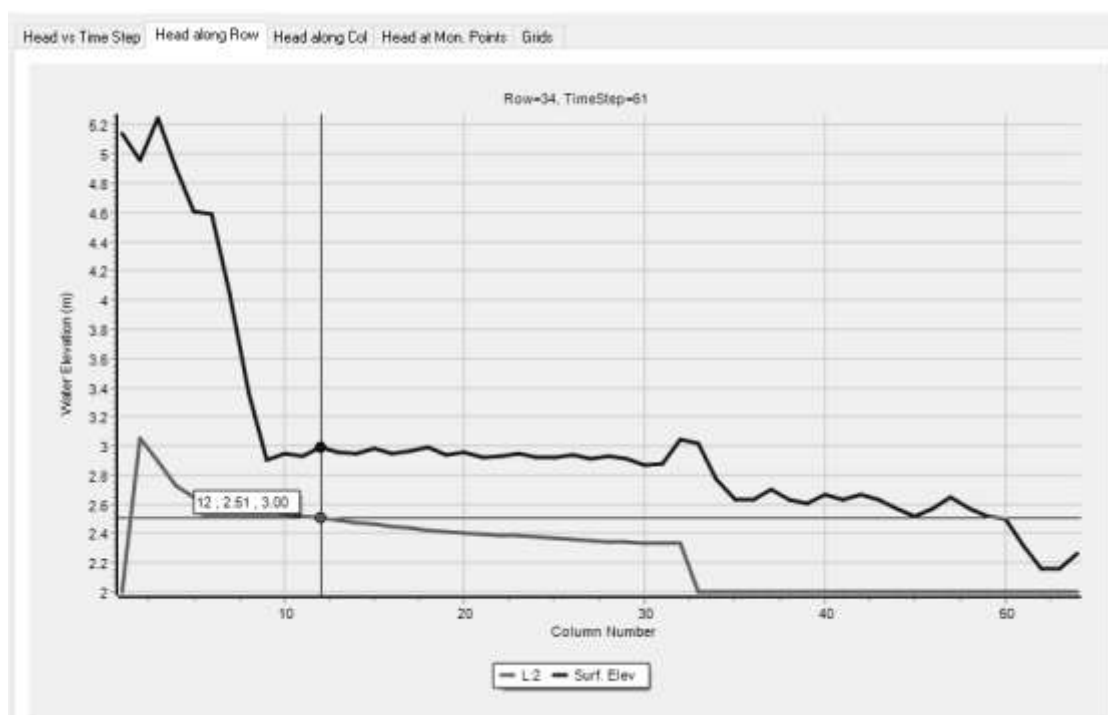


Figure 32. Wetbud Advanced Scenario Output at MW11B (C12, R34) at time step 61 (1 October 2015) prior to a storm event.

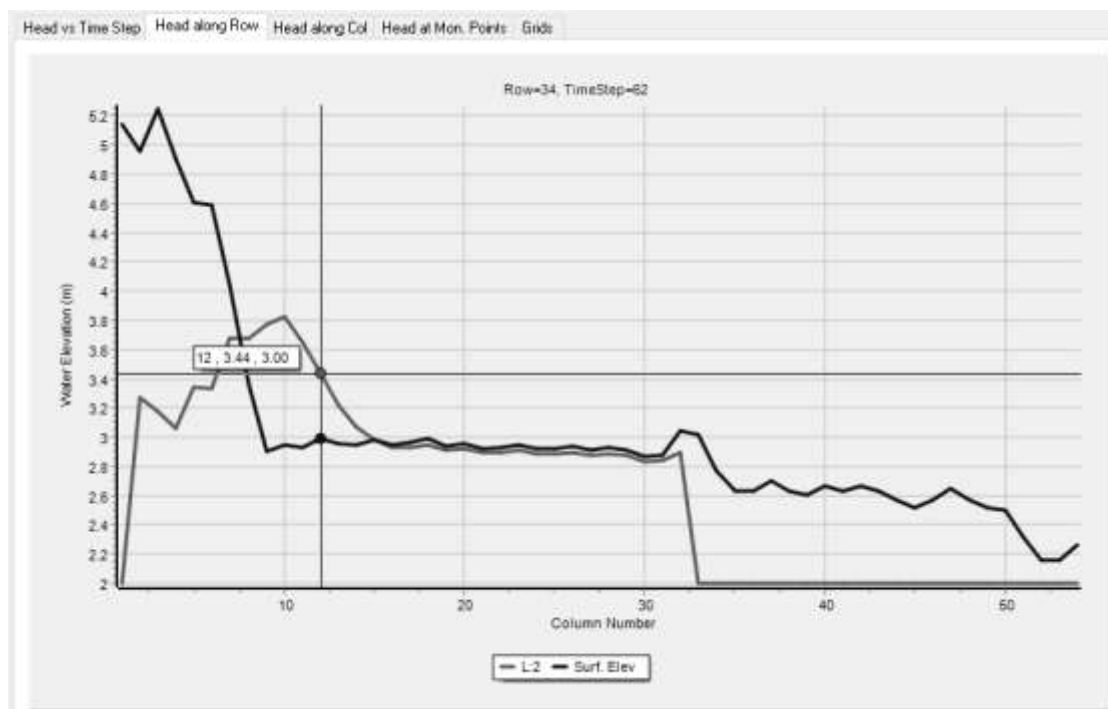


Figure 33. Wetbud Advanced Scenario Output at MW11B (C12, R34) at time step 62 (2 October 2015) during a storm event.

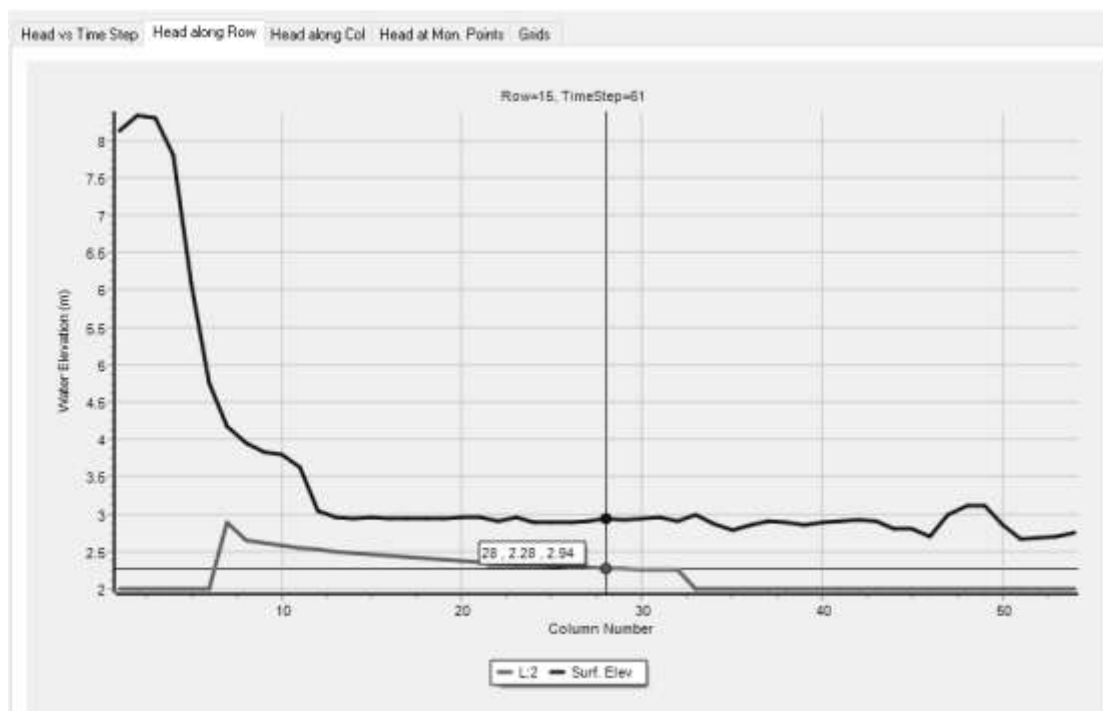


Figure 34. Wetbud Advanced Scenario Output at MW7B (C28, R15) at time step 61 (1 October 2015) prior to a storm event.

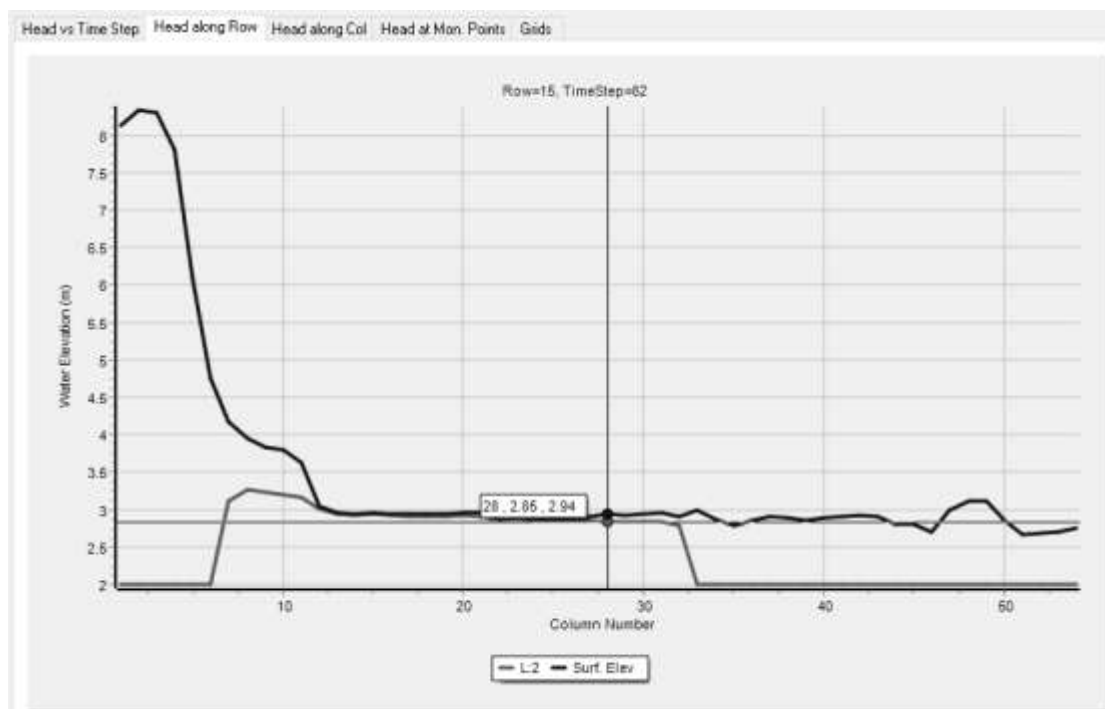


Figure 35. Wetbud Advanced Scenario Output at MW7B (C28, R15) at time step 62 (2 October 2015) during a storm event.

The row containing monitoring point MW7B demonstrated a downward water flow gradient across Pod 3B (Figure 34). The surface elevation is 2.94 m. On 1 October 2015, the water elevation was 2.28 m. During the 2 October 2015 storm, the water elevation increased to 2.85 m. The water table during the storm event was at or near the ground surface for the row containing MW7B and the groundwater gradient was significantly decreased (Figure 35).

Advanced Scenario Model Calibration

The Wetbud Advanced Scenario for Julie Metz was calibrated by comparing the modeled hydraulic head values at three monitoring well locations in the wetland, MW23, MW11B, and MW7B, to the observed hydraulic head values at the same locations from August 2015 to January 2016. Similar to the Wetbud Basic Scenario, the Advanced Scenario was calibrated

using Matlab to calculate the NSE and RMSE along with a graphical output displaying the difference in hydraulic head values during the six month calibration period (Figures 36 - 38).

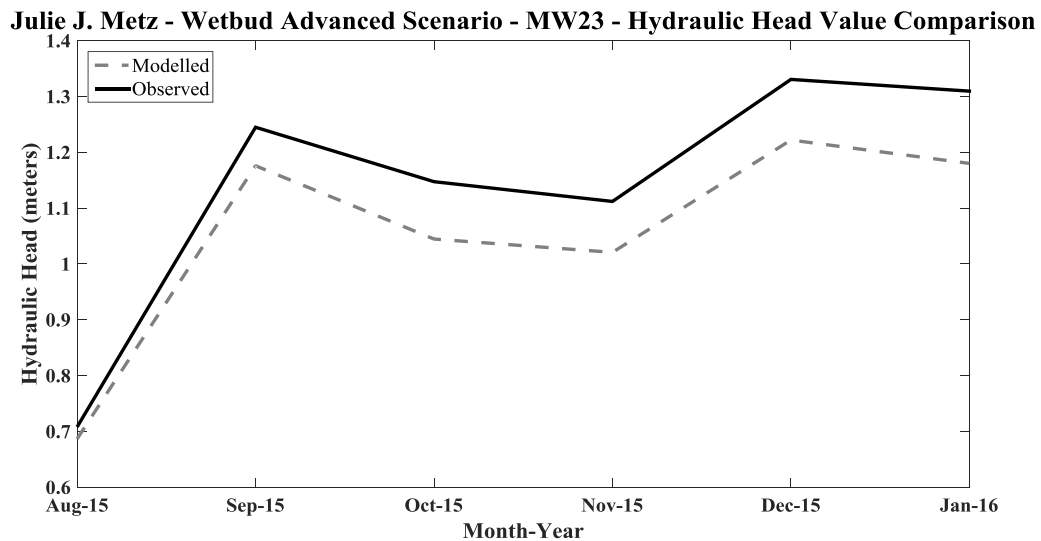


Figure 36. Julie Metz Advanced Scenario hydraulic head comparison graph for MW23 with NSE (0.80026) and RMSE (0.093665) results.

Julie J. Metz - Wetbud Advanced Scenario - MW11B - Hydraulic Head Value Comparison

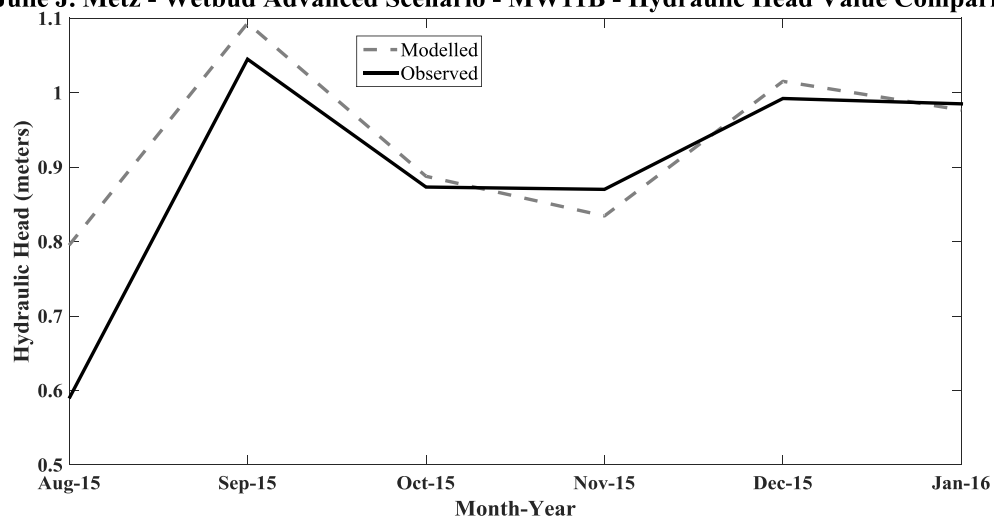


Figure 37. Julie Metz Advanced Scenario hydraulic head comparison graph for MW11B with NSE (0.65225) and RMSE (0.08833) results.

Julie J. Metz - Wetbud Advanced Scenario - MW7B - Hydraulic Head Value Comparison

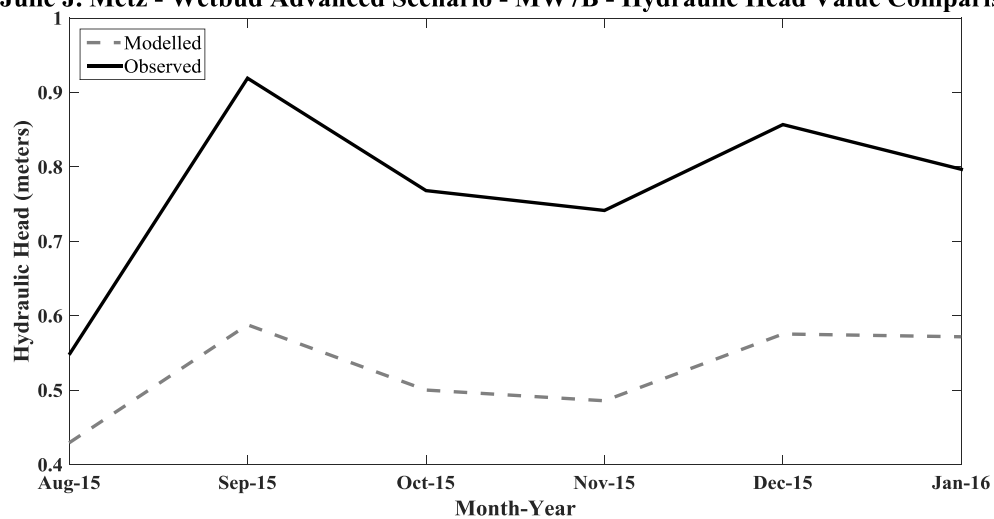


Figure 38. Julie Metz Advanced Scenario hydraulic head comparison graph for MW7B with NSE (-3.8365) and RMSE (0.25519) results.

A linear regression analysis and graph were also performed at MW23, MW11B, and MW7B. A R^2 and p-value were calculated in Matlab using the modeled and observed hydraulic head data (Figures 39 - 41). The highest NSE values with the corresponding lowest RMSE values were obtained by conducting 64 trials, adjusting the hydraulic conductivity, specific yield, drain conductance, cell zone placement, and grid zone placement. The three monitoring wells, MW23, MW11B, and MW7B, affected one another while adjusting their hydrogeologic characteristics during the calibration process. A sensitivity analysis was performed by adjusting one hydrologic characteristic at a time until the highest NSE and lowest RMSE values were attained for that characteristic. Subsequently, the other hydrologic characteristics were individually adjusted. Model calibration was attained when the NSE values for the three monitoring well locations were closest to one. At MW23 and MW11B, the NSE values were 0.80026 and 0.62552 respectively. These values are considered very good and good based on the Moriasi et al. (2007) categorizing method for NSE values. At MW7B, the NSE value was considered poor with a value of -3.8365. The hydraulic head comparison and the linear regression for MW7B show a similar trend visually and statistically ($R^2 = 0.86869$; p-value = 0.0067714) between the modeled and observed hydraulic head values, but the RMSE is 0.25519 meters (Figures 38 and 41).

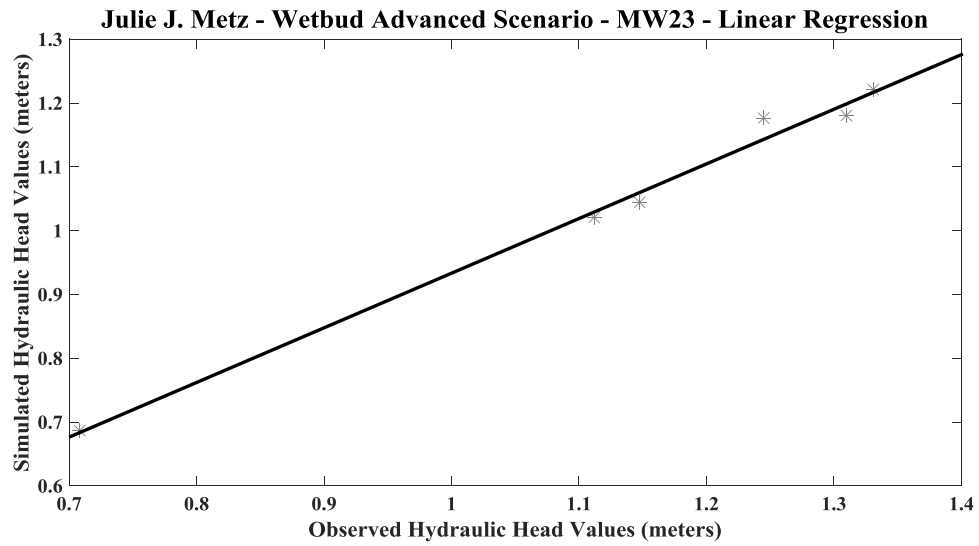


Figure 39. Julie Metz Advanced Scenario linear regression graph for MW23

with regression values ($y = 0.85649x + 0.07686$, $R^2 = 0.99102$,

$p\text{-value} = 0.000030314$).

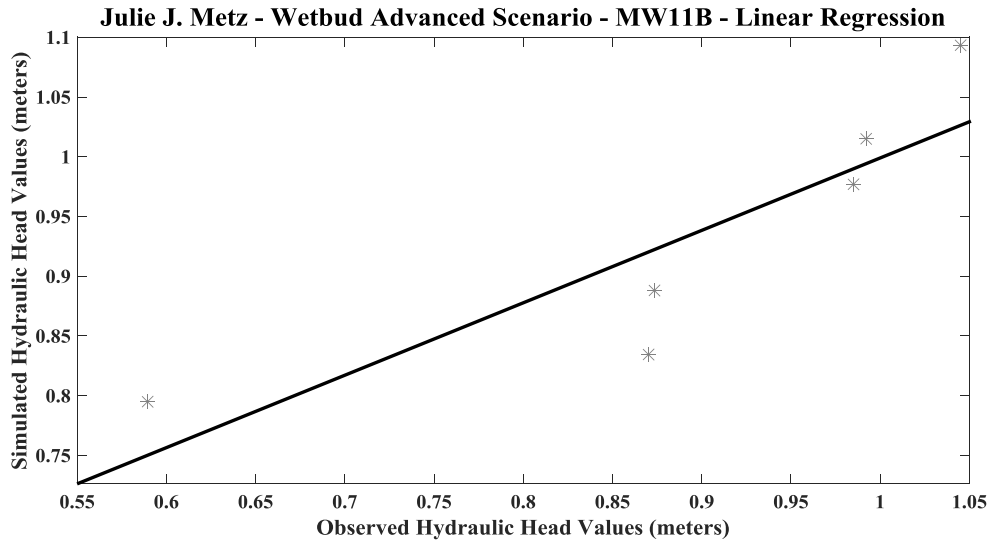


Figure 40. Julie Metz Advanced Scenario linear regression graph for MW11B with regression values ($y = 0.60621x + 0.39276$, $R^2 = 0.75901$, $p\text{-value} = 0.023811$).

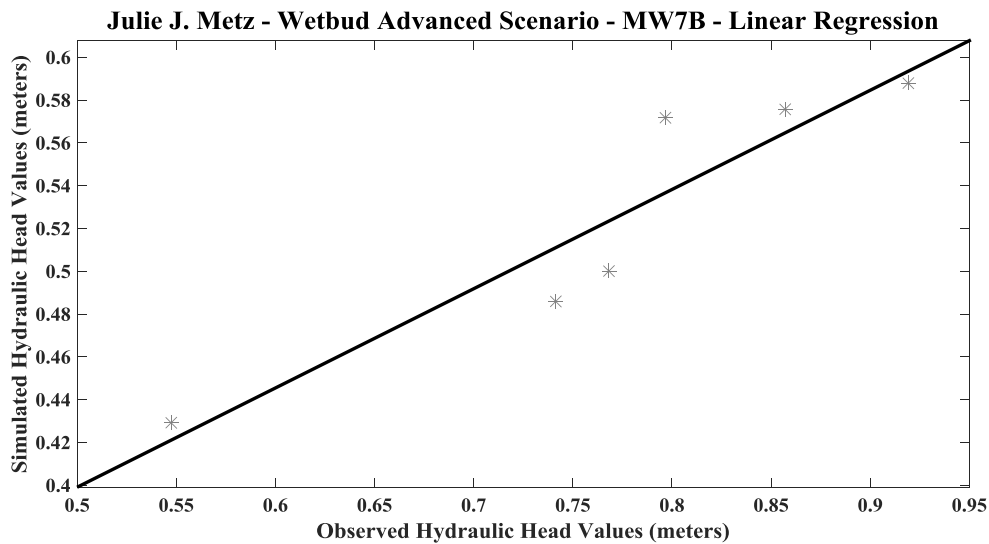


Figure 41. Julie Metz Advanced Scenario linear regression graph for MW7B with regression values ($y = 0.46377x + 0.1672$, $R^2 = 0.86869$, $p\text{-value} = 0.0067714$).

The dryness of the modeled hydraulic head data compared to the observed head data may be explained by the absence of surface flow runoff in the Wetbud Advanced model from neighboring Pod 2. Following a rain event in Fall 2015, a rack line of leaf litter and wood debris was pushed against the base of several trees separating Pod 2 from Pod 3B near the location of MW7B. The rack line indicated significant surface water had flowed from Pod 2 to Pod 3B (Figure 42).

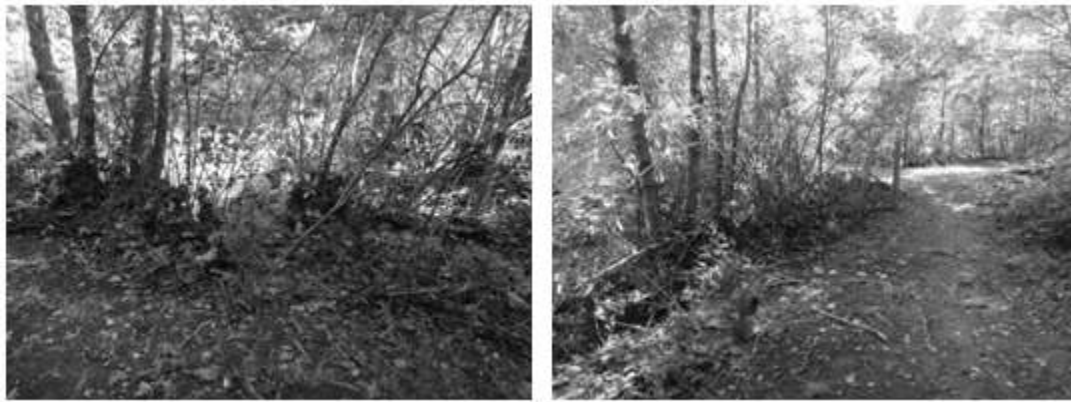


Figure 42. Photos of rack line along western boundary of Pod 3 on 5 October 2015.

The surface runoff from the neighboring Pod 2 was not included in the Wetbud Advanced Model Scenario and could account for the difference between the observed and modeled hydraulic head values.

Tidal Analysis

The tidal influence inland from the creek was calculated using the governing equation in one dimension and applying it to the equation from Jacob (1950). Assuming the cobble and gravel unit is approximately six meters thick with a hydraulic conductivity of $1\text{E-}03$ m/s, a tidal signal with an amplitude of 0.02 m would be observed approximately 39 m inland of the tidal creek. As a reference, MW9B is 25 m inland, MW8B is 60 m inland, and the Pod 3A - 3B bermed boundary is 85 m inland. The calculation supports the groundwater hydrographs and flow maps showing tidal influence in Pod 3A, but not in Pod 3B.

The tidal forcing at Neabsco Creek was also investigated using the T_TIDE Matlab function. Using the Neabsco Creek well data from Figure 10, the T_TIDE function separated the tidal signal into 35 components (Pawlowicz et al., 2002). Several lunar and solar components from the Neabsco Creek tidal signal were used to quantify the tidal type (diurnal, semidiurnal, mixed) using the Form Factor equation. The Form Factor equation uses the lunisolar diurnal, the principal lunar diurnal, the principal lunar semidiurnal, and the principal solar semidiurnal components to calculate a numerical result. The Neabsco Creek Form Factor result was 0.31. Form Factor values less than 0.25 are considered semidiurnal and mixed tides have values that range from 0.25 to 1.25. The Neabsco Creek result indicates a mixed tidal signal that is mainly semidiurnal. This result coincides with the Neabsco Creek tidal signal shown in the Pod 3A groundwater hydrograph. Throughout a given month, the Neabsco Creek tidal signal primarily has two flood tides and two ebb tides on a daily occurrence. However, for a few days throughout a given month, there will be only one flood tide or one ebb tide. This implies a mixed tidal signal.

The T_TIDE function also classified 46% of the components with lunar or solar attributes and 54% of the components with influence from the wind and regional watershed flow. To strengthen the T_TIDE classification results, groundwater data from the Washington, D.C. weather station were combined with the Neabsco Creek and MW9B groundwater data. The combined tidal data were displayed with an adjoining graph showing the wind speed and direction from the Washington, D.C. weather station during the same time period, 1 - 8 October 2014 (Figure 7). During this time period, the tidal peak on 4 October 2014 was expected to be caused by precipitation because Figure 10 shows a precipitation event on 4 October 2014. However, the amount of rainfall is not consistent with the elevated tidal peak. The elevated tidal peak corresponds with high wind gusts from the south after comparing the wind data and the tidal data from 4 October 2014.

Sea Level Rise Effects

The cross-sectional profile of Pod 3A and 3B at the Julie Metz wetland is shown in Figure 43.

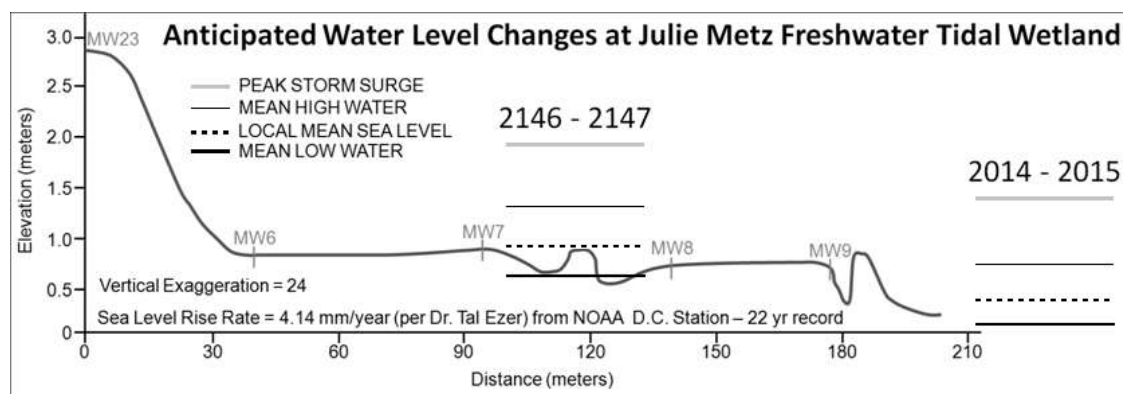


Figure 43. Cross-sectional profile across Pod 3 from the upland fan (MW23) to the tidal creek showing effects from sea level rise.

Using the current Washington D.C. sea level rise rate of 4.14 mm/yr (Ezer and Atkinson, 2015), anticipated water level changes to the wetland at Pod 3 are shown. In approximately 132 years, Pod 3 will be permanently inundated. In 22 years, Pod 3A will be consistently inundated during flood tide periods. As a reference, Pod 3A was inundated 10 times from August 2014 to October 2015 (Figure 44).

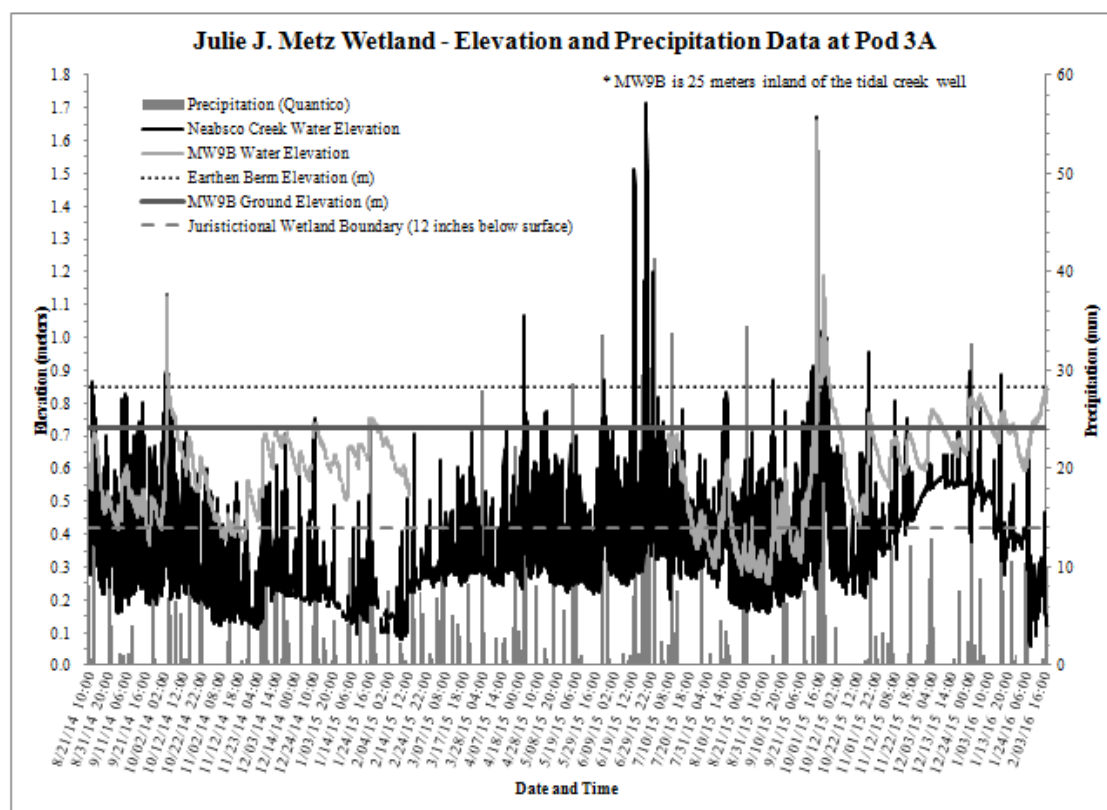


Figure 44. Graph displaying water elevation, ground elevation, and precipitation data at Pod 3A from 21 August 2014 - 4 February 2015.

During the next 22 years, the inundation frequency for Pod 3A will increase until it occurs on a consistent basis. The Pod 3A wetland will transition from a forested, shrub-scrub wetland to an emergent wetland. Ultimately, there will be wetland loss as sea level continues to rise.

CHAPTER IV

DISCUSSION AND CONCLUSIONS

Hydrogeology

Julie Metz is located on a Quaternary-aged alluvial fan deposited along the tidally influenced Neabsco Creek. The alluvial fan developed at the base of steep slopes in the flood plain areas of Neabsco Creek. The creek incised the surrounding and expansive Cretaceous sands and clays called the Potomac group, forming a valley that filled with Quartzite cobbles and Ordovician slate fragments. The cobbles and slate fragments were transported as sediment load downstream and were later covered by alluvial sediment (Figure 3). The finer grained sediment and slate fragments filled the void space between the larger quartzite cobbles that affected the hydraulic conductivity of the wetland. Using the table from Appendix B and the Pod 3 stratigraphic profile (Figure 8), hydraulic conductivity (K_{sat}) values were expected to range from 10^{-1} to 10^{-4} m/s. However, after performing the slug tests at the wells located in Pod 3, the K_{sat} values ranged from 10^{-4} m/s to 10^{-6} m/s (Table 6). The K_{sat} values provide an approximation of the soil permeability and indicate an overall moderate groundwater flow through Pod 3 at Julie Metz.

Hydrologic Analysis

The K_{sat} values, topography, groundwater, evapotranspiration, precipitation, and tidal forcing from Neabsco Creek affect the wetland hydrology at Pod 3. The topography sharply drops approximately 1.5 m from the alluvial fan to the lower-lying floodplain area. The toe from the alluvial fan was removed and semi-impermeable soil was placed above the gravel layer in the

Neabsco Creek flood plain (Figure 8). As a result, groundwater seeps into Pod 3B at the margin between the alluvial fan and the flood plain when the water table is near the ground surface. The groundwater elevation relative to the ground surface is primarily controlled by evapotranspiration and precipitation. Julie Metz evapotranspiration values calculated from the Wetbud Basic Scenario are shown in Figures 16 - 19. The values show increased evapotranspiration during warmer periods when there is leaf out. During the colder months, leaves are diminished or gone and the evapotranspiration is reduced. Because evapotranspiration is a net loss in a water budget, the groundwater elevation is closer to the ground surface during colder periods and deeper below the ground surface during warmer periods.

Precipitation is a net gain in the water budget and directly correlates to the groundwater elevation. Precipitation affects the groundwater in two ways at Pod 3 in Julie Metz: direct precipitation to the ground surface, and surface water flow. The groundwater elevation responds to rain events with a sudden increase followed by a gradual decrease (Figures 9 - 11). In Figure 9, the sharp increases in water elevations correlate with precipitation events. Precipitation in conjunction with the topography at Pod 3 causes surface water flow. During the storm event on 2 October 2015 (Figure 9), the groundwater elevations suddenly increased from 0.6 m to 1.7 m in conjunction with the large precipitation input at Julie Metz. The sharp rise in groundwater elevation was caused by the heavy precipitation (Figure 9) as well as the surface water flow (Figures 32 and 33). Precipitation that did not infiltrate the soil from the upland alluvial fan region flowed down gradient as surface water and eventually was directed through a three-foot diameter corrugated plastic culvert pipe to Pod 3B near MW11B. The sudden influx of surface water to Pod 3B temporarily reversed the hydraulic gradient between the toe slope well (MW11B) and the upland well (MW23) (Figure 11).

Figures 9 - 11, Figures 12 - 15, and Figures 30 - 35 demonstrate groundwater is the principal water source controlling water table variation across Pod 3. There is a baseline groundwater elevation regardless of precipitation, surface water flow, or evapotranspiration. Groundwater is affected by precipitation, surface water flow, and evapotranspiration based on the groundwater hydrographs, Wetbud actual water levels, and the Wetbud Advanced Scenario hydrographs.

Similar to precipitation, tidal forcing affects groundwater flow, but is not the principal component. The tidal forcing influences the groundwater gradient as shown in Figures 14 and 15. During flood tide, the groundwater gradient is lessened or non-existent. The gradient steepens during the ebb tide allow groundwater to exit the wetland more readily. Thus, the groundwater gradient fluctuation coincides with the tidal signal from Neabsco Creek. Groundwater remains the principal wetland hydrology component at Julie Metz, but is significantly influenced by precipitation and tidal forcings.

Tidal Analysis

The tidal forcing at Julie Metz was analyzed using the T_TIDE function in Matlab. The function separated the tidal signal into many components, designating 46% of the components as lunar or solar and 54% of the components as influenced by wind or regional watershed flow. Figure 7 illustrates the impact of wind. Strong winds from the South on 4 October 2014 correspond with the heightened water elevations at MW9B, Neabsco Creek, and the Washington, D.C. station during the same time period.

Sea Level Rise Analysis

As sea level continues to rise, wetlands will either adapt by migrating inland or become inundated and lost. At Julie Metz, the rate of sea level rise (4.14 mm/year) predicts consistent inundation will occur during flood tides at Pod 3A in 22 years. The Pod 3 will become completely inundated in 132 years (Figure 44). Julie Metz will be unable to migrate inland at a sufficient rate because the steep rise of the upland area from the flat floodplain area.

The inundation predictions at Julie Metz Pod 3 are based on the sea level rise rate. However, the inundation may occur sooner due to the continuing changes in the groundwater gradient as Neabsco Creek rises. Groundwater hydrology at the wetland is affected by the tidal signal. As sea level rises, the flood tide will become the new mean water level and the gradient will lessen over time. Eventually, the groundwater gradient could become negligible.

Wetland Water Budget Importance

A wetland is delineated by its soils, fauna, and groundwater elevation. Wetland soils must have hydric characteristics which include extended saturation, and flooding or ponding during the growing season. The fauna present in a wetland thrive in periodic flooded conditions. Groundwater creates the conditions that allow hydric soils and wetland fauna to flourish. Groundwater elevations must be within 12 inches of the surface during a percentage of the growing season for an area to be considered a wetland. Because groundwater affects the soils and fauna of an area, it should be considered the central part of wetland delineation. Thus, the Wetbud water budget software was developed to generate anticipated water levels based on weather and well data.

The Wetbud Basic Scenario and Advanced Scenario were tested at the Julie Metz wetland. The Basic Scenario pulled weather data and solar data, and used a WETS table to calculate a typical Dry, Normal, and Wet year at Julie Metz. Additionally, groundwater data from monitoring wells at Julie Metz were used to calculate the effective monthly recharge (W_{em}) and graphically displayed groundwater levels on a monthly scale. The Basic Scenario data was used as the foundation to generate the Advanced Scenario. The Advanced Scenario used a time solver on a daily scale and a grid format to spatially show the groundwater distribution at a given cell location and time step. The advantage for the Advanced Scenario is the ability to generate a model with a topographic profile and water level data at both a spatial and temporal scale. The Advanced Scenario is restricted by the number of layers available, four, and the daily time step limitation. At Julie Metz, the Advanced Scenario was not used to develop a model for the tidally-influenced Pod 3A because the time step could not be refined to an hourly time step. Fortunately, Julie Metz did not require more than four layers to generate an effective model for Pod 3B. Wetland systems with more than four distinct geologic layers would require some modification or unification to develop a water budget using the Wetbud Advanced Scenario. The unification of geologic layers may diminish the realistic model output of the Advanced Scenario.

Julie Metz is a unique wetland setting because of the combination of surface water, groundwater and tidal forcing components. Additionally, the wetland has a highly permeable basal gravel layer. The combination of the tidal forcing and highly permeable setting allows the tidal forcing to be shown in the wetland hydrology. The Julie Metz topography and permeable gravel layer provided a setting to observe the effects of precipitation and tidal forcings on the

groundwater hydrographs and support the hypothesis that groundwater is the principal water source controlling water variability.

Mitigation wetlands have previously been constructed by installing an impermeable clay layer to negate the groundwater component of the water budget. Developing a Wetbud water budget at Julie Metz increases the locations where mitigation wetlands can be constructed, adding highly permeable areas. However, Julie Metz revealed the limitations of Wetbud. The water budget software would not be ideal for constructing or enhancing wetlands in a tidal setting.

Wetbud's strength is its ability to predict water levels during specific time periods allows consultants to use the software for wetland enhancement or construction. Wetbud water budget software would aid consultants in constructing mitigated wetlands in highly permeable settings with shallow water tables, but not in tidal settings. Regulators could use Wetbud to efficiently delineate a wetland area using groundwater elevations as a starting point, followed by the soil type and fauna present.

REFERENCES CITED

- Aungsakul, K., Jaroensutasinee, M., & Jaroensutasinee, K. 2011. Numerical study of principal tidal constituents in the Gulf of Thailand and the Andaman Sea. *Walailak Journal of Science and Technology (WJST)*, 4(1), 95-109.
- Allen, R. 2005. Penman–Monteith Equation. *Encyclopedia of Soils in the Environment*, p. 180-188. doi:10.1016/b0-12-348530-4/00399-4.
- Barlow, P. M., & Harbaugh, A. W. 2006. USGS directions in MODFLOW development. *Groundwater*, 44(6), 771-774.
- Brinson, M. M. 1993. *A hydrogeomorphic classification for wetlands*. East Carolina University, Greenville, NC.
- Brown S. and Veneman, P. 1998. *Compensatory Wetland Mitigation in Massachusetts*, Research Bulletin Number 746, Massachusetts Agricultural Experiment Station, University of Massachusetts, Amherst.
- DeWeese, J. 1994. An Evaluation of Selected Wetland Creation Projects Authorized through the Corps of Engineers Section 404 Program, U.S. Fish and Wildlife Service, Sacramento, CA.
- Dingman, S. L. 2015. *Physical hydrology*. Waveland press.
- Dobbs, K.M., Stone, S.F., Agioutantis, Z., Hiza, B., Haering, K.C., Neuhaus, E., Wynn-Thompson, T., Whittecar, G.R., Daniels, W.L. WETBUD PLUS Wetland Water Budget Modeling Software User's Manual. 2016.
- Ezer, T., & Atkinson, L. P. 2015. Sea Level Rise in Virginia—Causes, Effects and Response. *Virginia Journal of Science*, 66(3),8.
- Fetter, C.W. 2001. *Applied Hydrogeology*, 4th ed., Upper Saddle River, New Jersey: Prentice Hall.
- Kent, D. M. 2001. *Applied wetlands science and technology*. Boca Raton, FL: Lewis Publishers.
- Gallihugh, J. L. 1998. *Wetland Mitigation and 404 Permit Compliance Study*, Vol. 1. Report and Appendices A, B, C, D, E, U.S. Fish and Wildlife Service, Barrington, IL.
- Hammer, Donald A., ed. *Constructed wetlands for wastewater treatment: municipal, industrial and agricultural*. CRC Press, 1989. Chapter 2 pp 10-12.
- Hey, D. L., & Philippi, N. S. 1999. *A case for wetland restoration*. New York: Wiley.

- Jacob, C. 1950. Flow of groundwater. *Engineering hydraulics*, 5, 321.
- Lim, K. J., Engel, B. A., Muthukrishnan, S., & Harbor, J. 2006. Effects of Initial Abstraction and Urbanization on Estimated Runoff Using Cn Technology1.
- Lu, J., Sun, G., McNulty, S. G., & Amatya, D. M. 2005. A comparison of six potential evapotranspiration methods for regional use in the southeastern United States.
- Maidment, D. R. 1993. *Handbook of hydrology*. New York: McGraw-Hill.
- McLeod, J.M. 2013. Hydrogeologic analysis of factors that influence pitcher plant bog viability at the Joseph Pines Preserve, Sussex, Virginia [M.S. Thesis]: Old Dominion University, Norfolk, VA, 77 p.
- Meng, A. A., & Harsh, J. F. 1988. *Hydrogeologic framework of the Virginia coastal plain*. US Government Printing Office.
- Merwade, V. 2012. Creating SCS Curve Number Grid using HEC-GeoHMS. *Purdue University*.
- Mitsch, J. M., & Gosselink, J. G. 1993. *Wetlands*. International Thomson Publishing, Inc.
- Mixon, R.B., Southwick, D.L., and Reed, J.C. 1972. *Geologic map of the Quantico Quadrangle, Prince William and Stafford Counties, Virginia, and Charles County, Maryland* [map]. (ca. 1:24,000) Retrieved from http://ngmdb.usgs.gov/Prodesc/proddesc_10589.htm.
- Moriasi, D. N., J. G. Arnold, M. W. Van Liew, R. L. Bingner, R. D. Harmel, and T. L. Veith. 2007. Model evaluation guidelines for systematic quantification of accuracy in watershed simulations. *Transactions of the Asabe* 50(3):885-900.
- Myers, D. R. 2002. Uncertainty for Satellite and Station Solar Data in the Updated NSRDB. *Solar Energy*, 73(5), 307-317.
- Nash, J.E. and Sutcliffe, J.V. 1970. River flow forecasting through conceptual models part I – A discussion of principles: *Journal of Hydrology*, v.10, p. 282-290.
- National Mitigation Bank Association. 2011. Julie J. Metz Wetland Bank, Woodbridge. Available online at <http://www.mitigationbanking.org/mitigationbanks/index.html>. Accessed [03/09/2015].
- National Research Council. 2001. *Compensating for Wetland Losses Under the Clean Water Act*, National Academy Press, Washington, D.C., pp. 82, 160-4
- Natural Resource Conservation Service (NRCS). http://www.nrcs.usda.gov/wps/portal/nrcs/detail/soils/use/hydric/?cid=nrcs142p2_053961. Accessed [02/03/2016].

- Pawlowicz, R., Beardsley, B., & Lentz, S. 2002. Classical tidal harmonic analysis including error estimates in MATLAB using T_TIDE. *Computers & Geosciences*, 28(8), 929-937.
- Pierce, G.J. 1993. Planning hydrology for constructed wetlands, Poolesville, MD: Wetland Training Institute.
- Pitt, R. 2005. WinTR55 for Watershed Analyses.
- Redmond, A. 1991. Report on the Effectiveness of Permitted Mitigation, Florida Department of Environmental Regulation.
- Sanford, W. E., & Selnick, D. L. 2013. Estimation of Evapotranspiration Across the Conterminous United States Using a Regression With Climate and Land-Cover Data. *JAWRA Journal of the American Water Resources Association*, 49(1), p. 217- 230.
- Soil Survey Staff, Natural Resources Conservation Service, United States Department of Agriculture. Web Soil Survey. Available online at <http://websoilsurvey.nrcs.usda.gov/>. Accessed [02/03/2016].
- Sprecher, S. W., & Warne, A. G. 2000. *Accessing and using meteorological data to evaluate wetland hydrology* (No. ERDC/EL-TR-WRAP-00-1). ENGINEER RESEARCH AND DEVELOPMENT CENTER VICKSBURG MS ENVIRONMENTAL LAB.
- Titus, J.G., & Anderson, K.E. 2009. *Coastal sensitivity to sea-level rise: a focus on the mid-Atlantic region*. Government Printing Office.
- USDA. 1986. Natural Resources Conservation Service (NRCS). *Technical Release 55: Urban hydrology for small watersheds*, 2nd ed., Washington, D.C.
- Wetland Studies and Solutions, Inc (WSSI). 2011. Corporate Biography. Available online at <http://www.wetlandstudies.com/about-wssi/mission-statement.html>. Accessed [03/10/2015].
- Whittecarr, G. R., Dobbs, K. M., Stone, S. A., McLeod, J. M., Thornton, T. L., & Smith, J. C. 2017. Use of the Effective Monthly Recharge model to assess long-term water-level fluctuations in and around groundwater-dominated wetlands. *Ecological Engineering*, 99, 462-472.
- Whittecarr, G. R., & Lawrence, J. R. 1999. Hydrology and Geomorphology of Green Pond—a High-elevation Depressional Wetland in the Blue Ridge of Virginia. *Banisteria*, 13, 149-159.
- Whittecarr, G.R., Newell, W.L., and Eaton, L.S. 2016. Landscape Evolution in Virginia, pg. 259-291. In: The Geology of Virginia. Bailey, C.M., Eaton, L.S., and Sherwood, W.C. (eds.), Virginia Museum of Natural History, Special Publication 18.

Xiong, Y., & Berger, C. R. 2010. Chesapeake Bay Tidal Characteristics. *Journal of Water Resource and Protection*, 2(07), 619.

APPENDIX A

BOREHOLE LOGS AND WELL COMPLETION REPORTS

Borehole Log

Project: Julie J. Metz Wetland Bank

Location: Julie Metz Wetland – WOODBRIDGE, VA

Lat: 38.605900

Long: -77.277470

Borehole Name: SB 1

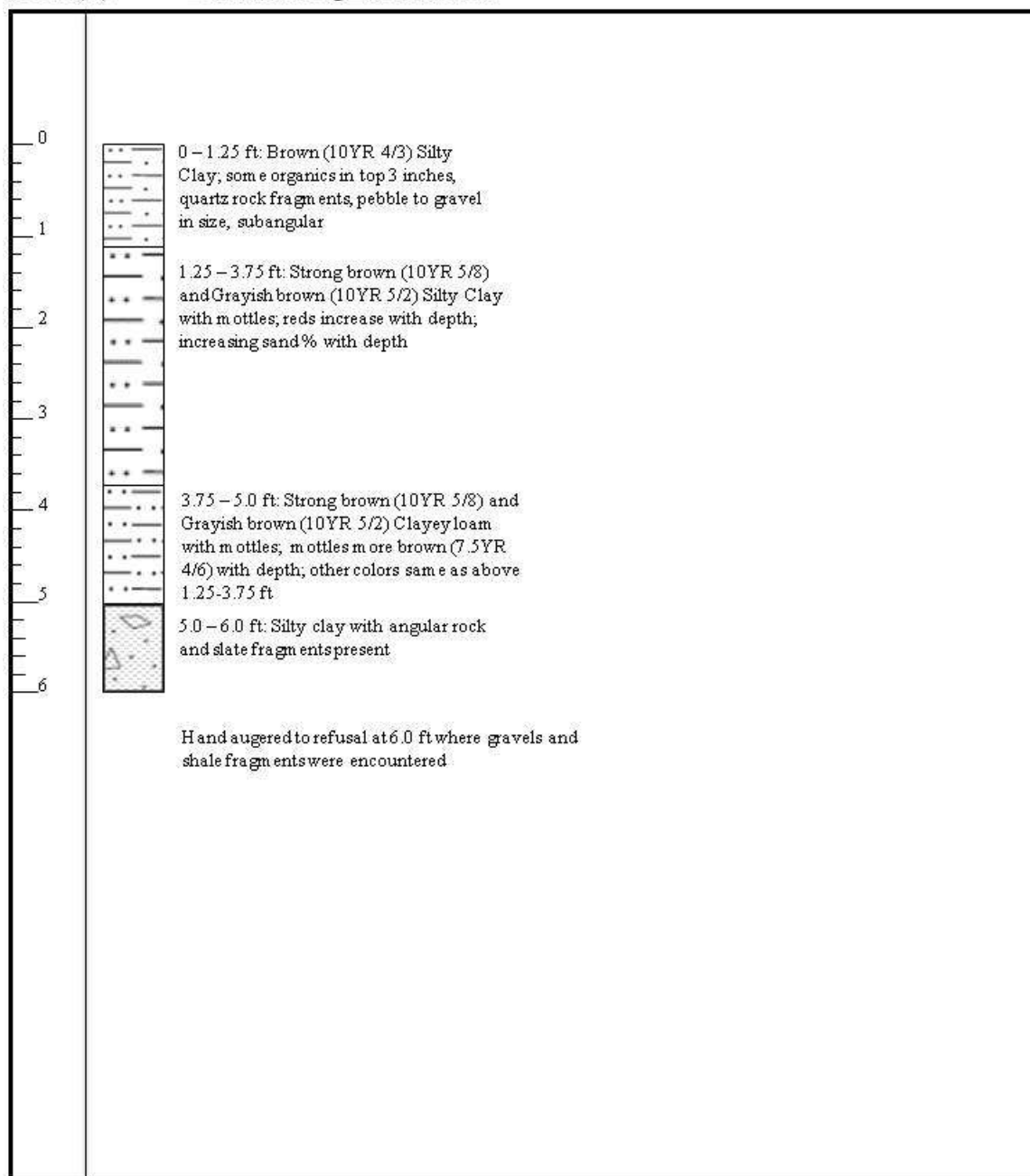
Completed by: B. Hiza, S. Stone

Construction Date: 05/29/2014

Auger Type: Hand auger

Scale (ft)

Borehole Log Information



Borehole Log

Project: Julie J. Metz Wetland Bank

Location: Julie Metz Wetland – WOODBRIDGE, VA

Lat: 38.607660

Long: -77.278790

Borehole Name: SB2

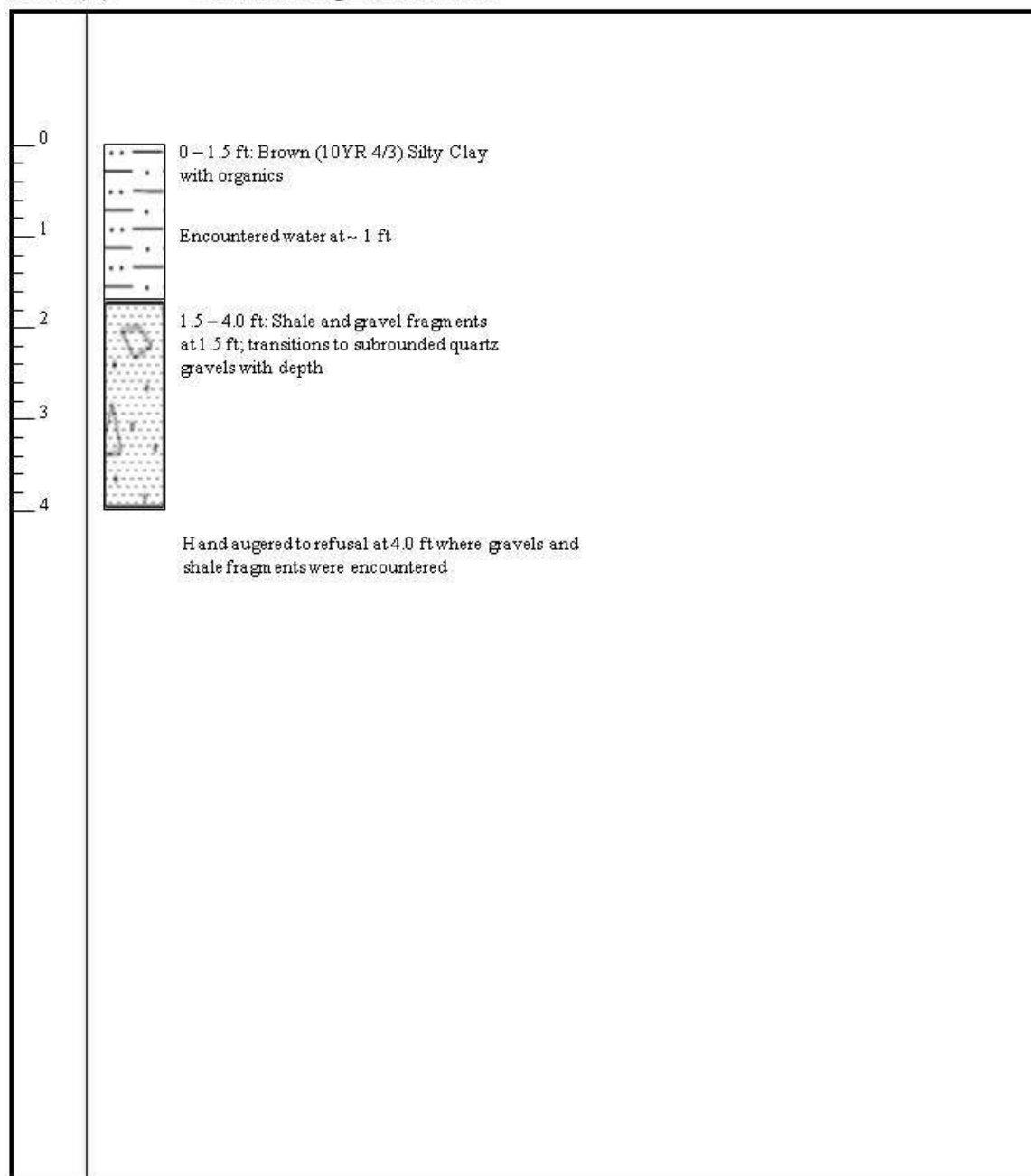
Completed by: B. Hiza, S. Stone

Construction Date: 06/16/2014

Auger Type: Hand auger

Scale (ft)

Borehole Log Information



Borehole Log

Project: Julie J. Metz Wetland Bank

Location: Julie Metz Wetland – WOODBRIDGE, VA

Lat: 38.607540

Long: -77.278370

Borehole Name: SB3

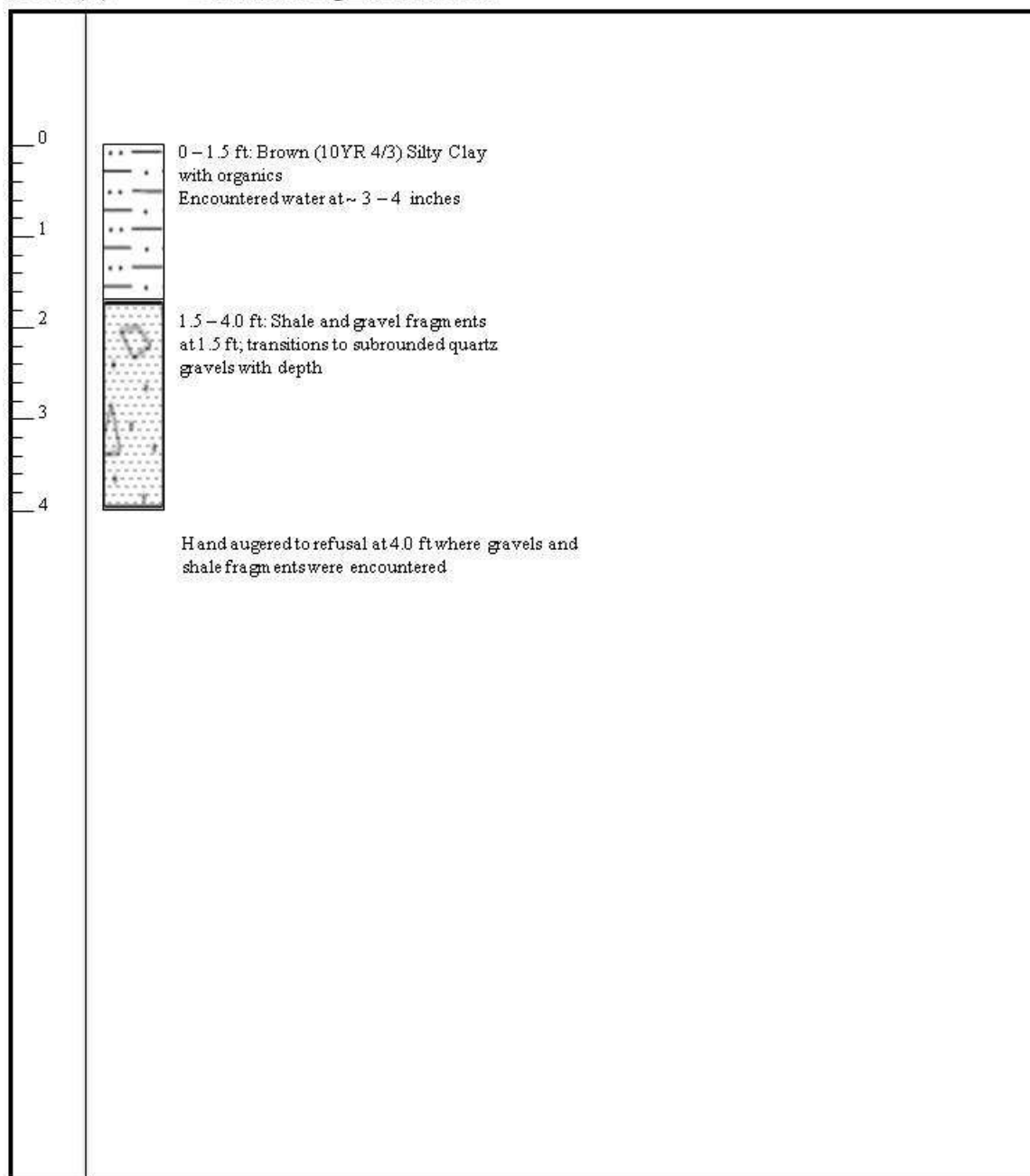
Completed by: B. Hiza, S. Stone

Construction Date: 06/16/2014

Auger Type: Hand auger

Scale (ft)

Borehole Log Information



Borehole Log

Project: Julie J. Metz Wetland Bank

Location: Julie Metz Wetland – WOODBRIDGE, VA

Lat: 38.606720

Long: -77.276060

Borehole Name: SB4

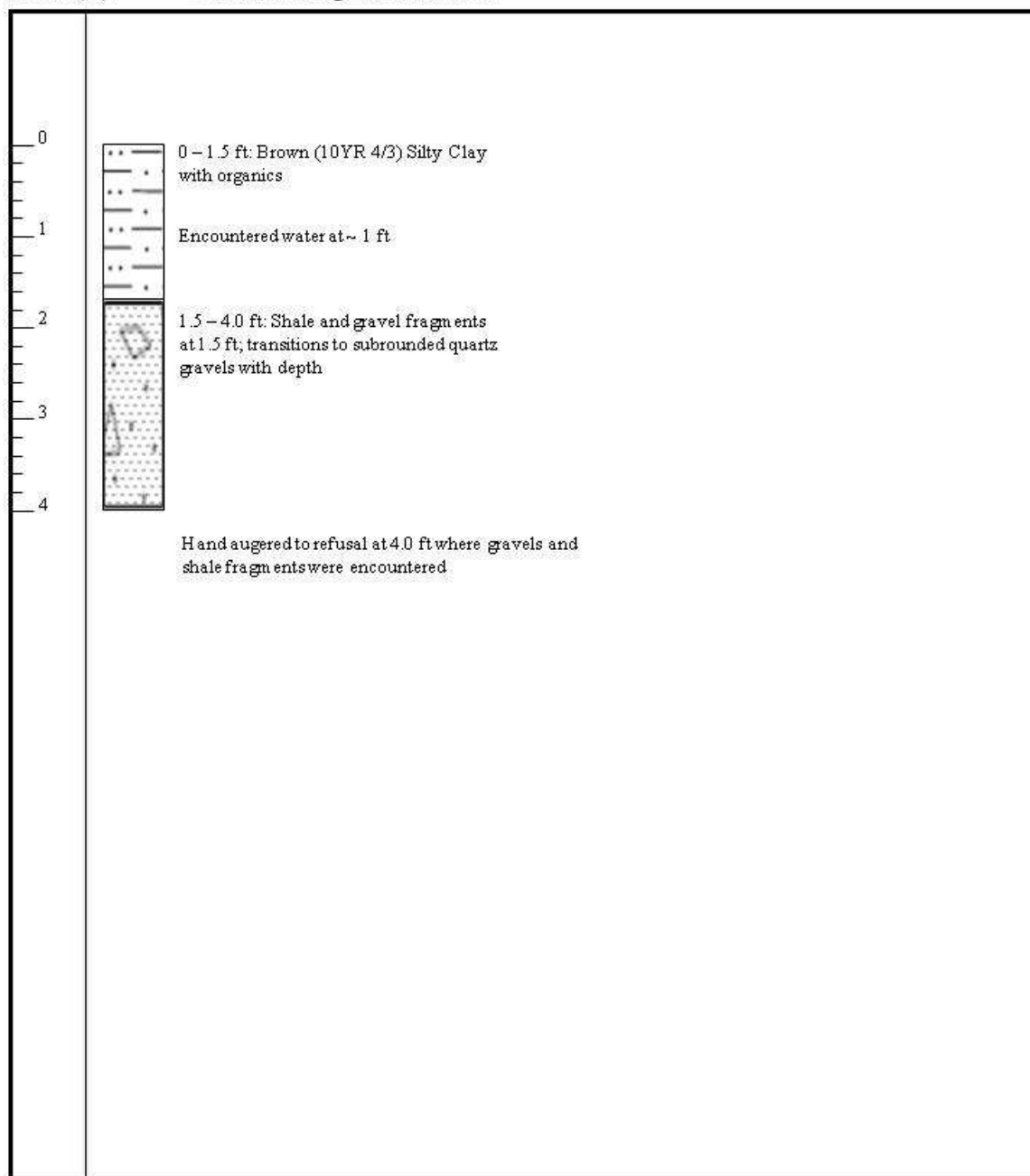
Completed by: B. Hiza, S. Stone

Construction Date: 06/16/2014

Auger Type: Hand auger

Scale (ft)

Borehole Log Information



Borehole Log

Project: Julie J. Metz Wetland Bank

Location: Julie Metz Wetland – WOODBRIDGE, VA

Lat: 38.606570

Long: -77.276480

Borehole Name: SB5

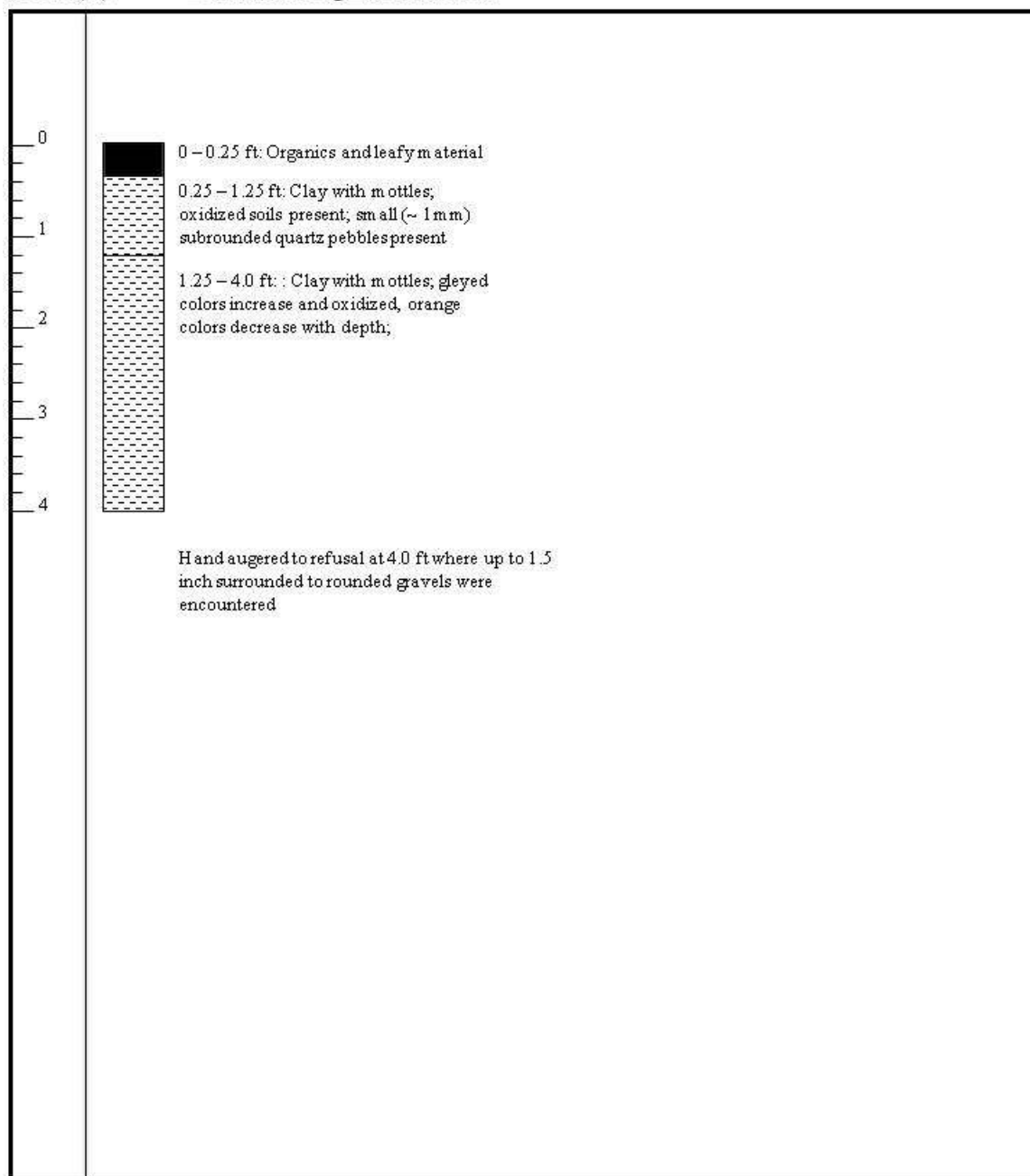
Completed by: B. Hiza, S. Stone

Construction Date: 06/16/2014

Auger Type: Hand auger

Scale (ft)

Borehole Log Information



Borehole Log

Project: Julie J. Metz Wetland Bank

Location: Julie Metz Wetland – WOODBRIDGE, VA

Lat: 38.605660

Long: -77.277690

Borehole Name: SB6

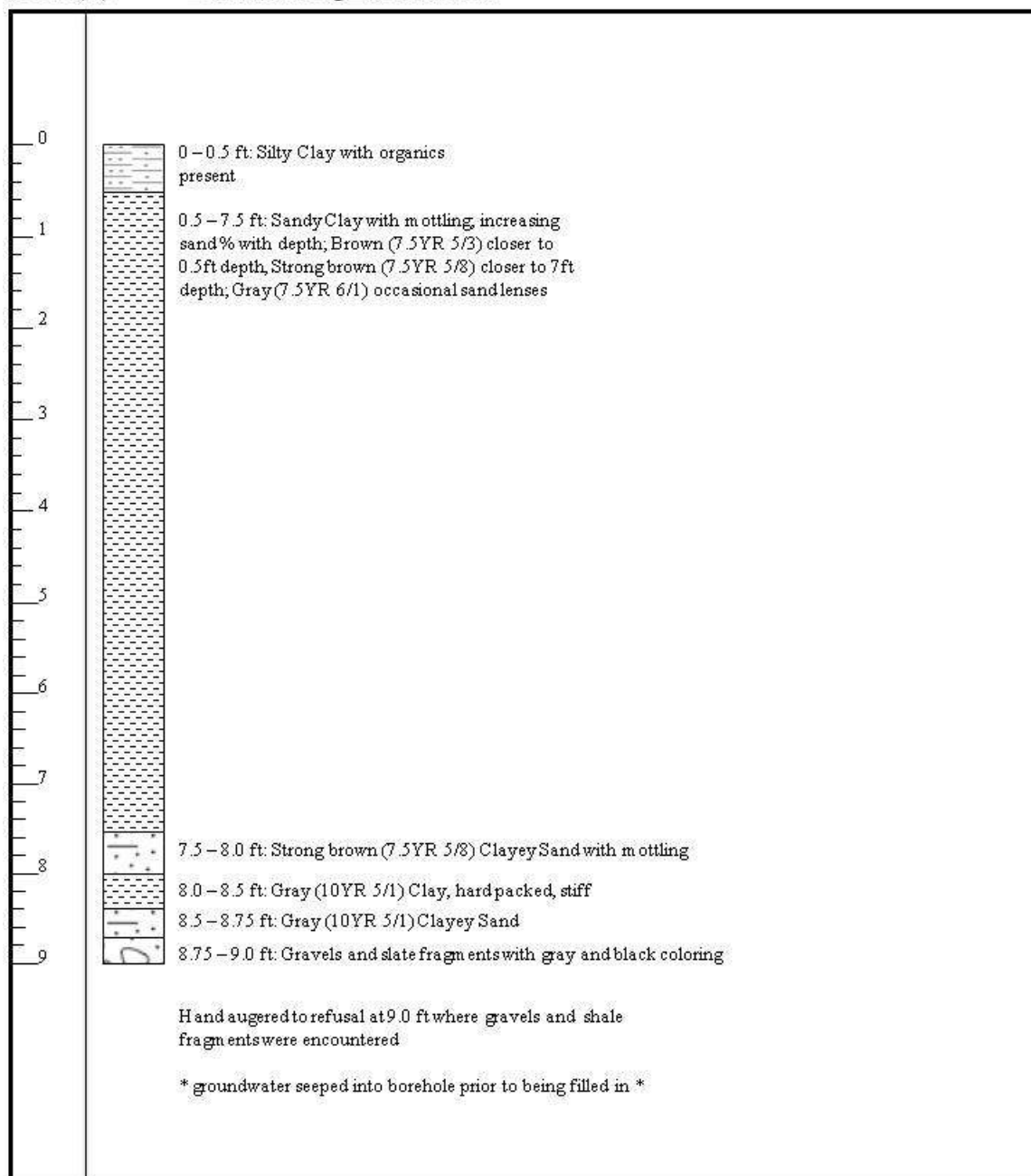
Completed by: B. Hiza, S. Stone

Construction Date: 06/16/2014

Auger Type: Hand auger

Scale (ft)

Borehole Log Information



Borehole Log

Project: Julie J. Metz Wetland Bank

Location: Julie Metz Wetland – WOODBRIDGE, VA

Lat: 38.605230

Long: -77.274410

Borehole Name: SB7

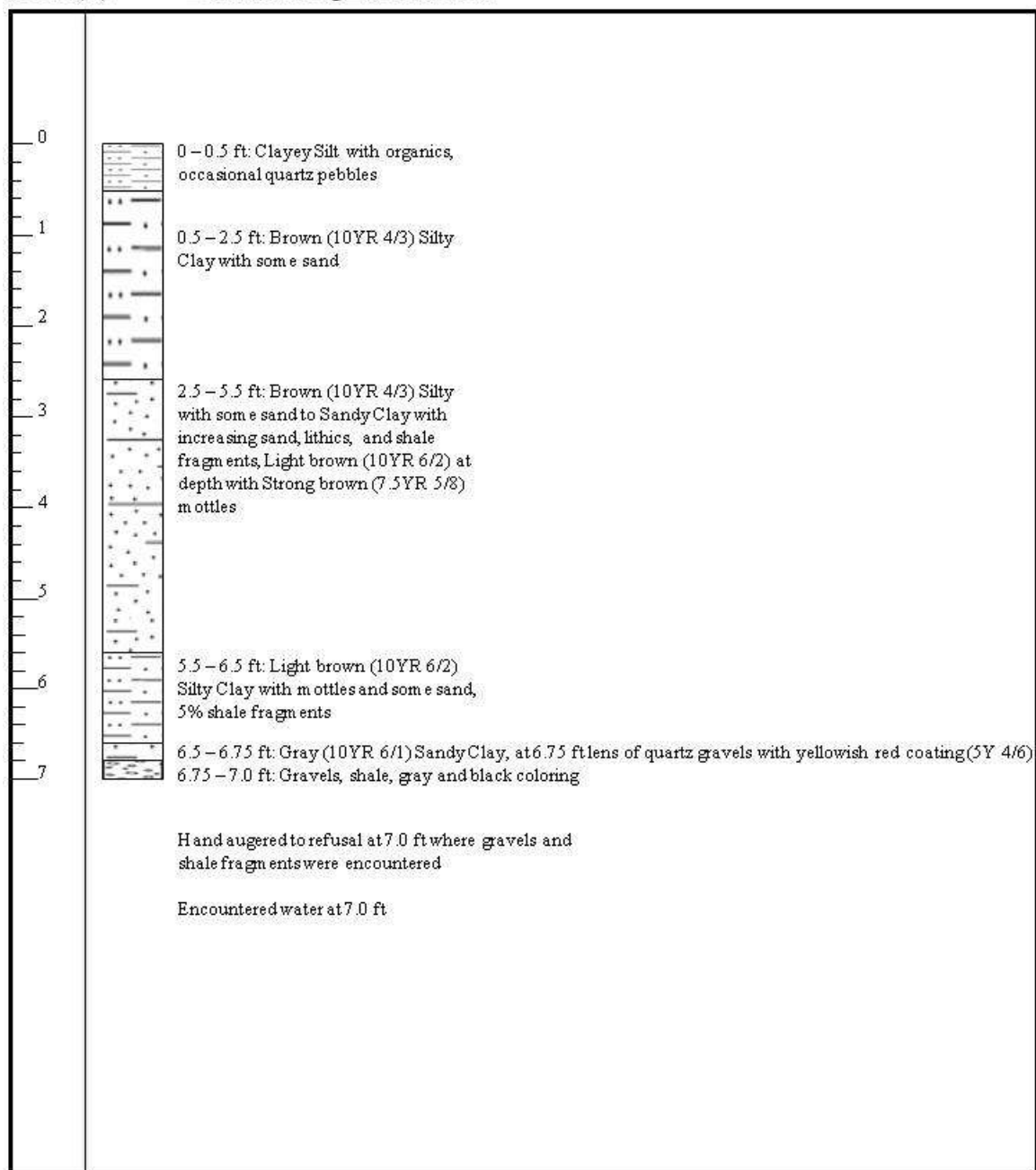
Completed by: B. Hiza, S. Stone

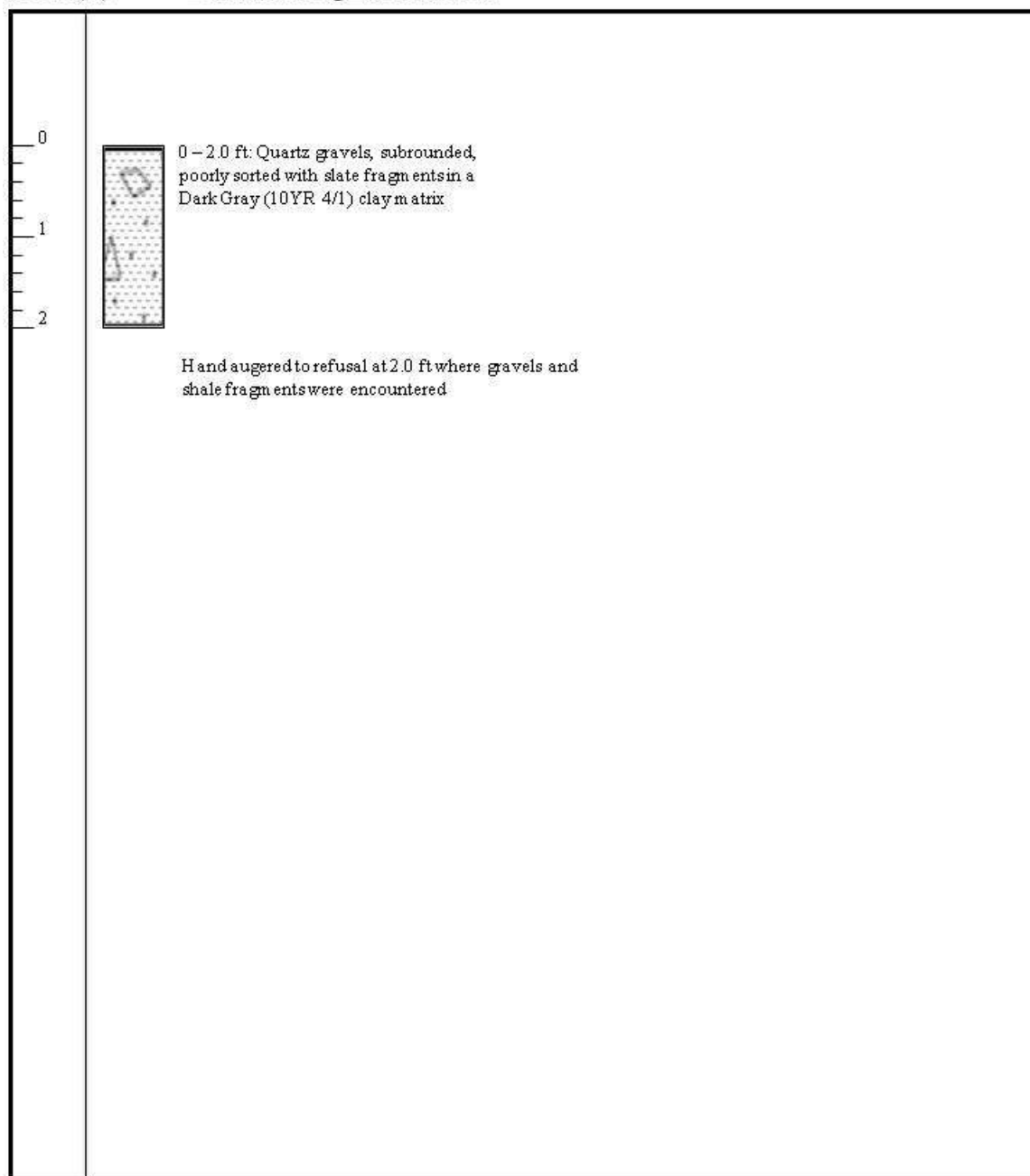
Construction Date: 06/16/2014

Auger Type: Hand auger

Scale (ft)

Borehole Log Information



Borehole Log**Project:** Julie J. Metz Wetland Bank**Location:** Julie Metz Wetland – WOODBRIDGE, VA**Lat:** 38.606890**Long:** -77.278830**Borehole Name:** SB8**Completed by:** B. Hiza, S. Stone**Construction Date:** 07/30/2014**Auger Type:** Hand auger**Scale (ft)****Borehole Log Information**

Borehole Log

Project: Julie J. Metz Wetland Bank

Location: Julie Metz Wetland – WOODBRIDGE, VA

Lat: 38.606690

Long: -77.278750

Borehole Name: SB9

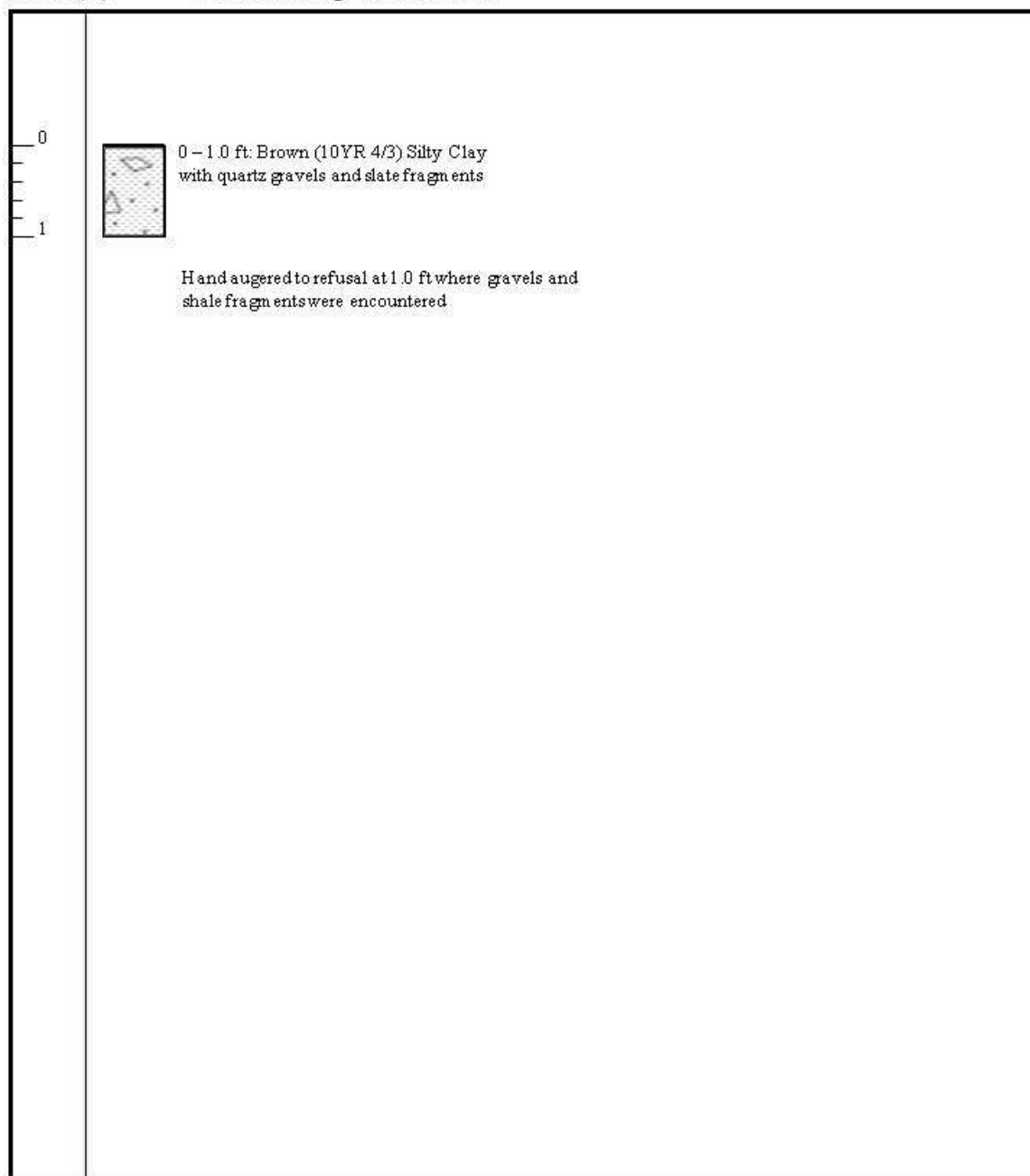
Completed by: B. Hiza, S. Stone

Construction Date: 07/30/2014

Auger Type: Hand auger

Scale (ft)

Borehole Log Information



Well Completion Report

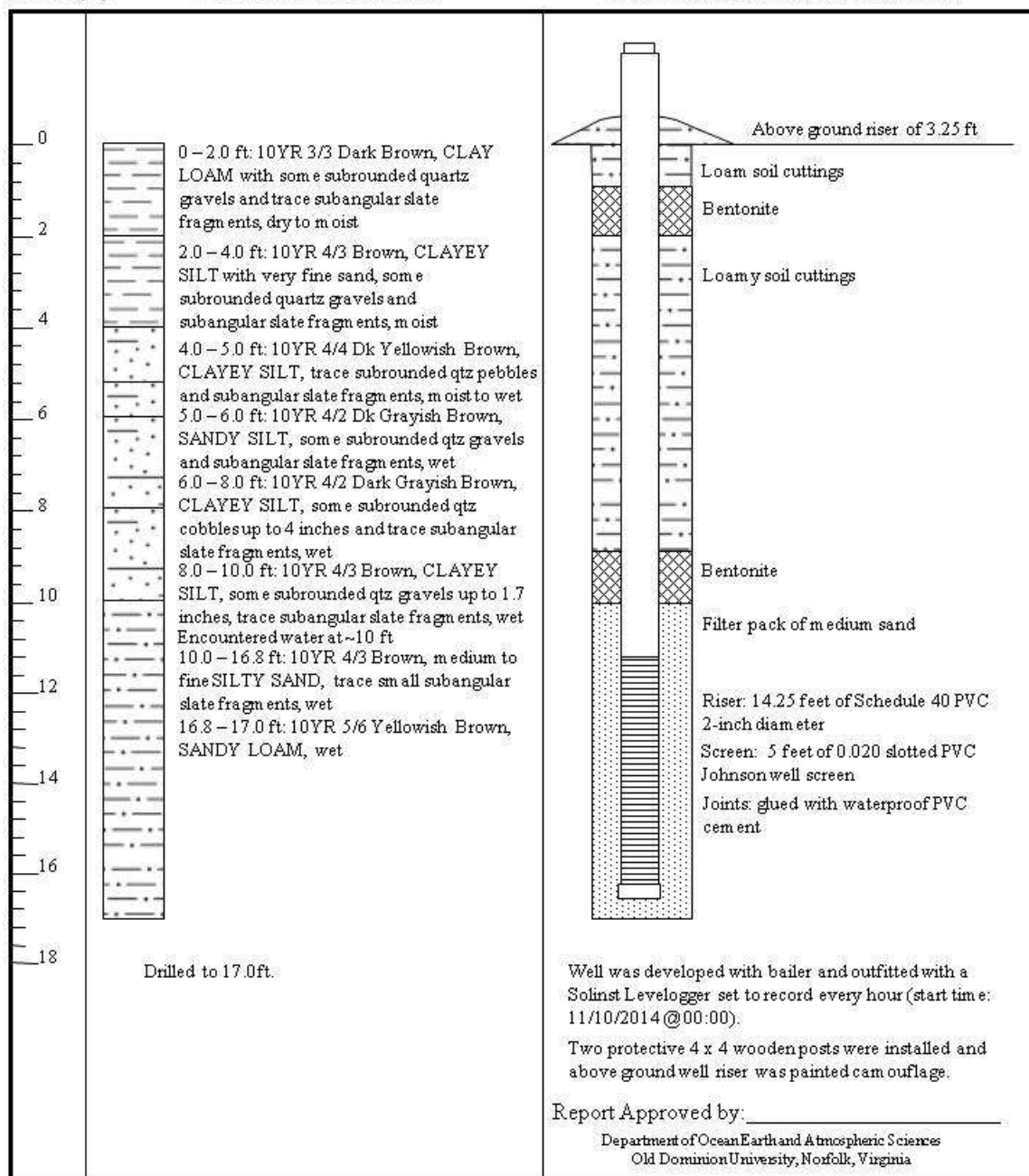
Project: Julie J. Metz Wetland Bank
Location: Julie Metz Wetland – WOODBRIDGE, VA
Lat: 38.605845
Long: -77.279189
Top of casing elevation: 9.86 feet

Well Name: MW23
Constructed by: S. Nagle, B. Hiza, S. Stone
Construction Date: 11/05/2014
Auger Type: Drilled with 6-inch hollow-stem auger

Scale (ft)

Borehole Information

Well Construction Information



Well Completion Report

Project: Julie J. Metz Wetland Bank

Location: Julie Metz Wetland – WOODBRIDGE, VA

Lat: 38.605475

Long: -77.277869

Top of casing elevation: 10.71 feet

Well Name: MW24

Constructed by: S. Nagle, B. Hiza, S. Stone

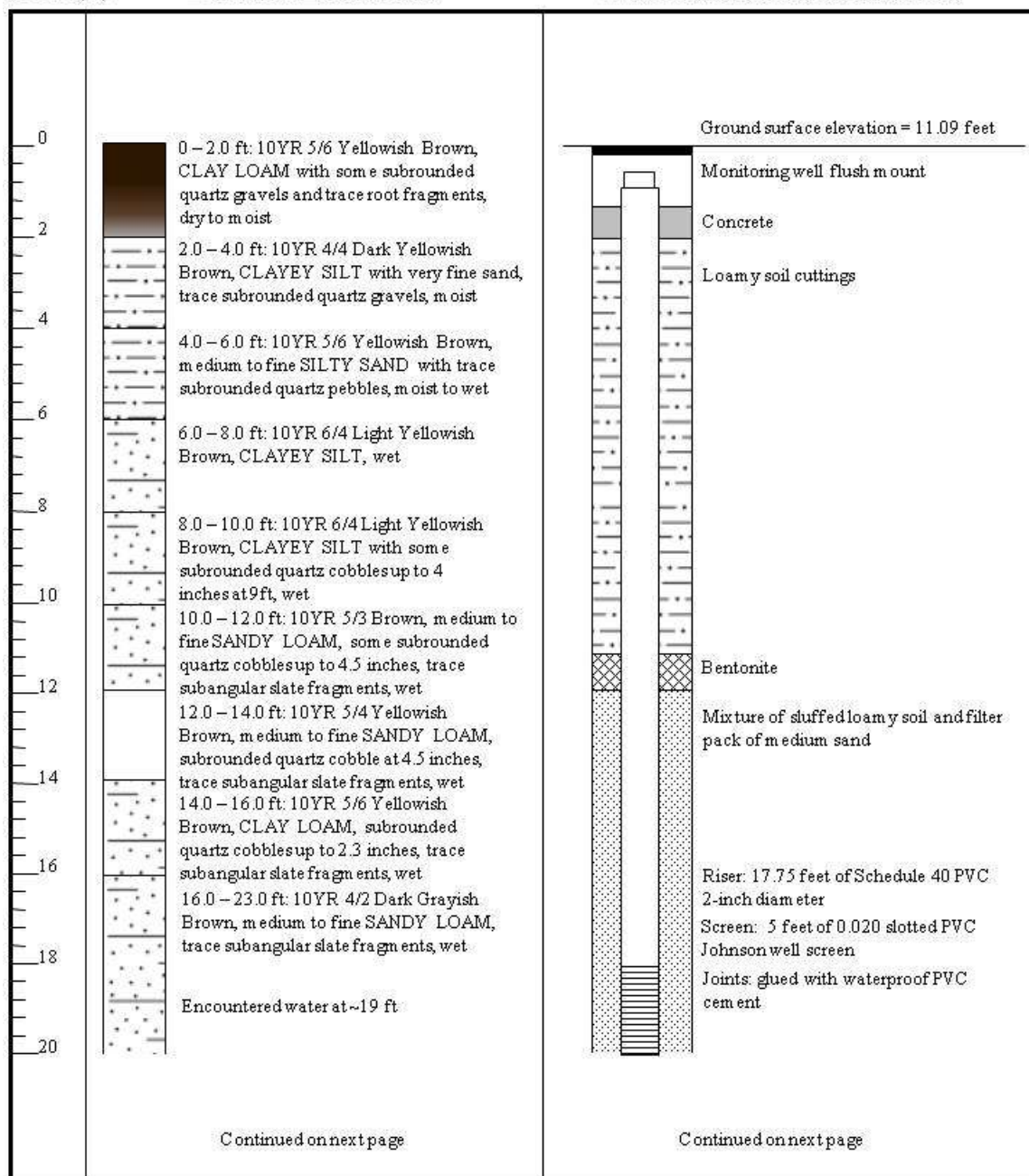
Construction Date: 11/05/2014

Auger Type: Drilled with 6-inch hollow-stem auger

Scale (ft)

Borehole Information

Well Construction Information



Well Completion Report (cont.)

Project: Julie J. Metz Wetland Bank

Location: Julie Metz Wetland – WOODBRIDGE, VA

Lat: 38.605475

Long: -77.277869

Top of casing elevation: 10.71 feet

Well Name: MW24

Constructed by: S. Nagle, B. Hiza, S. Stone

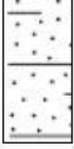
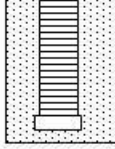
Construction Date: 11/05/2014

Auger Type: Drilled with 6-inch hollow-stem auger

Scale (ft)

Borehole Information

Well Construction Information

<p>20</p> <p>22</p> <p>24</p>	 <p>Drilled to 23.0 ft.</p>	 <p>Well was developed with bailer and outfitted with a Solinst Levellogger set to record every hour (start time: 11/10/2014 @ 00:00).</p>
<p>Report Approved by: _____</p> <p>Department of Ocean Earth and Atmospheric Sciences Old Dominion University, Norfolk, Virginia</p>		

Well Completion Report

Project: Julie J. Metz Wetland Bank

Location: Julie Metz Wetland – WOODBRIDGE, VA

Lat: 38.607694

Long: -77.278889

Top of casing elevation: 4.406 feet

Well Name: Neabsco Creek

Constructed by: B. Hiza, S. Stone

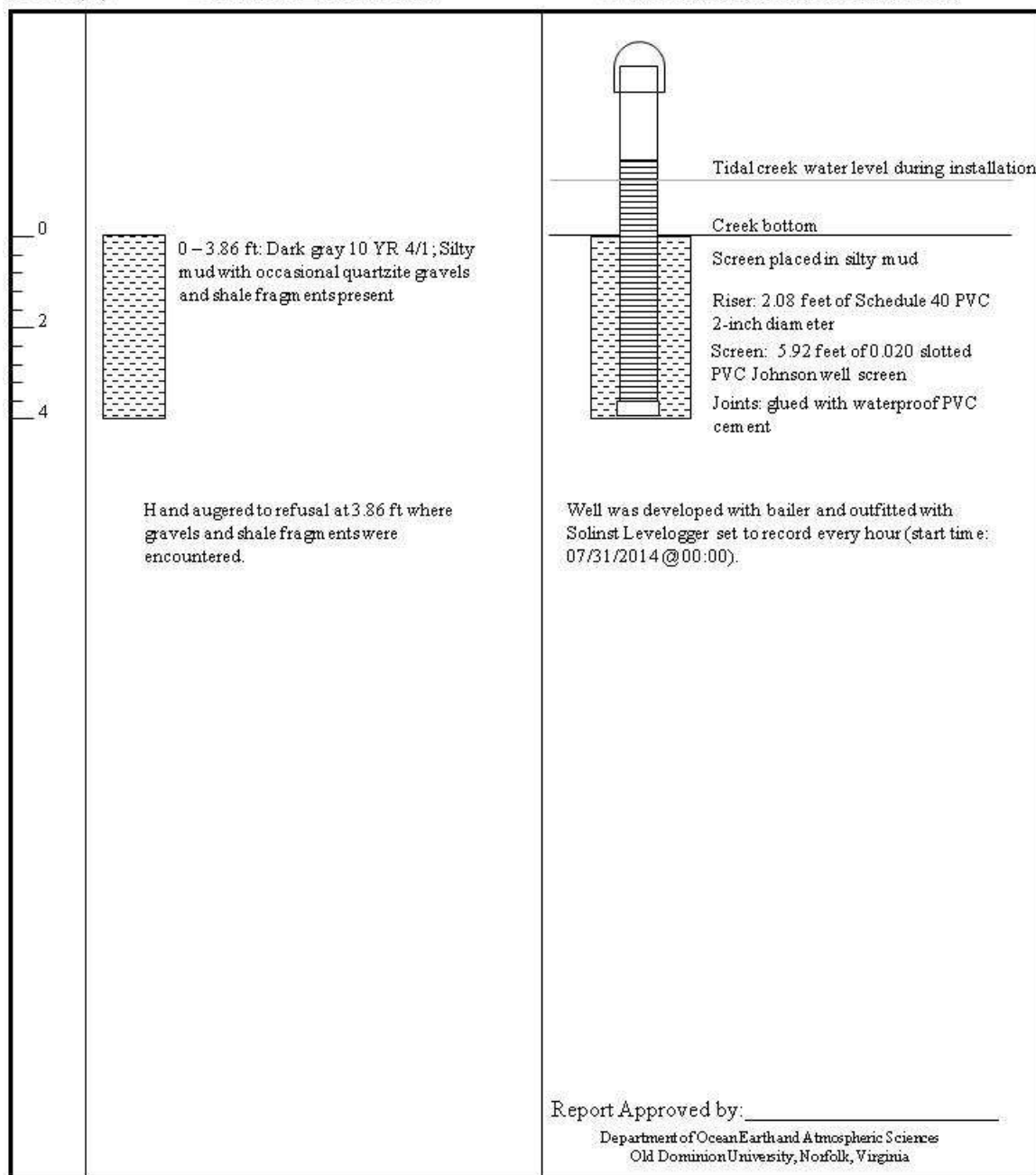
Construction Date: 07/30/2014

Auger Type: Hand auger

Scale (ft)

Borehole Information

Well Construction Information



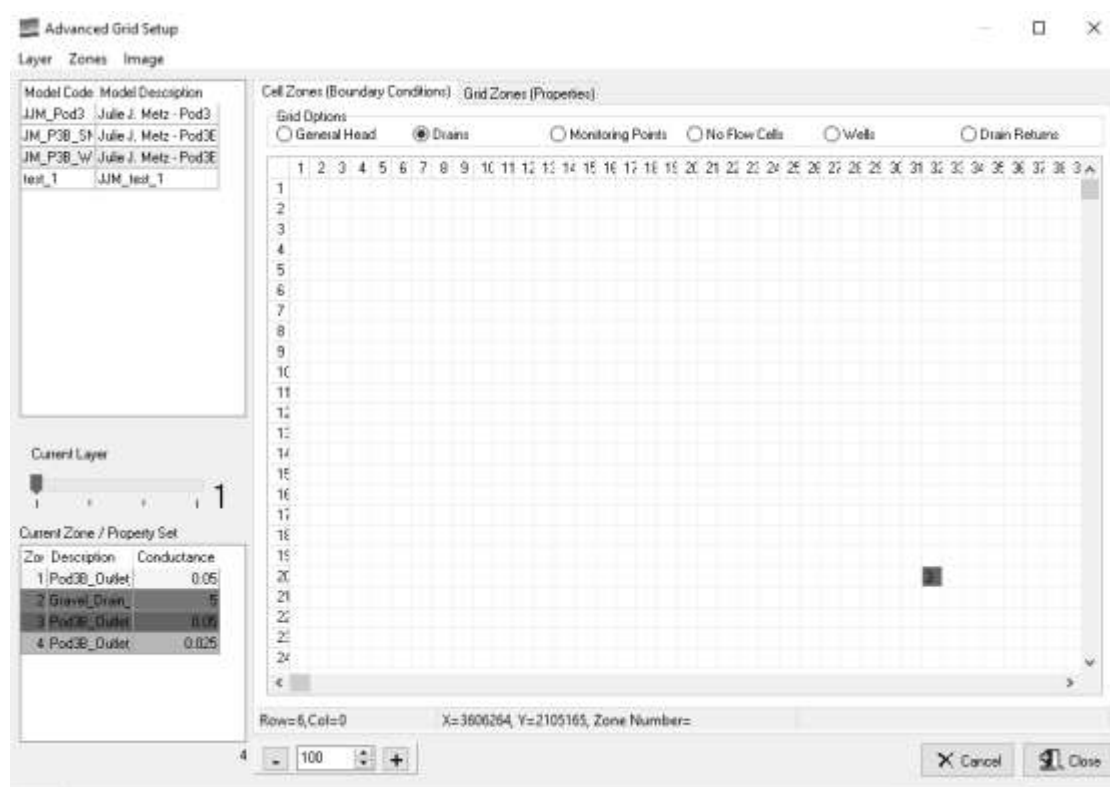
APPENDIX B
COMMON K_{sat} AND S_y VALUES

COMMON K_{sat} AND S_y VALUES

Sediment or Material Type	Hydraulic conductivity* (K_{sat})	Specific yield (S_y)**
	--- m/sec ---	--- % ---
Clean gravel	10^{-2} - 1	20 - 50
Clean coarse sand	10^{-4} - 10^{-2}	15 - 35
Fine sand	10^{-5} - 10^{-3}	10 - 30
Silty sand	10^{-5} - 10^{-4}	10 - 30
Clayey sand	10^{-6} - 10^{-4}	5 - 25
Silt	10^{-10} - 10^{-5}	3 - 20
Clay	10^{-12} - 10^{-8}	0 - 5
Uniformly graded coarse aggregate	0.4 - 10^{-3}	10 - 30
Well-graded coarse aggregate	10^{-5} - 10^{-3}	5 - 25
Concrete sand, variable dust content	10^{-8} - 10^{-4}	5 - 20
Compacted silt	10^{-10} - 10^{-8}	< 5
Compacted clay	< 10^{-9}	< 1

(Dobbs et al., 2016)

APPENDIX C**WETBUD DRAIN CELL ZONE LAYOUT IMAGE**

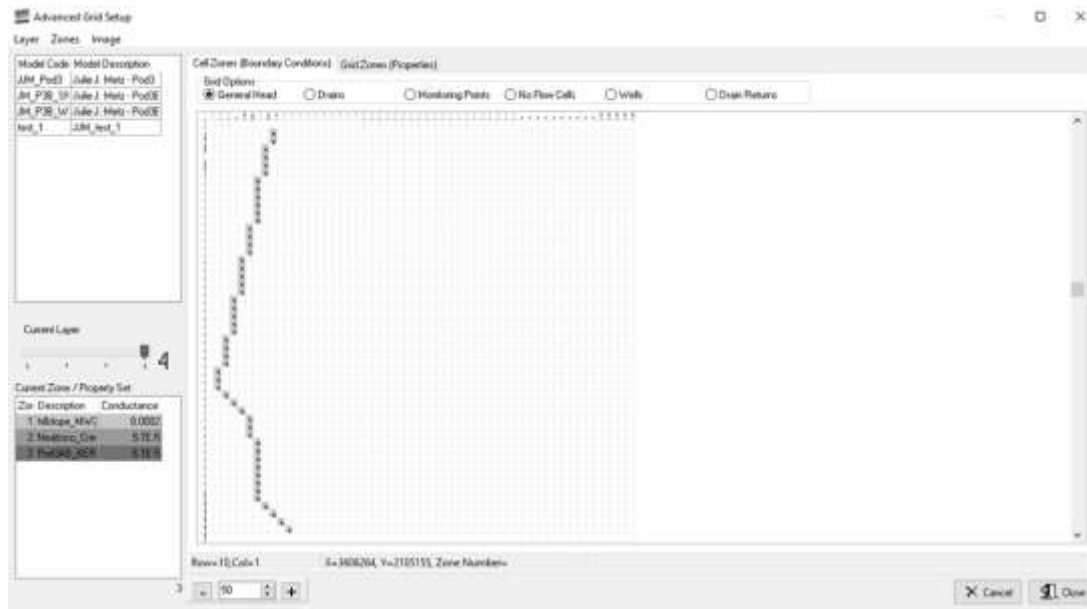


Julie Metz cell zone layout image with the drain location for layer 1 and the conductance value. The drain locations for layers 2 and 3 are the same as in layer 1.

DRAIN CELL LAYER INFORMATION - BOTTOM LEFT OF WETBUD DRAIN CELL ZONE IMAGE

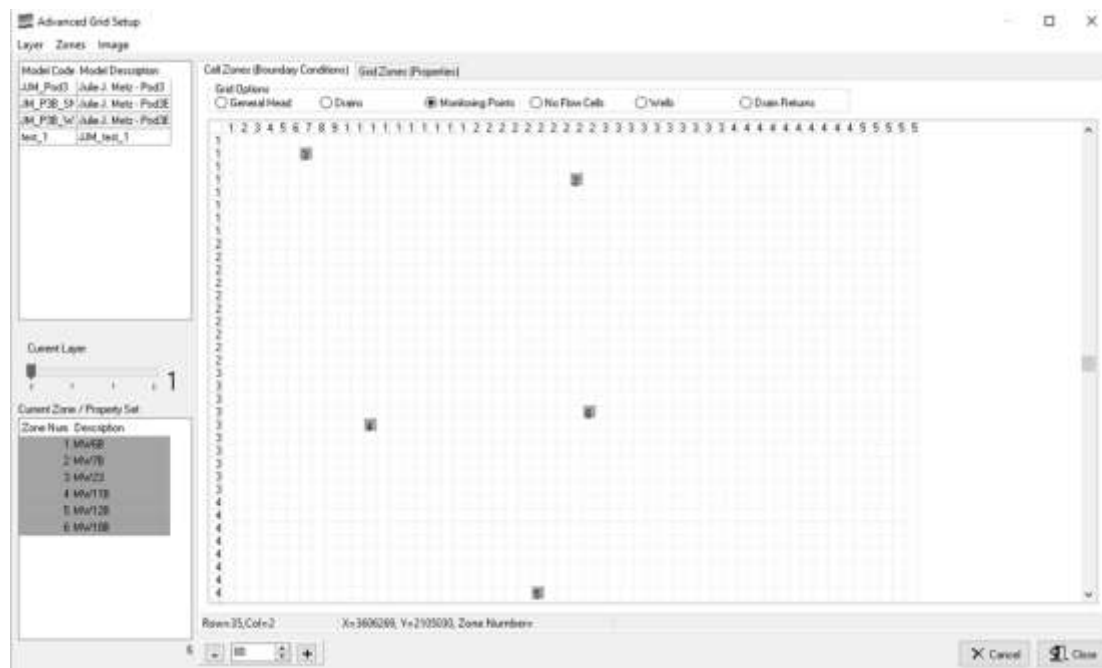
Zone	Layer	Conductance
1	2	0.05
2	N/A	N/A
3	1	0.05
4	3	0.025

APPENDIX D**WETBUD GENERAL HEAD CELL ZONE LAYOUT IMAGE**



Julie Metz cell zone layout image with the general head locations for layer 4 and the conductance value (0.0002).

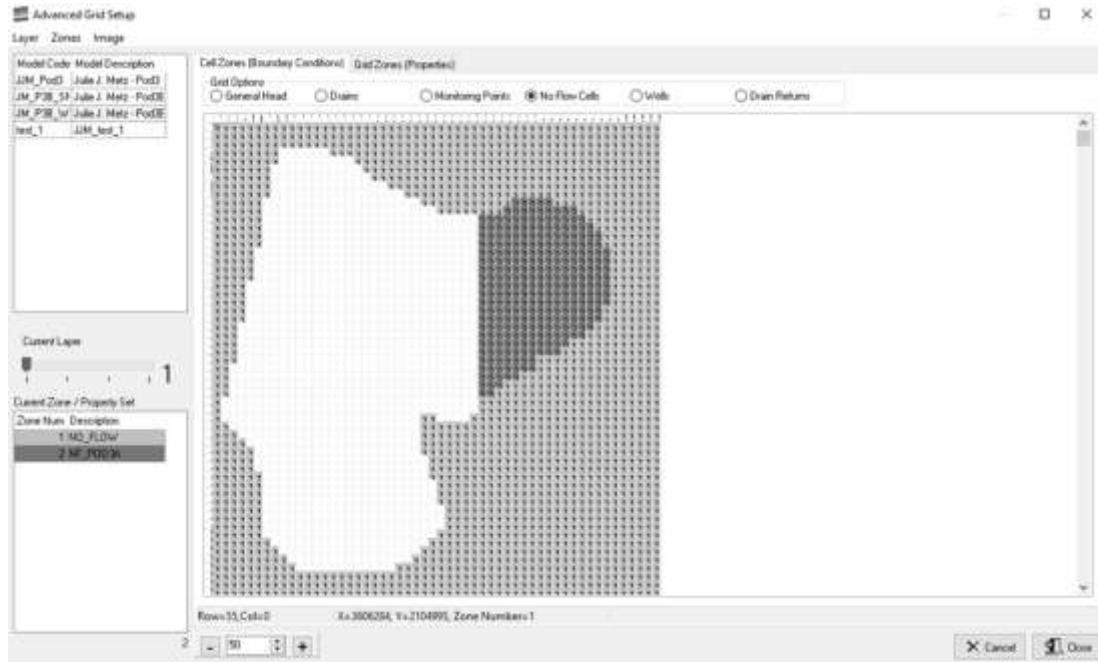
APPENDIX E**WETBUD MONITORING POINT CELL ZONE LAYOUT IMAGE**



Julie Metz cell zone layout image with the monitoring point locations for layer 1.

Layers 2 - 4 have the same monitoring point locations as layer 1.

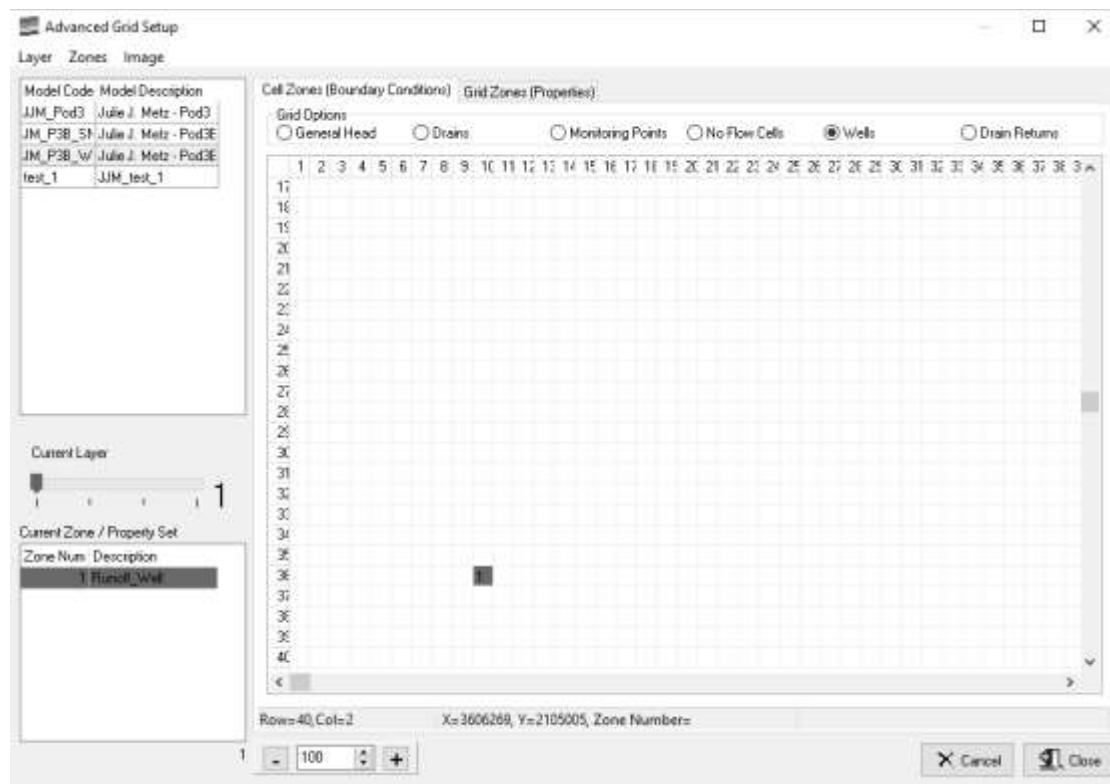
APPENDIX F**WETBUD NO FLOW CELL ZONE LAYOUT IMAGE**



Julie Metz cell zone layout image with the no flow cell locations for layer 1.

Layers 2 - 4 have the same no flow cell locations as layer 1.

APPENDIX G**WETBUD RUNOFF WELL LOCATION IN CELL ZONE LAYOUT IMAGE**



Julie Metz cell zone layout image with the runoff well location in layer 1.

APPENDIX H

WETBUD HYDRAULIC CONDUCTIVITY GRID ZONE LAYOUT IMAGES

Advanced Grid Setup

Layer Zones Image

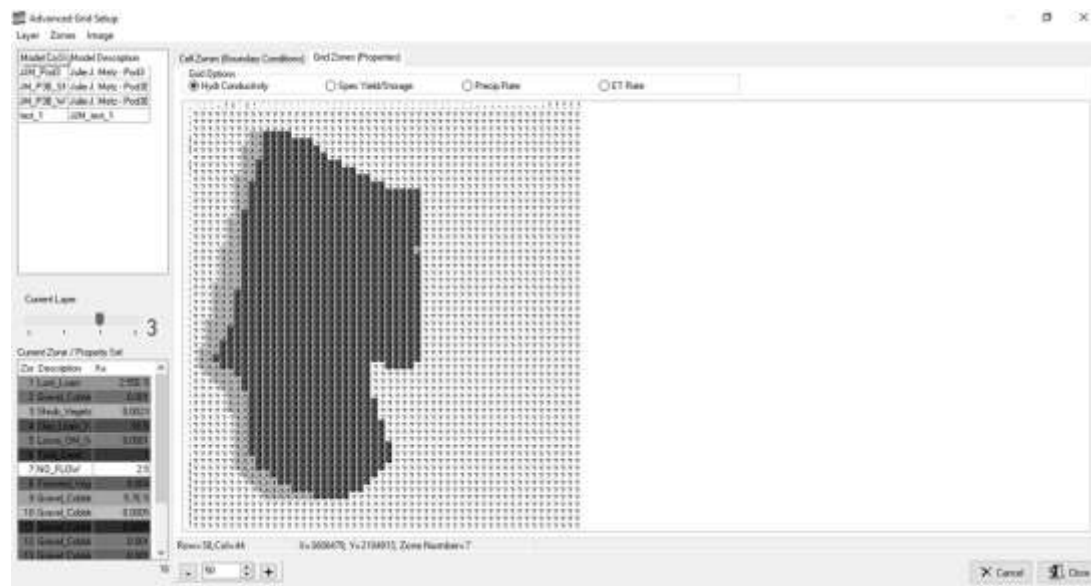
Model Code/Model Description

Model Code	Model Description
JH1_P0d1	Zone 1, Mat: P0d1
JH1_P0d2	Zone 2, Mat: P0d2
JH1_P0d3	Zone 3, Mat: P0d3
JH1_P0d4	Zone 4, Mat: P0d4
JH1_P0d5	Zone 5, Mat: P0d5
JH1_P0d6	Zone 6, Mat: P0d6
JH1_P0d7	Zone 7, Mat: P0d7
JH1_P0d8	Zone 8, Mat: P0d8
JH1_P0d9	Zone 9, Mat: P0d9
JH1_P0d10	Zone 10, Mat: P0d10
JH1_P0d11	Zone 11, Mat: P0d11
JH1_P0d12	Zone 12, Mat: P0d12
JH1_P0d13	Zone 13, Mat: P0d13
JH1_P0d14	Zone 14, Mat: P0d14
JH1_P0d15	Zone 15, Mat: P0d15
JH1_P0d16	Zone 16, Mat: P0d16
JH1_P0d17	Zone 17, Mat: P0d17
JH1_P0d18	Zone 18, Mat: P0d18
JH1_P0d19	Zone 19, Mat: P0d19
JH1_P0d20	Zone 20, Mat: P0d20
JH1_P0d21	Zone 21, Mat: P0d21
JH1_P0d22	Zone 22, Mat: P0d22
JH1_P0d23	Zone 23, Mat: P0d23
JH1_P0d24	Zone 24, Mat: P0d24
JH1_P0d25	Zone 25, Mat: P0d25
JH1_P0d26	Zone 26, Mat: P0d26
JH1_P0d27	Zone 27, Mat: P0d27
JH1_P0d28	Zone 28, Mat: P0d28
JH1_P0d29	Zone 29, Mat: P0d29
JH1_P0d30	Zone 30, Mat: P0d30
JH1_P0d31	Zone 31, Mat: P0d31
JH1_P0d32	Zone 32, Mat: P0d32
JH1_P0d33	Zone 33, Mat: P0d33
JH1_P0d34	Zone 34, Mat: P0d34
JH1_P0d35	Zone 35, Mat: P0d35
JH1_P0d36	Zone 36, Mat: P0d36
JH1_P0d37	Zone 37, Mat: P0d37
JH1_P0d38	Zone 38, Mat: P0d38
JH1_P0d39	Zone 39, Mat: P0d39
JH1_P0d40	Zone 40, Mat: P0d40
JH1_P0d41	Zone 41, Mat: P0d41
JH1_P0d42	Zone 42, Mat: P0d42
JH1_P0d43	Zone 43, Mat: P0d43
JH1_P0d44	Zone 44, Mat: P0d44
JH1_P0d45	Zone 45, Mat: P0d45
JH1_P0d46	Zone 46, Mat: P0d46
JH1_P0d47	Zone 47, Mat: P0d47
JH1_P0d48	Zone 48, Mat: P0d48
JH1_P0d49	Zone 49, Mat: P0d49
JH1_P0d50	Zone 50, Mat: P0d50
JH1_P0d51	Zone 51, Mat: P0d51
JH1_P0d52	Zone 52, Mat: P0d52
JH1_P0d53	Zone 53, Mat: P0d53
JH1_P0d54	Zone 54, Mat: P0d54
JH1_P0d55	Zone 55, Mat: P0d55
JH1_P0d56	Zone 56, Mat: P0d56
JH1_P0d57	Zone 57, Mat: P0d57
JH1_P0d58	Zone 58, Mat: P0d58
JH1_P0d59	Zone 59, Mat: P0d59
JH1_P0d60	Zone 60, Mat: P0d60
JH1_P0d61	Zone 61, Mat: P0d61
JH1_P0d62	Zone 62, Mat: P0d62
JH1_P0d63	Zone 63, Mat: P0d63
JH1_P0d64	Zone 64, Mat: P0d64
JH1_P0d65	Zone 65, Mat: P0d65
JH1_P0d66	Zone 66, Mat: P0d66
JH1_P0d67	Zone 67, Mat: P0d67
JH1_P0d68	Zone 68, Mat: P0d68
JH1_P0d69	Zone 69, Mat: P0d69
JH1_P0d70	Zone 70, Mat: P0d70
JH1_P0d71	Zone 71, Mat: P0d71
JH1_P0d72	Zone 72, Mat: P0d72
JH1_P0d73	Zone 73, Mat: P0d73
JH1_P0d74	Zone 74, Mat: P0d74
JH1_P0d75	Zone 75, Mat: P0d75
JH1_P0d76	Zone 76, Mat: P0d76
JH1_P0d77	Zone 77, Mat: P0d77
JH1_P0d78	Zone 78, Mat: P0d78
JH1_P0d79	Zone 79, Mat: P0d79
JH1_P0d80	Zone 80, Mat: P0d80
JH1_P0d81	Zone 81, Mat: P0d81
JH1_P0d82	Zone 82, Mat: P0d82
JH1_P0d83	Zone 83, Mat: P0d83
JH1_P0d84	Zone 84, Mat: P0d84
JH1_P0d85	Zone 85, Mat: P0d85
JH1_P0d86	Zone 86, Mat: P0d86
JH1_P0d87	Zone 87, Mat: P0d87
JH1_P0d88	Zone 88, Mat: P0d88
JH1_P0d89	Zone 89, Mat: P0d89
JH1_P0d90	Zone 90, Mat: P0d90
JH1_P0d91	Zone 91, Mat: P0d91
JH1_P0d92	Zone 92, Mat: P0d92
JH1_P0d93	Zone 93, Mat: P0d93
JH1_P0d94	Zone 94, Mat: P0d94
JH1_P0d95	Zone 95, Mat: P0d95
JH1_P0d96	Zone 96, Mat: P0d96
JH1_P0d97	Zone 97, Mat: P0d97
JH1_P0d98	Zone 98, Mat: P0d98
JH1_P0d99	Zone 99, Mat: P0d99
JH1_P0d100	Zone 100, Mat: P0d100

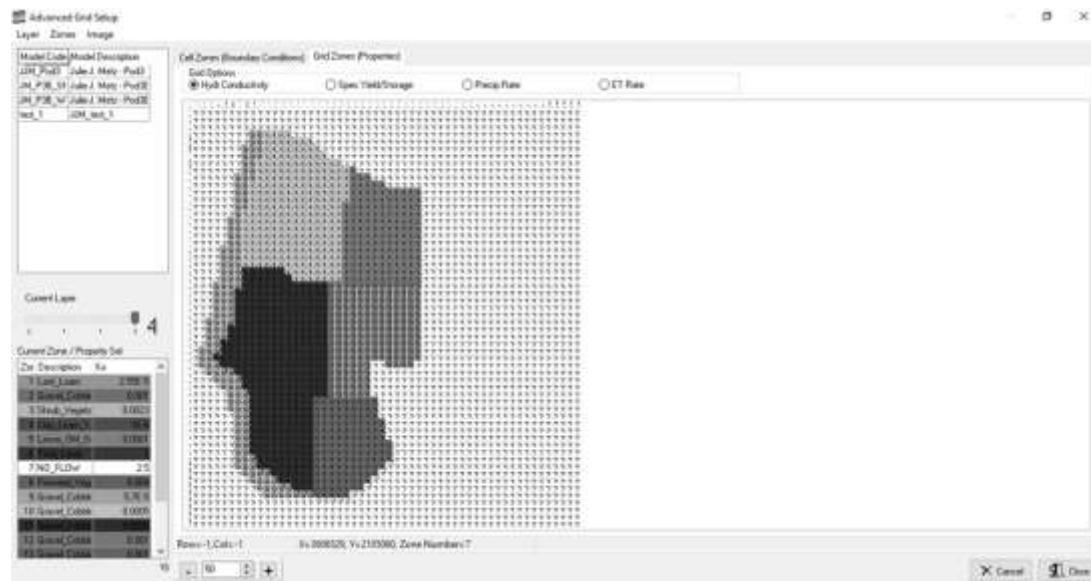
Current Layer

Current Zone / Property Set

Julie Metz grid zone layout with the hydraulic conductivity types and values for layer 2.



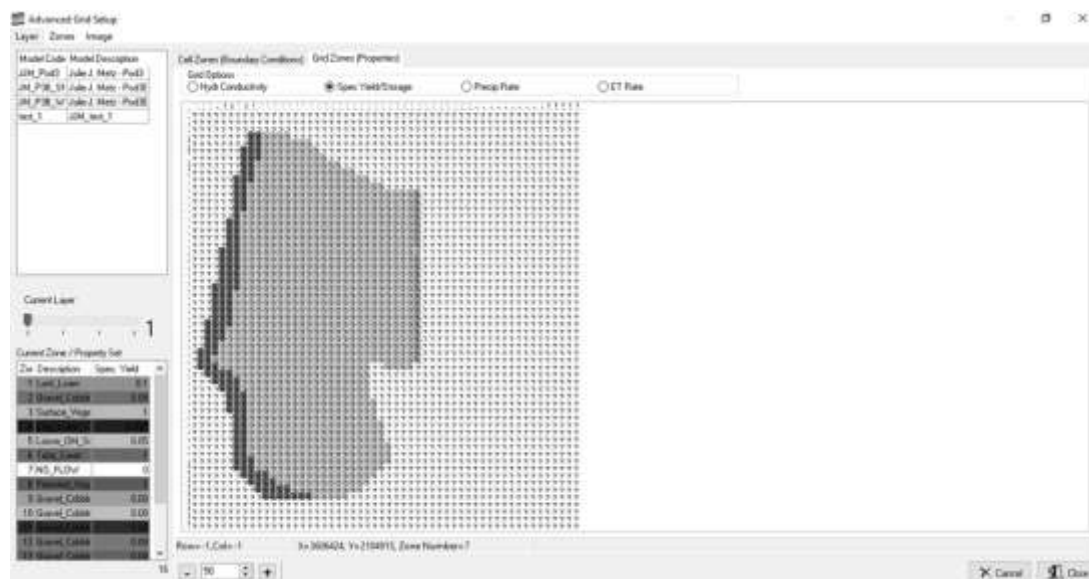
Julie Metz grid zone layout with the hydraulic conductivity types and values for layer 3.



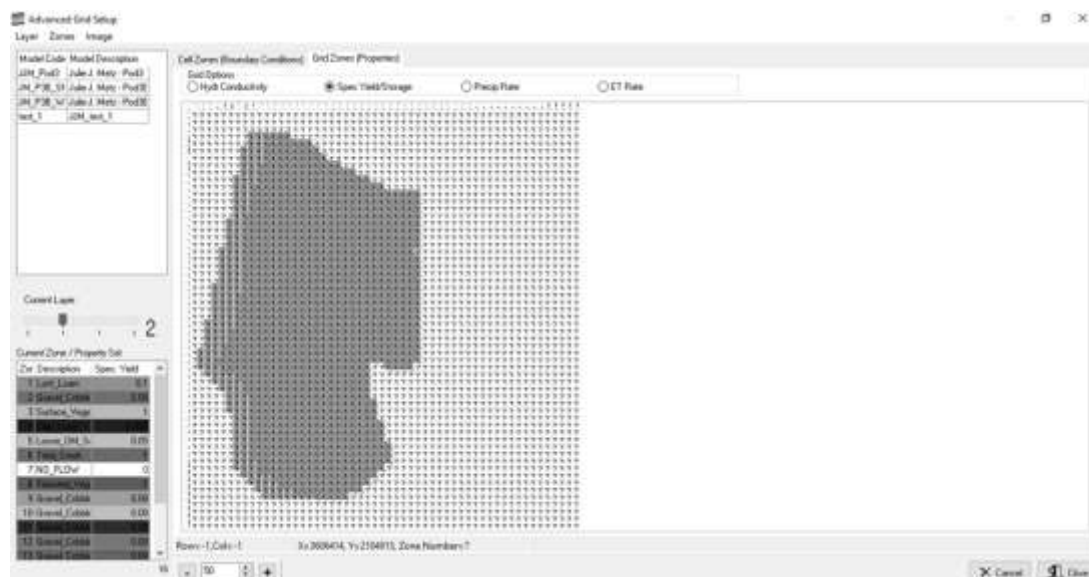
Julie Metz grid zone layout with the hydraulic conductivity types and values for layer 4.

APPENDIX I

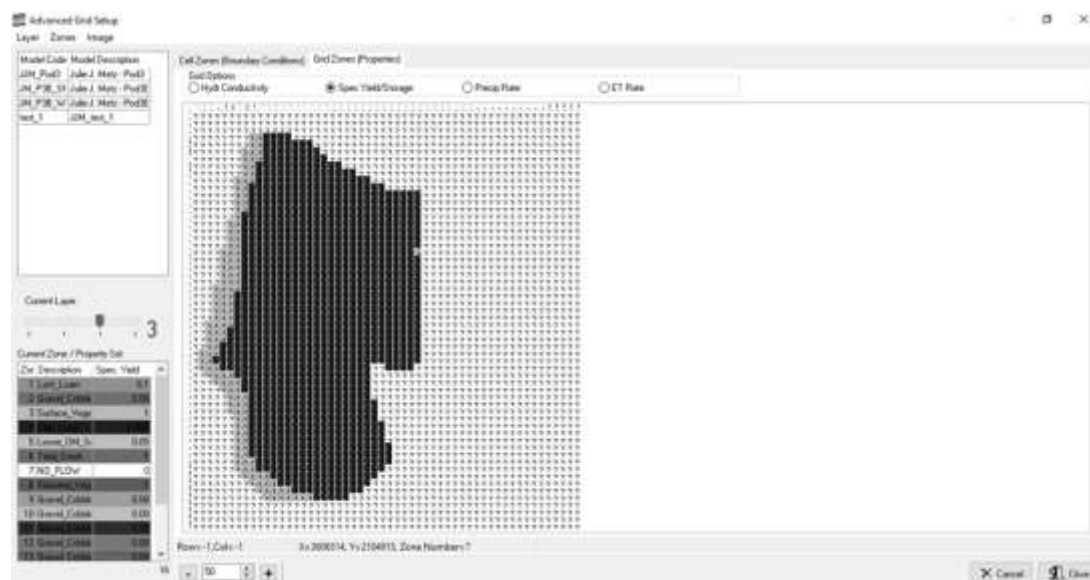
WETBUD SPECIFIC YIELD GRID ZONE LAYOUT IMAGES



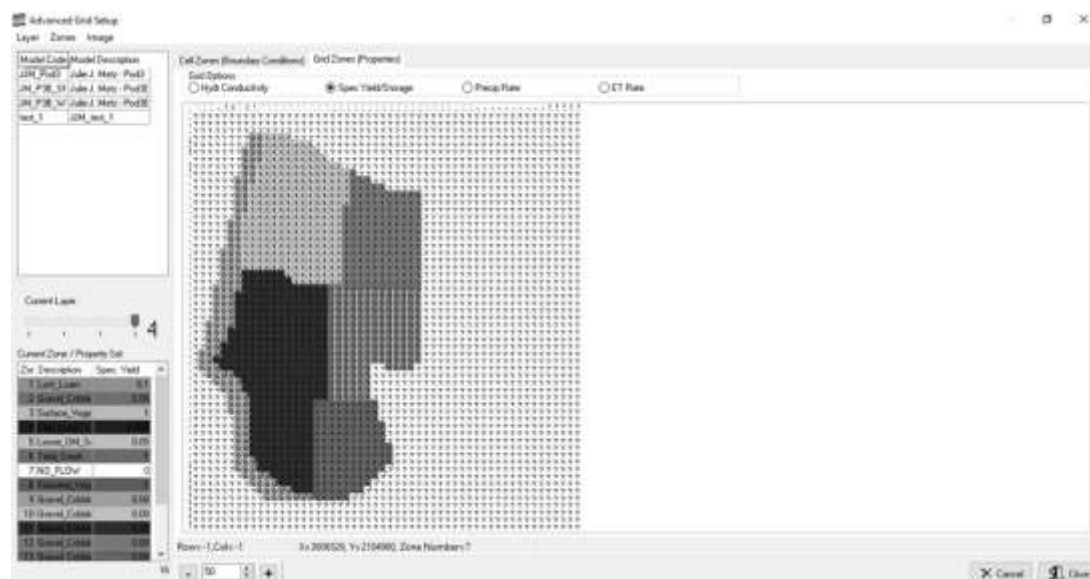
Julie Metz grid zone layout with the specific yield types and values for layer 1.



Julie Metz grid zone layout with the specific yield types and values for layer 2.



Julie Metz grid zone layout with the specific yield types and values for layer 3.



Julie Metz grid zone layout with the specific yield types and values for layer 4.

VITA

Benjamin Stuart Hiza

Ocean, Earth, and Atmospheric Sciences

4600 Elkhorn Ave. Old Dominion University, Norfolk, VA, 23529

EDUCATION

M.S. Ocean and Earth Sciences, Old Dominion University, Norfolk, VA, May 2017

B.S. Ocean and Earth Sciences, Old Dominion University, Norfolk, VA, May 2013

B.S. Environmental Science, Virginia Polytechnic Institute and State University,
Blacksburg, VA, May 2000

HONORS

Diversity Champion Award – ODU, April 2016

Lee Entsminger Scholarship for Coastal Geology – ODU, October 2015